

**THE EFFECT OF LDL-C ON T-CELL METABOLISM AND ITS  
IMPLICATIONS FOR CEREBROVASCULAR FUNCTION**

by

Theodore M. DeConne

A dissertation submitted to the Faculty of the University of Delaware in partial fulfillment of the requirements for the degree of Doctor of Philosophy in Applied Physiology

Summer 2023

© 2023 DeConne  
All Rights Reserved

**THE EFFECT OF LDL-C ON T-CELL METABOLISM AND ITS  
IMPLICATIONS FOR CEREBROVASCULAR FUNCTION**

by

Theodore M. DeConne

Approved: \_\_\_\_\_  
David G. Edwards, Ph.D.  
Chair of the Department of Kinesiology and Applied Physiology

Approved: \_\_\_\_\_  
William B. Farquhar, Ph.D.  
Dean of the College of Health Sciences

Approved: \_\_\_\_\_  
Louis F. Rossi, Ph.D.  
Vice Provost for Graduate and Professional Education and  
Dean of the Graduate College

I certify that I have read this dissertation and that in my opinion it meets the academic and professional standard required by the University as a dissertation for the degree of Doctor of Philosophy.

Signed:

---

Christopher R. Martens, Ph.D.  
Professor in charge of dissertation

I certify that I have read this dissertation and that in my opinion it meets the academic and professional standard required by the University as a dissertation for the degree of Doctor of Philosophy.

Signed:

---

David G. Edwards, Ph.D.  
Member of dissertation committee

I certify that I have read this dissertation and that in my opinion it meets the academic and professional standard required by the University as a dissertation for the degree of Doctor of Philosophy.

Signed:

---

Ibra S. Fancher, Ph.D.  
Member of dissertation committee

I certify that I have read this dissertation and that in my opinion it meets the academic and professional standard required by the University as a dissertation for the degree of Doctor of Philosophy.

Signed:

---

Daniel W. Trott, Ph.D.  
Member of dissertation committee

## **ACKNOWLEDGMENTS**

To paraphrase the late Christopher Hitchens, an educated person is someone who knows enough to know how ignorant they are. In this regard, I can attest that my graduate education has been a truly humbling process. I entered the program expecting to obtain a complete understanding of human physiology, but soon learned how naive this expectation was. While one might believe this realization would cause feelings of disillusionment, I would argue that it is an important part of the experience as a trainee, and quite inspiring. The scientific method is a tool that can be employed to objectively discern what is and is not likely to be false; however, those employing it are subject to many forms of bias. Furthermore, unexpected experimental results and failures, competing hypotheses or models, or challenging inquiries may cause doubt and/or cognitive dissonance. It is in these scenarios that it is important to remember our ignorance. Rather than doubling down, being able to question our own ideas and objectively analyze new information will help advance our understanding of the world. It is the knowledge of our ignorance that is inspiring, as this should be coupled with excitement of all there is left to learn.

I am extremely grateful for the mentors that I have had throughout this process. For without them, I would not have had the opportunities and experiences that led me to this philosophy. Dr. David Sauer was the first person that inspired me to pursue a career as a scientist. I met Dr. Sauer when I was a personal trainer at the local YMCA, and throughout my tenure at the YMCA he became a close friend and mentor. He inspired and supported me to pursue this career and throughout the process has always

been willing to listen and help guide me when facing a difficult decision. He has nearly limitless patience and is one of the most kind and generous people that I know. I would next like to acknowledge my academic mentors at my undergraduate alma mater, Southern Connecticut State University. Dr. Marc Robertson and Dr. Robert Axtell were my mentors in the Exercise Physiology program, and they helped cultivate my passion for Exercise Physiology. I am very grateful for their willingness to answer my questions, offer career guidance, and support my undergraduate research efforts. I would also like to thank my committee members Dr. David Edwards, Dr. Ibra “Drew” Fancher, and Dr. Daniel Trott for supporting my research interests, providing their technical and scientific knowledge, and allowing me to pursue this research question. I am also very grateful that Dr. Trott, Dr. Arit Ghosh, and the late Mr. Richard West taught me to perform flow cytometry. They were always willing to answer my questions and provide their knowledge and technical experience when I encountered a problem. Without these mentors, this project would not have been possible.

Lastly, I would like to thank my PhD advisor, Dr. Christopher Martens. Prior to working in Dr. Martens’ laboratory, I had very limited research experience. He took a risk by making me his first hire, but I am extremely thankful that he gave me this opportunity. Dr. Martens taught me many fundamental research skills and was always willing to answer questions and offer his assistance when I encountered a problem that I could not solve. He also consistently tried to include his trainees on various professional (e.g., grant writing & laboratory management) and service (e.g., peer review) related tasks to ensure we left the program as well-rounded scientists. Despite being a trainee, I always felt that my opinions and arguments were respected, and his mentoring style cultivated an environment of open communication. He also supported

my multitude of research ideas, responded to my late night/early morning emails, and provided countless edits and detailed feedback on documents. I believe that Dr. Martens is a great mentor, and I could not have asked for a better advisor to guide me through this process.

While not mentors, I would also like to acknowledge the individuals who helped me complete my degree and this research project. I would like to thank all our laboratory managers, including Joshua Hobson, Elizabeth Habash, and Catherine Awad for going above and beyond their roles as laboratory managers. While Josh and Elizabeth did not assist with my dissertation projects, their work laid the foundation for the laboratory as it is today. Cat continued to build upon their work and contributed to the participant recruitment and data collection by making herself available to assist with the flow cytometry experiments. I also appreciate the work of our former undergraduate volunteer, Houston Ward, who assisted with the data collection for the preliminary experiments for this study. I would like to thank the other members of the Neurovascular Aging Laboratory, who include Dr. Faria Sanjana, Dr. Kevin Decker, Mr. Nicholas Rizzi, and Ms. Fiona Horvat for assisting with blood draws, moving their study visits to accommodate mine, and listening and providing their input about technical, conceptual, and scientific aspects of the project.

Lastly, I would like to thank my fiancé, Alexa Brenner. Despite not being in the field, Alexa always made herself available to eagerly listen to my presentations and my many, many research ideas. She also supported me through the moments when I failed; the many experimental failures, rejected grant applications, and challenging presentations. She understood the sacrifices required to complete a PhD, and would

help care for me, our dog, Maple, and our home when she knew I had to stay late or work through the weekend. I am very grateful and thankful that she stood by my side.

I hope that I can hold onto the skills and lessons that I learned from everyone who helped me achieve a PhD throughout the rest of my scientific career. I will undoubtedly face failure and uncertainty in the future, but I will remember these moments offer the opportunity to learn and grow.

## TABLE OF CONTENTS

LIST OF FIGURES .....	xi
LIST OF TABLES .....	xii
ABSTRACT .....	xiii

### Chapter

1	REVIEW OF THE LITERATURE .....	1
1.1	Introduction .....	1
1.2	Overview of the Immune System .....	3
1.2.1	The Innate Immune System .....	4
1.2.2	The Adaptive Immune System .....	6
1.3	The Effect of Cardiometabolic Risk Factors on T-cell Function .....	9
1.3.1	T-cell Activation .....	9
1.3.2	T-cell Senescence .....	12
1.3.3	T-cell Mitochondrial Function .....	13
1.4	The Role of Vascular Dysfunction in Alzheimer’s Disease .....	18
1.5	The Role of Lymphocytes in Regulating Vascular Function .....	22
1.5.1	The Role of B-cells in Regulating Vascular Function .....	22
1.5.2	The Role of T-cells in Regulating Vascular Function .....	23
1.5.2.1	The Effect of Cardiometabolic Risk Factors on T-cell Function and the Implications for Vascular Function .....	28
1.6	Summary .....	34
2	THE ASSOCIATION BETWEEN T-CELL AND CEREBROVASCULAR FUNCTION IN MID-LIFE ADULTS. ....	36
2.1	Introduction .....	36
2.2	Materials and Methods .....	38
2.2.1	Participant Recruitment .....	38
2.2.2	Questionnaires .....	39
2.2.3	Blood Draw .....	40
2.2.4	Blood Pressure .....	41
2.2.5	Anthropometric Measurements .....	41
2.2.6	Peripheral Blood Mononuclear Cell Isolation .....	41

2.2.7	Positive T-cell Separation .....	42
2.2.8	T-cell Mitochondrial Respirometry .....	43
2.2.9	Measuring Cerebrovascular Reactivity .....	46
2.2.10	Statistical Analysis .....	49
2.3	Results .....	50
2.4	Discussion .....	62
3	<b>THE EFFECT OF EXOGENOUS LOW-DENSITY LIPOPROTEIN CHOLESTEROL ON T-CELL FUNCTION .....</b>	<b>67</b>
3.1.	Introduction .....	67
3.2.	Materials and Methods .....	68
3.2.1.	Participant Recruitment .....	68
3.2.2.	Questionnaires .....	69
3.2.3.	Blood Draw .....	70
3.2.4.	Blood Pressure .....	70
3.2.5.	Height and Weight .....	71
3.2.6.	Peripheral Blood Mononuclear Cell Isolation .....	71
3.2.7.	Positive T-cell Separation and LDL-C Treatment .....	72
3.2.8.	T-cell Mitochondrial Respirometry .....	73
3.2.9	Negative T-cell Separation and LDL-C Treatment .....	74
3.2.10	Flow Cytometry Experiments .....	75
3.2.11.	Statistical Analysis .....	79
3.3.	Results .....	80
3.4.	Discussion .....	97
4	<b>CONCLUSIONS .....</b>	<b>102</b>
4.1.	Summary .....	102
4.2	Perspectives .....	103
	<b>REFERENCES .....</b>	<b>104</b>
	Appendix	
	Appendix A .....	121
	SUPPLEMENTARY FIGURES .....	121
	SUPPLEMENTARY METHODS .....	123
	Appendix B .....	125

IRB APPROVED PROTOCOL ..... 125

## LIST OF FIGURES

<b>Figure 1.1</b>	Innate and Adaptive Immune Cells.....	4
<b>Figure 1.2</b>	CD4+ and CD8+ T-cell Anatomy.....	7
<b>Figure 1.3</b>	CD4+ T-cell activation.....	10
<b>Figure 1.4</b>	Cellular Bioenergetics. ....	13
<b>Figure 1.5</b>	Mitochondrial Regulation of T-cells.....	16
<b>Figure 1.6</b>	Muscular Artery Cross-Section and Endothelial Nitric Oxide Production.....	17
<b>Figure 2.1</b>	Agilent Seahorse XF Cell Mito Stress Test.....	46
<b>Figure 2.2</b>	Breath-Hold Protocol.....	48
<b>Figure 2.3</b>	Mediation Analysis.....	61
<b>Figure 2.4</b>	Spearman correlations.....	62
<b>Figure 3.1</b>	Representative Gating Strategy. ....	78
<b>Figure 3.2</b>	Gating strategy for CD69 marker.....	79
<b>Figure 3.3</b>	The Effect Of LDL-C on CD4+ bioenergetics. ....	83
<b>Figure 3.4</b>	The Effect Of LDL-C on CD8+ bioenergetics. ....	85
<b>Figure 3.5</b>	The Effect Of LDL-C on CD4+ T-cell Function. ....	90
<b>Figure 3.6</b>	The Effect Of LDL-C on CD8+ T-cell Function.....	91
<b>Figure 3.7</b>	The Effect Of LDL-C on CD4+ and CD8+ T-cell Cytokine Production. .....	93
<b>Figure 3.8</b>	The Associations Between Measures of CD4+ and CD8+ T-cell Function in Response to LDL-C.....	96
<b>Supplementary Figure A.1</b>	Seeding Density Titration Experiment.....	122

## LIST OF TABLES

<b>Table 2.1</b>	Descriptive Statistics.....	51
<b>Table 2.2</b>	Clinical Blood Chemistry.....	52
<b>Table 2.3</b>	Lifestyle, Health, and Behavioral Factors.....	53
<b>Table 2.4</b>	Baseline Physiologic Cerebrovascular Reactivity Data. ....	55
<b>Table 2.5</b>	Cerebrovascular Reactivity Responses.....	56
<b>Table 2.6</b>	CD4 <sup>+</sup> Mitochondrial Respiration and Glycolysis vs. Cerebrovascular Reactivity.....	59
<b>Table 2.7</b>	CD8 <sup>+</sup> Mitochondrial Respiration and Glycolysis vs. Cerebrovascular Reactivity.....	60
<b>Table 3.1</b>	Descriptive Statistics.....	80
<b>Table 3.2</b>	Clinical Blood Chemistry.....	81
<b>Table 3.3</b>	The Effect of LDL-C on CD4 <sup>+</sup> Mitochondrial Respiration and Glycolysis.....	84
<b>Table 3.4</b>	The Effect of LDL-C on CD8 <sup>+</sup> Mitochondrial Respiration and Glycolysis.....	86

## ABSTRACT

**INTRODUCTION:** Alzheimer’s disease (AD) mortality is the fifth leading cause of death in adults 65 years and older. Aging is the greatest risk factor for AD, and is associated with an increase in chronic, sterile, low-grade inflammation termed “inflammaging”. Inflammaging is caused, in part, by dysregulation of the immune system. Adaptive immune cells called T-lymphocytes (T-cells) are primary contributors to inflammaging. T-cells become dysregulated with aging because of impaired mitochondrial function, oxidative stress, and repetitive activation, which shift T-cells towards a pro-inflammatory or senescent state. T-cells have also recently been recognized as important regulators of cerebrovascular function in animals, and impaired cerebrovascular function is a hallmark of AD. However, whether T-cell function relates to human cerebrovascular function is not known. Further, the cause of T-cell dysregulation is not entirely understood. We and others have shown that higher endogenous low-density lipoprotein cholesterol (LDL-C) is related to lower immune cell mitochondrial function and treating T-cells with exogenous LDL-C impaired ATP production. Additionally, animal models have shown that LDL-C can act as a “neo-antigen”, resulting in the activation of T-cells. **OBJECTIVES:** Therefore, the objectives of this study were to (1) determine whether T-cell mitochondrial respiration is predictive of cerebrovascular function in middle-aged humans and (2) determine whether treatment with a high concentration of LDL-C impairs mitochondrial respiration, induces activation and senescence, and increases intracellular cytokine production and mitochondrial oxidative stress, compared to treatment with a low concentration of LDL-C. **HYPOTHESES:** (1) We hypothesized that higher T-cell mitochondrial respiration would be predictive of greater cerebrovascular function and

that higher T-cell glycolysis would be predictive of lower cerebrovascular function and (2) treatment with a high concentration of exogenous LDL-C would lower mitochondrial respiration, increase activation and glycolysis, pro-inflammatory cytokine production, and mitochondrial oxidative stress, and induce senescence in CD4<sup>+</sup> and CD8<sup>+</sup> T-cells from middle-aged adults. **METHODS:** Twenty middle-aged adults were recruited to assess the relation between mitochondrial respiration and cerebrovascular function, and eighteen middle-aged adults were recruited to determine the effect of exogenous LDL-C on T-cell function. T-cells were separated from peripheral blood mononuclear cells using magnetic bead separation. For the first objective, mitochondrial respiration was assessed by measuring oxygen consumption rate (OCR), and glycolysis was assessed by measuring extracellular acidification rate using extracellular flux analysis. Cerebrovascular function was assessed by measuring the change in blood flow velocity in the middle-cerebral artery (MCAv) during a 30-second breath-hold. The breath-hold index (BHI) was calculated as the main outcome measure for cerebrovascular reactivity. For the second objective, CD4<sup>+</sup> and CD8<sup>+</sup> T-cells were treated with a high and low physiological concentration of exogenous LDL-C for 20-hours. Mitochondrial respiration and extracellular acidification rate (ECAR) were measured using extracellular flux analysis, and all other measures of T-cell function were measured using flow cytometry. **RESULTS:** We found that higher CD8<sup>+</sup> basal was predictive of lower MCAv BHI ( $\beta=-2.20$ ,  $R^2=0.29$ ,  $P=0.015$ ), likely by modulating the sympathetic pressor response to the breath-hold. No measure of CD4<sup>+</sup> T-cell mitochondrial respiration or ECAR were predictive of MCAv BHI. We also found that treatment with a high concentration of LDL-C impaired CD4<sup>+</sup> T-cell basal (low:  $0.75 \pm 0.34$  vs. high:  $0.65 \pm 0.35$  pMol/min/10,000 cells,  $p=0.022$ ), and

impaired CD4<sup>+</sup> and CD8<sup>+</sup> T-cell ATP-linked OCR (CD4<sup>+</sup> low:  $0.84 \pm 0.31$  vs. CD4<sup>+</sup> high:  $0.64 \pm 0.33$  pMol/min/10,000 cells,  $p < 0.0001$ ; & CD8<sup>+</sup> low:  $0.85 \pm 0.35$  vs. CD8<sup>+</sup> high:  $0.64 \pm 0.14$  pMol/min/10,000 cells,  $p = 0.0024$ ). Treatment with high LDL-C also increased glycolysis in CD8<sup>+</sup> T-cells (low:  $0.20 \pm 0.072$  vs. high:  $0.23 \pm 0.089$  mpH/min/10,000 cells,  $p = 0.025$ ). Additionally, treatment with high LDL-C induced activation (CD4<sup>+</sup> low:  $6.78 \pm 5.77$  vs. CD4<sup>+</sup> high:  $19.16 \pm 20.51\%$ ,  $p = 0.0093$ ; & CD8<sup>+</sup> low:  $12.75 \pm 11.73$  vs. CD8<sup>+</sup> high:  $27.91 \pm 26.87\%$ ,  $p = 0.0009$ ) and senescence (CD4<sup>+</sup> low:  $1.04 \pm 1.40$  vs. CD4<sup>+</sup> high:  $2.40 \pm 2.52\%$ ,  $p = 0.0021$ ; & CD8<sup>+</sup> low:  $13.01 \pm 7.78$  vs. CD8<sup>+</sup> high:  $14.86 \pm 8.10\%$ ,  $p = 0.030$ ) and increased the production of intracellular cytokines, such as IL-6 (CD4<sup>+</sup> low:  $72.49 \pm 21.47$  vs. CD4<sup>+</sup> high:  $77.19 \pm 22.42\%$ ,  $p = 0.0092$ ; & CD8<sup>+</sup> low:  $74.48 \pm 25.54$  vs. CD8<sup>+</sup> high:  $78.72 \pm 26.45\%$ ,  $p = 0.0044$ ) and mitochondrial oxidative stress (CD4<sup>+</sup> low:  $11.23 \pm 7.12$  vs. CD4<sup>+</sup> high:  $36.04 \pm 35.43\%$ ,  $p = 0.0026$ ; & CD8<sup>+</sup> low:  $4.90 \pm 5.35$  vs. CD8<sup>+</sup> high:  $20.17 \pm 22.19\%$ ,  $p = 0.0024$ ) in both CD4<sup>+</sup> and CD8<sup>+</sup> T-cells, compared to the treatment with low LDL-C. **CONCLUSION:** Higher CD8<sup>+</sup> T-cell glycolysis was associated with lower cerebrovascular function in humans. We also found that treatment with a high concentration of LDL-C impaired mitochondrial respiration and shifted T-cells towards glycolytic metabolism. Additionally, high LDL-C induced activation and senescence and the production of pro-inflammatory cytokine and mitochondrial oxidative stress. To prevent increases in T-cell inflammation and oxidative stress and preserve mitochondrial function it is important to maintain low concentrations of LDL-C with aging. Therapeutics targeting T-cells may provide novel treatments or preventative strategies for the development of age-related inflammatory diseases, such as AD.

# Chapter 1

## REVIEW OF THE LITERATURE

### 1.1 Introduction

Alzheimer's disease (AD) mortality has risen by 145% from 2000 to 2019 <sup>4</sup>, and the incidence will likely further increase considering the number of adults in the U.S. over the age of 65 is projected to double by 2050 <sup>5</sup>. The “amyloid cascade hypothesis” has traditionally been the accepted explanation for the etiology of AD. The amyloid cascade hypothesis generally states that a build-up of amyloid- $\beta$  plaques in the brain, the primary pathological feature of AD, is also the root cause of AD. However, there are several problems that the Amyloid Cascade Hypothesis fails to account for <sup>6</sup>. This has led to the development of alternative hypotheses in which processes such as cellular senescence, oxidative stress, metabolic dysfunction, inflammation, and vascular dysfunction lead to AD <sup>7,8</sup>. In this regard, multiple studies have shown that cerebrovascular function is lower in people with AD and cognitive impairment and poor cerebrovascular function is a risk factor for neurodegenerative disease <sup>9-16</sup>.

It is now well recognized that cardiovascular diseases (CVD) and AD share many similar cardiometabolic risk factors, including aging, high cholesterol, hypertension, and arterial stiffness <sup>17</sup>. Starting in mid-life, the accumulation of cardiometabolic risk factors over time may significantly increase later life AD risk <sup>18-22</sup>. Thus, it is important to delay the accumulation of cardiometabolic risk factors for

as long as possible. Cardiometabolic risk factors also contribute to “inflammaging”<sup>23</sup>, a process characterized by an age-related imbalance of pro-inflammatory cytokines to anti-inflammatory cytokines, resulting in a low-grade, sterile chronic inflammation<sup>24–26</sup>. Inflammaging is thought to be caused, in-part, by T-lymphocytes (T-cells) that become dysfunctional<sup>27–29</sup>. T-cells are specialized cells in the adaptive immune system and have recently been identified to be involved in the pathogenesis of AD<sup>30–33</sup> and CVD<sup>34–36</sup>. T-cells become dysfunctional with normal aging, resulting in a shift towards a pro-inflammatory phenotype<sup>28,37,38</sup>. Importantly, T-cells have also been shown to influence cerebrovascular endothelial function in various animal models, likely by modulating inflammation<sup>39–41</sup>. While generally recognized for their ability to produce ATP, the mitochondria are also necessary for regulating proper T-cell activation, effector and memory function, proliferation, in addition to other functions<sup>3,42</sup>. The mitochondria are subject to age-related changes, resulting in impaired mitochondrial respiration<sup>43,44</sup>. Impaired mitochondrial respiration, in turn leads to increased oxidative stress<sup>45</sup>, resulting in a pro-inflammatory phenotype that drives early T-cell senescence<sup>3,28,46,47</sup>.

In this regard, impairing mitochondrial respiration in T-cells from young mice induced pre-mature aging, as well as widespread senescence and physiological dysfunction<sup>42</sup>. Despite these data, it is not known whether T-cell mitochondrial dysfunction is associated with accelerated vascular aging in humans. The age-related processes that lead to changes in mitochondrial function are also not fully known. Cardiometabolic risk factors, such as elevated endogenous low-density lipoprotein cholesterol (LDL-C) have recently been linked to impaired mitochondrial respiration<sup>48,49</sup> in human peripheral immune cells, which include T-cells. LDL-C has been shown

to induce mitochondrial dysfunction in other immune cells<sup>50</sup>. Our preliminary data suggest that LDL-C may be activating T-cells. Additionally, LDL-C and the particle responsible for carrying LDL-C (e.g., apolipoprotein B-100; apoB) can become a “neo-antigen” for T-cells<sup>51–53</sup>, possibly resulting in their repetitive activation. Over time, repetitive activation induces senescence and shifts T-cells to a more pro-inflammatory state<sup>28,37,38,54–56</sup>. Aging is associated with an increase in endogenous LDL-C, and peaks in mid-life<sup>57,58</sup>. Thus, it may be that elevated LDL-C with aging induces T-cell activation, and overtime this may lead to T-cell senescence and pro-inflammatory phenotype<sup>28,37,38,54–56</sup>. Thus, this review will focus on the effect of LDL-C on T-cell function (e.g., mitochondrial function, inflammation, activation, senescence, and oxidative stress) and the role that T-cell function plays in regulating endothelial function, specifically the endothelium in brain.

## **1.2 Overview of the Immune System**

The immune system protects the body against foreign pathogens and substances using both humoral (e.g., antibodies) and cell-mediated immunity (e.g., phagocytosis, cytokines, & antigen-specific cellular apoptosis), provided by the innate and adaptive immune systems<sup>1</sup>. Innate and adaptive immunity have separate roles but work closely together to protect the body against pathogens<sup>1</sup>. The innate immune system provides general protection against the infiltration of foreign pathogens or substances and is also the body’s first response to foreign molecules that have infiltrated the body<sup>1</sup>. These responses are rapid and non-specific, which end in pathogen elimination<sup>1</sup>. In contrast to innate immunity, adaptive immunity is antigen-specific, but the initial response is slower<sup>1</sup>. This is because the adaptive immune

system possesses “immunological memory”, and immune cells with receptors for the specific antigen are required for the response <sup>1</sup>. The response to a novel antigen is slower (e.g., primary response), as the body only possess a limited number of immune cells with a specificity for a given antigen <sup>1</sup>. The speed with which the adaptive immune system responds also depends on previous encounters with the antigen and the presentation of the antigen by the innate immune cells <sup>1</sup>. Importantly, each subsequent encounter with a previously encountered antigen allows for a more rapid and robust secondary immune response <sup>1</sup>. The protection the immune system offers against foreign pathogens is one of its most well-known characteristics; however, immune system dysfunction has more recently been recognized as a major contributor to the development of a multitude of chronic diseases, including endothelial dysfunction.

### 1.2.1 The Innate Immune System

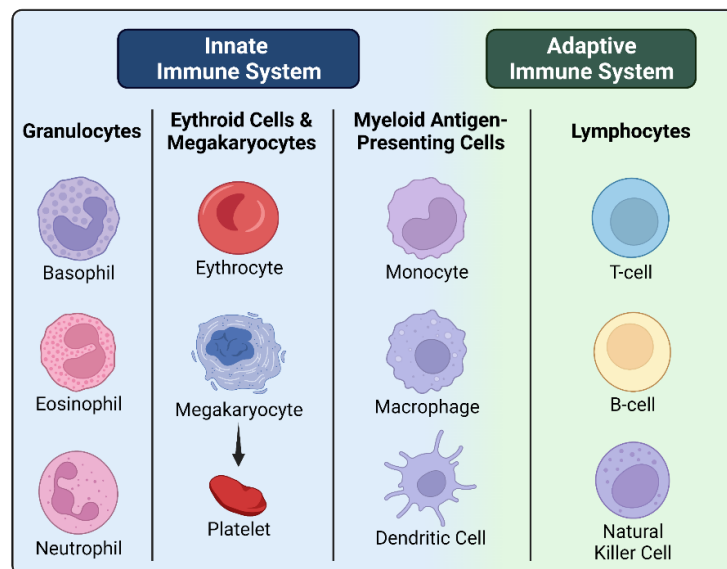


**Figure 1.1** Innate and Adaptive Immune Cells. Information in this figure can be found in Punt et al., 2018 <sup>1</sup>. Created with BioRender.com.

The innate immune system is comprised of differentiated myeloid progenitor cells that committed to the myeloid lineage from hematopoietic stem cells found in the bone marrow <sup>1</sup>. These immune cells include granulocytes, myeloid antigen-presenting cells, erythroid cells, and megakaryocytes (Fig. 1.1) <sup>1</sup>. Granulocytes are comprised of neutrophils, eosinophils, basophils, and mast cells <sup>1</sup>. These cells are generally the first to respond to a foreign pathogen or substance and have a variety of different functions depending on the cell type <sup>1</sup>. Myeloid antigen-presenting cells include monocytes, macrophages, and dendritic cells <sup>1</sup>. While considered part of the innate immune system, these cells connect the innate and adaptive immune systems via their ability to present antigens to the adaptive immune cells (e.g., antigen presenting cells, APCs) <sup>1</sup>. In addition to their role as APCs, these cells also engulf bacteria, cells or liquids (e.g., phagocytes and pinocytes), initiate immune responses, and regulate inflammation and immune cell communication and activation at sites of infection or damage <sup>1</sup>.

The primary function of erythroid cells or erythrocytes (red blood cells) is the transport of oxygen or carbon dioxide via a protein called hemoglobin. However, erythrocytes also have a small role in the immune system. In this respect, erythrocytes have the ability to express surface markers to attract macrophages and also damage microbes <sup>1</sup>. Megakaryocytes are platelet-producing cells found in the bone marrow <sup>1</sup>. Platelets act as barrier cells, as they are important for forming blood clots, which prevent pathogens from entering the body <sup>1</sup>. While outside the scope of this review, the innate immune system contributes to endothelial dysfunction, however, little literature exists exploring the relation between the innate immune system and cerebrovascular endothelial dysfunction within the context of healthy aging. In this regard, neutrophils <sup>59-63</sup>, monocytes and macrophages <sup>64,65</sup>, contribute to endothelial

dysfunction and/or atherosclerosis, a condition preceded by endothelial dysfunction<sup>66,67</sup>.

### **1.2.2 The Adaptive Immune System**

The adaptive immune system is comprised of three groups of lymphocytes that differentiate from lymphoid lineage cells<sup>1</sup>. These include B-lymphocytes (B-cells), T-cells, and innate lymphoid cells (ILCs), of which natural killer (NK) cells are the most common (Figure 1.1)<sup>1</sup>. Lymphocytes can be differentiated by uniquely expressed surface proteins (e.g., clusters of differentiation, CD)<sup>1</sup>. For example, T-cells can be subdivided into T-helper (T<sub>H</sub>) and cytotoxic T-cells (T<sub>C</sub>) via their respective surface markers (CD4<sup>+</sup> vs. CD8<sup>+</sup>)<sup>1</sup>. The function of lymphocytes depends on where they are in their life cycle. Newly formed lymphocytes are called “naïve” and have not yet encountered an antigen<sup>1</sup>. Once an antigen encounters a naïve cell with a specific receptor for that antigen (antigen-specific receptor), the cell begins to rapidly proliferate and differentiate, producing more cells with identical antigen-specific receptors<sup>1</sup>. Naïve lymphocytes differentiate into effector cells, and a subset of effector cells will differentiate into memory cells<sup>1,68</sup>. The effector cells are responsible for initiating the immune response<sup>1</sup>. A small proportion of effector cells will survive following the immune response and will return to a quiescent state as memory cells<sup>1</sup>. Memory cells have a longer half-life and are what provide us with “immunological memory”, mediating a faster and more robust secondary immune response in response to the same antigen in the future<sup>1</sup>. The differentiation process can differ depending on the type of lymphocyte.

B-cells are formed in the bone marrow <sup>1</sup>. Mature B-cells can be identified by the expression of a B-cell receptor (BCR) <sup>1</sup>. This receptor is responsible for binding antigens to an antibody bound to the B-cell's membrane <sup>1</sup>. The surface antibody is antigen specific, and each B-cell expresses a different surface antibody <sup>1</sup>. Once activated, B-cells have a variety of functions. Activated B-cells act as APCs and stimulate T-cell activation; the latter results in B-cell differentiation into effector B-cells or plasma B-cells via CD4<sup>+</sup> T<sub>H</sub> cell mediated cytokine cross-talk <sup>1</sup>. Plasma cells are responsible for the production and secretion of antigen specific antibodies, and those that survive the antigen encounter remain in circulation as memory B-cells <sup>1</sup>.

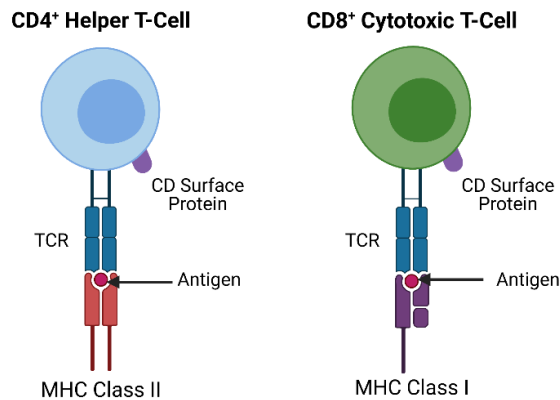


**Figure 1.2.** CD4+ and CD8+ T-cell Anatomy. Adapted from Punt et al. 2018 <sup>1</sup>. Created with BioRender.com. Abbreviations: MHC, major histocompatibility complex; CD, cluster of differentiation; & TCR, T-cell receptor.

Like B-cells, T-cells also derive their name from their point of maturation, which is in the thymus <sup>1</sup>. T-cell progenitor cells can develop into two different lineages, including  $\alpha\beta$  and  $\gamma\delta$  T-cell subsets <sup>69</sup>.  $\alpha\beta$  T cells are the most abundant lineage (95-99.5%) <sup>70</sup>, thus this review will primarily focus on this subset. T-cells do

not produce antibodies, and instead either assist other immune cells in responding to an antigen ( $CD4^+$ ) or by directly eliminating the antigen ( $CD8^+$ )<sup>1</sup>. T-cells express a T-cell receptor (TCR), which is a surface receptor that binds to specific antigen fragments (Figure. 1.2)<sup>1</sup>. These antigen fragments must be presented to T-cells bound to major histocompatibility complexes (MHC) on the cell membranes of APCs<sup>1</sup>.  $CD4^+$  T-cells recognize MHC class II (MCH-II) molecules, whereas  $CD8^+$  T-cells recognize MHC class I (MCH-I) molecules<sup>1</sup>.  $CD4^+$  T-cells are considered  $T_H$  cells, and generally assist with mediating the immune responses of other immune cells (e.g., B-cells &  $CD8^+$  T-cells)<sup>1</sup>. Naïve  $CD4^+$  T-cells are activated once they recognize an antigen fragment bound to MHC-II, and will then proliferate and differentiate into a variety of effector subsets ( $T_{EFF}$ )<sup>1</sup>. These subsets can be recognized by their uniquely expressed surface proteins (e.g., CDs) and cytokines that they produce<sup>1</sup>. Naïve  $CD4^+$  T-cells can also undergo a separate lineage commitment and differentiate into regulatory T-cells ( $T_{REG}$ )<sup>1</sup>. Rather than assisting other immune cells to initiate an immune response,  $T_{REG}$  act as inhibitors<sup>1</sup>. These regulatory cells are necessary to prevent immune responses to self-antigens (e.g., autoimmune responses) and an uninhibited immune response<sup>1</sup>. Effector  $T_{REG}$  and  $T_{EFF}$  will eventually differentiate terminally into central memory  $T_H$ <sup>68</sup>. With the help from  $CD4^+$   $T_H$ , naïve  $CD8^+$   $T_C$  are activated once they encounter a receptor specific antigen bound to an MHC-I complex and then proliferate and differentiate into central memory, effector memory, and eventually terminally differentiated T-cells<sup>1,68</sup>. However, unlike  $CD4^+$   $T_H$ ,  $CD8^+$   $T_C$  directly eliminate non-self-antigens<sup>1</sup>.

Innate lymphoid cells (ILCs) are the last group of lymphocytes<sup>1</sup>. They can be divided into three subgroups (e.g., ILC1, ILC2, and ILC3), but the most well-known

ILC are natural killer cells (NK) within the ILC1 subgroup<sup>1</sup>. ILCs do not have an antigen-specific receptor and are instead categorized by the cytokines produced<sup>1</sup>. ILCs are found in the skin and mucous, making them one of the first barriers for foreign antigens to bypass before accessing the body<sup>1</sup>. NK cells are cytotoxic and eliminate cells by either releasing cytotoxic granules that attack cells that do not have MHC-I complexes or by binding antibodies to their surface receptors<sup>1</sup>. The antibodies bind to antigens on infected cells, allowing the NK cells to release their cytotoxic granules resulting in cellular death<sup>1</sup>. Research investigating the role that NK cells play in endothelial dysfunction is scarce. Thus, the subsequent sections of this review will focus primarily on B-cells and T-cells.

### **1.3 The Effect of Cardiometabolic Risk Factors on T-cell Function**

#### **1.3.1 T-cell Activation**

In order to combat a foreign antigen, naïve T-cells needed to be activated in order to proliferate and differentiate into their effector and memory subtypes. If a naïve T-cell does not encounter an antigen bound to a compatible MHC on APCs, it will re-enter the circulation and continue its search in other tissues<sup>1</sup>. The accepted explanation for naïve T-cell activation is called the “two-signal hypothesis”<sup>1</sup>. Despite its name, this hypothesis postulates that there are three signals necessary for T-cell activation<sup>1</sup>. The first signal is the interaction between the TCR from the T-cell and the MHC-antigen complex from an APC, and the CD4<sup>+</sup> and CD8<sup>+</sup> surface proteins act as co-receptors that bind to their respective MHC-antigen complexes<sup>1</sup>.

To induce proliferation *in vitro*, monoclonal CD3 antibodies can be used as a surrogate for the TCR and MHC-antigen complex interaction (e.g., signal 1)<sup>1</sup>. The second signal involves the interaction between the CD28 receptor on T-cells and co-stimulatory ligands on the APC (e.g., CD80/CD86)<sup>1</sup>. As a result of the first and second signal, cytokines are produced (e.g., IL-2) that initiate T-cell proliferation and differentiation via polarizing cytokines<sup>1</sup>. The cytokines act as the third signal in T-cell activation, which determines the fate of the naïve T-cell<sup>1</sup>. An example of CD4<sup>+</sup> T<sub>H</sub> cell activation is depicted in Figure 1.3.

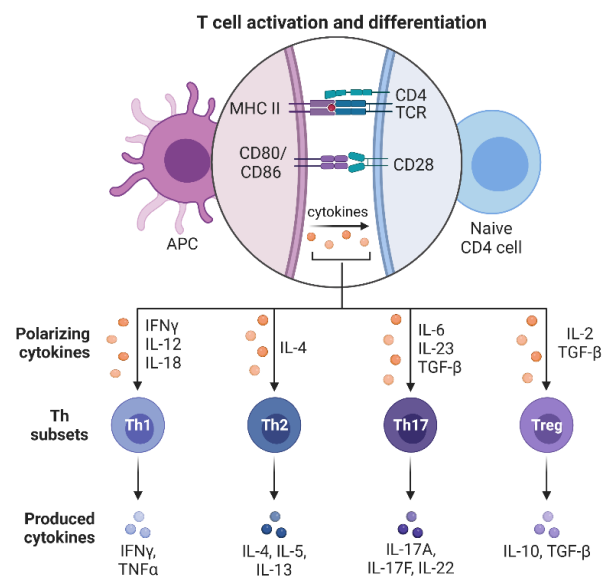


**Figure 1.3.** CD4<sup>+</sup> T-cell activation. Adapted from BioRender.com and Punt et al., 2018<sup>1</sup>. Created with BioRender.com. Abbreviations: APC, antigen-presenting cell; MHC II, major histocompatibility complex-II; CD, cluster of differentiation; TCR, T-cell receptor; IL, interleukin; IFN $\gamma$ , interferon  $\gamma$ ; TGF- $\beta$ , transforming growth factor  $\beta$ ; & TNF- $\alpha$ , tumor necrosis factor  $\alpha$ .

Aging is associated with an imbalance of naïve to memory T-cells because of thymic involution and repetitive activation<sup>28,71</sup>. The thymus is responsible for the generation of naïve T-cells and is also where T-cell development occurs<sup>71</sup>. As the thymus becomes involuted, the number of naïve T-cells generated decreases, while the pool of effector and effector memory T-cells increases as a result of activation<sup>28,72,73</sup>. In a study of healthy children and adults, the ratio of memory to naïve T-cells began to decrease at 37.4 and 29.5 years of age for CD4<sup>+</sup> and CD8<sup>+</sup> T-cells, respectively<sup>74</sup>. This loss of T-cell repertoire increases the risk of severe infection in older populations<sup>28,71</sup>, and the increased pool of circulating memory T-cells contributes to inflammaging<sup>28</sup>. Importantly, naïve T-cell activation can occur independent of viral antigen encounters, such as through the interaction with neo-antigens (e.g., LDL-C)<sup>51-53</sup>.

In this regard, T-cells from atherosclerotic mice immunized with oxidized LDL-C were activated in response to LDL-C exposure by APC, but not oxidized LDL-C exposure<sup>53</sup>. The recognition of LDL-C as a neo-antigen may depend on the T-cell subtype being exposed. For example, exogenous LDL-C treatment inhibited V $\gamma$ 9V $\delta$ 2 T cell activation<sup>75</sup>. V $\gamma$ 9V $\delta$ 2 T cells do not require MHC antigen presentation or co-stimulation, and function as both innate and adaptive immune cells acting as APCs<sup>76</sup>. They are also one of the least abundant T-cells in humans,<sup>77</sup> and given their different activation pathway, their reactivity to LDL-C may not represent that of the more abundant  $\alpha\beta$  T-cell lineage. As endogenous LDL-C increases with aging<sup>57,58</sup>, it may be that increased endogenous LDL-C in mid-life contributes to the accumulation of activated memory T-cells, via repetitive T-cell activation. Over time, repeated activation leads to senescent T-cells with a shift towards a more pro-inflammatory phenotype and inflammaging<sup>28,37,38,54-56</sup>.

### 1.3.2 T-cell Senescence

For the purposes of this review, T-cell senescence will be defined as age-related T-cell dysregulation because of a build-up of terminally differentiated T-cells<sup>28,55</sup>. Senescent T-cells produce and secrete a greater amount of pro-inflammatory cytokines, exhibit increased mitochondrial dysfunction, and also become less responsive to stimulation resulting in decreased proliferation<sup>28,55</sup>. As previously mentioned, T-cell senescence is a result of repetitive activation resulting in telomere shortening (e.g., replicative senescence); however, T-cell senescence can also be induced by cellular stress from other external stresses, such as pre-mature senescence caused by T<sub>REG</sub> signaling<sup>56</sup>. Effector memory and terminally differentiated T-cells exhibit the greatest proportion of senescent cells compared to naïve and central memory T-cells<sup>78</sup>. It appears that certain T-cell subtypes have more resilience against senescence, for example CD4<sup>+</sup> T<sub>H</sub> appear resist senescence more than CD8<sup>+</sup> T<sub>C</sub><sup>28</sup>. Aging increased the populations of pro-inflammatory and cytotoxic CD4<sup>+</sup> T<sub>H</sub> cells, mimicking a phenotype similar to CD8<sup>+</sup> T<sub>C</sub><sup>37</sup>. Additionally, aging also appears to increase TH17 cells, which are a pro-inflammatory type of CD4<sup>+</sup> T<sub>H</sub> and a decrease in anti-inflammatory CD4<sup>+</sup> T<sub>REG</sub><sup>38</sup>. Mittlebrunn and Kroemer., (2021) argue that the resilience to senescence that CD4<sup>+</sup> T<sub>H</sub> exhibit might be due to the higher oxidative capacity of CD4<sup>+</sup> T<sub>H</sub> compared to CD8<sup>+</sup> T<sub>C</sub><sup>28</sup>. Indeed, impairing oxidative phosphorylation in CD4<sup>+</sup> T<sub>H</sub> induced wide-spread premature senescence in young mice and the T-cells from these mice exhibited a pro-inflammatory phenotype similar to that of aged mice, which led to an increase in systemic inflammation<sup>42</sup>.

### 1.3.3 T-cell Mitochondrial Function

In this review, mitochondrial dysfunction will be defined as the impaired ability for the electron transport chain (ETC) to produce ATP in response to an energetic demand, with a shift towards increased production of reactive oxygen species (ROS) and a decrease in ATP production. Mitochondrial respiration is a measure of the oxygen consumption by the ETC in the mitochondria and is indicative of the mitochondria's ability to produce energy via oxidative phosphorylation. The mitochondria are essential for T-cell function<sup>3</sup>, and are the major organelle responsible for the production of ATP in mammalian cells<sup>79</sup>. The ETC uses the energy stored in electron donors produced by the oxidation of carbohydrates and fats, and protein via in glycolysis, the tricarboxylic acid (TCA) cycle and fatty acid oxidation (Figure. 1.4)<sup>79,80</sup>.

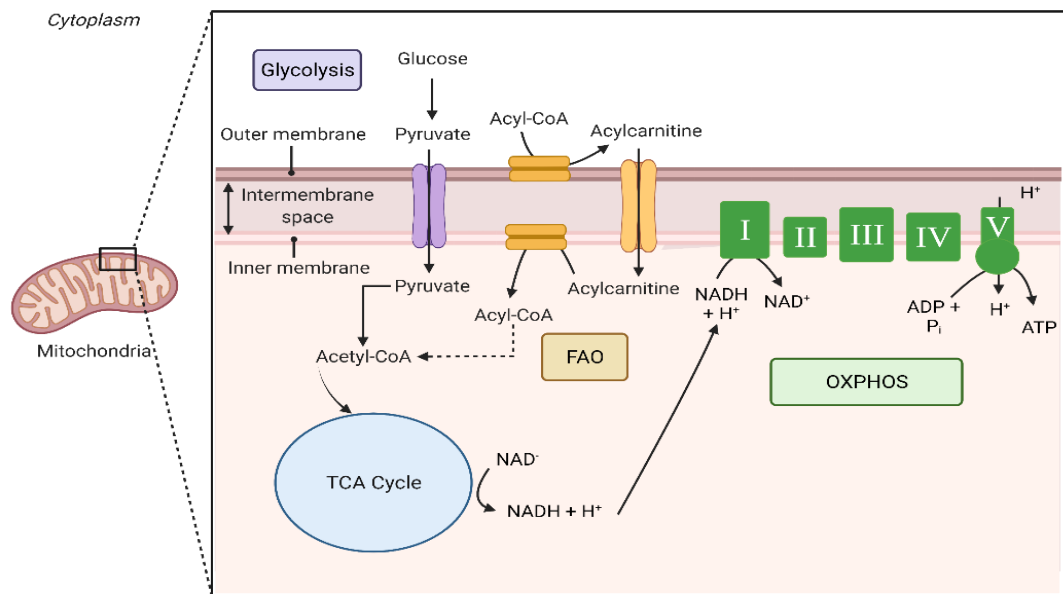


**Figure 1.4.** Cellular Bioenergetics. Adapted and recreated from Nsiah-Sefaa & McKenzie, 2016<sup>2</sup>. Created with BioRender.com. Abbreviations: FOA, fatty acid oxidation; NADH, nicotinamide adenine dinucleotide + hydrogen ion; NAD,

nicotinamide adenine dinucleotide; tricarboxylic acid, TCA; and OXPHOS, oxidative phosphorylation.

The ETC is comprised of four protein complexes (e.g., complex I – complex IV) and two electron carriers in the intermembrane space <sup>79,80</sup>. The electron carriers pass electrons across complexes in the ETC to produce energy to allow for protons to be pumped against their concentration gradient from the mitochondrial membrane into the intermembrane space at complexes I, III, and IV <sup>79,80</sup>. Additionally, the electrons are donated in complex IV convert O<sub>2</sub> to H<sub>2</sub>O to transfer an additional proton for each electron transporter <sup>79,80</sup>. The electrons are supplied by the electron transporters nicotinamide adenine dinucleotide (NADH) and flavin adenine dinucleotide (FADH<sub>2</sub>) that are by-products of the TCA cycle and fatty acid oxidation <sup>79,80</sup>. These electron transporters are then oxidized to NAD<sup>+</sup> and FADH. When the protons are transported against their concentration gradient this creates an electrochemical gradient that causes the F<sub>1</sub> domain of ATP-synthase (e.g., complex V) to act as a rotor <sup>79,80</sup>. The rotation of the F<sub>1</sub> domain of complex V induces a conformational change at binding sites of the F<sub>0</sub> domain, resulting in the phosphorylation of bound ADP to ATP <sup>79,80</sup>. However, oxidative phosphorylation is not always coupled to the production of ATP and can lead to the production of mitochondrial ROS (mtROS). mtROS are produced as a product of mitochondrial respiration <sup>81</sup>, which may act as important signaling molecules <sup>82</sup>. primarily produced at complex I, II, and III <sup>81,83</sup>. Complex I is one of the larger generators of mtROS <sup>83</sup>, and it generates mtROS via multiple mechanism. The first is caused by a reduction in the mitochondrial respiration rate, which causes a buildup of NADH, leading to an increase in the NADH/NAD<sup>+</sup> ratio and a resultant increase in the production of mtROS <sup>83</sup>. Complex I can also produce mtROS via

reverse electron transport, where electrons are shuttled backward in the ETC to complex I because of a change in the proton motor force as a result of low ATP production, and  $\text{NAD}^+$  is reduced to  $\text{NADH}$  <sup>83</sup>. Complexes II and III are also mtROS generators, but the production is generally low under normal physiologic conditions <sup>81,83</sup>. mtROS can also be generated from other mitochondrial enzymes <sup>83</sup>, but this review is mainly concerned with the mtROS production from the ETC complexes. For a more comprehensive review of the mtROS production by the mitochondria, refer to a review by Murphy, (2009) <sup>83</sup>.

T-cell metabolism changes depending on the stage in the life cycle of the T-cell. Naïve T-cells produce most of their energy via oxidative phosphorylation <sup>3,84-86</sup>. Following activation, naïve T-cells proliferate and differentiate into  $T_{\text{EFF}}$  and switch from oxidative to primarily glycolytic metabolism to meet the high energetic demand during proliferation via aerobic glycolysis <sup>3,84,85</sup>. This process is termed the Warburg Effect, where in the presence of oxygen, glucose is metabolized to lactate <sup>84</sup>. However, this is not to say that activated T-cells are entirely glycolytic, because the oxidative phosphorylation is required in early stages of T-cell activation <sup>84,86</sup>. Thus, oxidative metabolism also increases following antigen presentation <sup>84,86</sup>. Similar to naïve T-cells, quiescent memory T-cells primarily utilize fatty acid oxidation and oxidative phosphorylation, but upon activation, they shift predominately towards aerobic glycolysis <sup>84,85</sup>. With aging, cells become senescent, and senescent T-cells have impaired oxidative metabolism resulting in increased mtROS production <sup>85,87</sup>. Senescent cells are also more inflammatory compared to non-senescent cells, and this may be driven, in-part, by mitochondrial dysfunction <sup>3,28,55</sup>. In this regard, pro-inflammatory T-cells tend to utilize glycolytic metabolism, whereas, anti-

inflammatory T-cells utilize more oxidative metabolism<sup>84</sup>. Additionally, promoting oxidative metabolism shifts T-cells to be more anti-inflammatory, whereas conditions that favor glycolysis promotes pro-inflammatory T-cells<sup>3</sup>. It should be noted that mitochondria are essential for many other functions other than energy production in T-cells. These include events such as T-cell activation and effector and memory function, in addition to other functions (Figure 1.5)<sup>3</sup>. More comprehensive reviews on both T-cell metabolism and the role that the mitochondria play in T-cell function can be found here<sup>3,84-87</sup>.

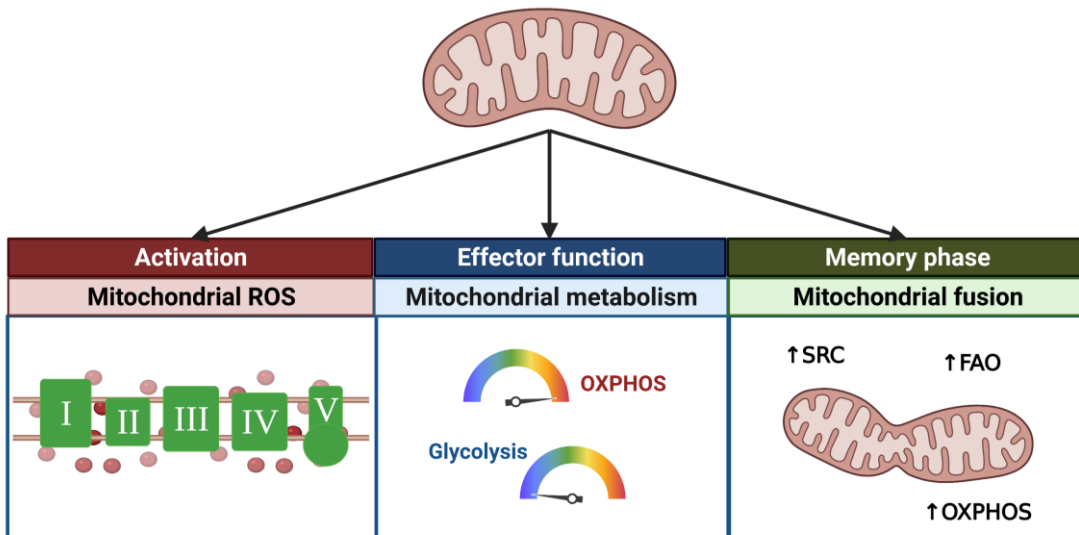


**Figure 1.5.** Mitochondrial Regulation of T-cells. Adapted and recreated from Desdín-Micó, Soto-Heredero, & Mittlebrunn, 2018<sup>3</sup>. Created with BioRender.com. Abbreviations: ROS, reactive oxygen species; SRC, spare respiratory capacity; FOA, fatty acid oxidation; and OXPHOS, oxidative phosphorylation.

Aging appears to induce metabolic changes in T-cells, and has been associated with a decrease mitochondrial respiration in T-cells in both mice and humans <sup>42-44</sup>. However, this is not conclusive across all studies and may depend on the T-cell subtype being studied <sup>88,89</sup>. The decrease in mitochondrial respiration increases pro-inflammatory cytokine production in CD4<sup>+</sup> T<sub>H</sub> <sup>42</sup>, and impairing mitochondrial respiration can induce premature senescence <sup>90</sup>. Despite these data, it is not known what physiological processes with aging induce mitochondrial dysfunction. One explanation might be an increase in endogenous LDL-C that occurs with age. Indeed, our laboratory and others have found that endogenous LDL-C concentration is associated with lower mitochondrial respiration in human peripheral blood mononuclear cells <sup>48,49</sup>, which includes T-cells.

*Ex vivo* data also shows that treatment with exogenous LDL-C impaired ATP-production and decreased mitochondrial DNA and mitochondrial mass in V $\gamma$ 9V $\delta$ 2 T cells, although this was not associated with an increase in ROS or inflammatory cytokine production <sup>75</sup>. Additionally, cholesterol impairs mitochondrial function via several mechanisms in other immune cells, such as macrophages <sup>50</sup>. Unbound - cholesterol in the cell enters the mitochondria, where its metabolism to oxysterol results in a decrease in endogenous antioxidants and an increase in mtROS and oxidative stress, resulting in increased mitochondrial DNA damage and decreased respiration <sup>50</sup>. More mtROS are produced because of the impaired respiration, resulting in a vicious cycle <sup>50</sup>. This cycle is exacerbated by a decrease in antioxidant transport into the mitochondria by the accumulation of cholesterol in mitochondrial membrane <sup>50</sup>. These processes ultimately result in the cell adopting a pro-inflammatory phenotype <sup>50</sup>. Importantly, aging appears to increase the accumulation of

cholesterol in CD4<sup>+</sup> T<sub>H</sub> and CD8<sup>+</sup> T<sub>C</sub><sup>91</sup>, and treatment with exogenous LDL-C increases intracellular cholesterol in Vγ9Vδ2 T cells<sup>75</sup>. Thus, the accumulation of intracellular cholesterol from LDL-C with age may induce mitochondrial dysfunction in T-cells in similar fashion leading to premature senescence.

#### **1.4 The Role of Vascular Dysfunction in Alzheimer's Disease**

The vasculature has recently been recognized to play a causal role in the development of AD<sup>7,8</sup>, including dysfunction in the peripheral<sup>92</sup> and cerebrovasculature<sup>9-16,93-95</sup>. Cerebrovascular dysfunction associated with AD can be characterized by cerebral hypoperfusion<sup>93-95</sup> or reduced reactivity of the cerebral vessels to a stimuli (e.g., cerebrovascular reactivity, CVR) such as an increased partial-pressure of arterial CO<sub>2</sub> (e.g., hypercapnia)<sup>9-16</sup>. For the purposes of this review, the reactivity of the cerebral vessels to hypercapnia will be discussed. Our laboratory has successfully induced hypercapnia using multiple methods to increase cerebral blood flow in adults across the lifespan. Because of our prior experience using the breath-hold assessment, and the sensitivity of breath-hold to detect differences between healthy controls, and patients with pre-clinical and Alzheimer's disease<sup>96</sup>, a breath-hold protocol will be used in this study. There are multiple mechanisms which govern the CVR response to hypercapnia, including smooth muscle cell tone and the function of the endothelium, pericytes, and astrocytes<sup>97</sup>.

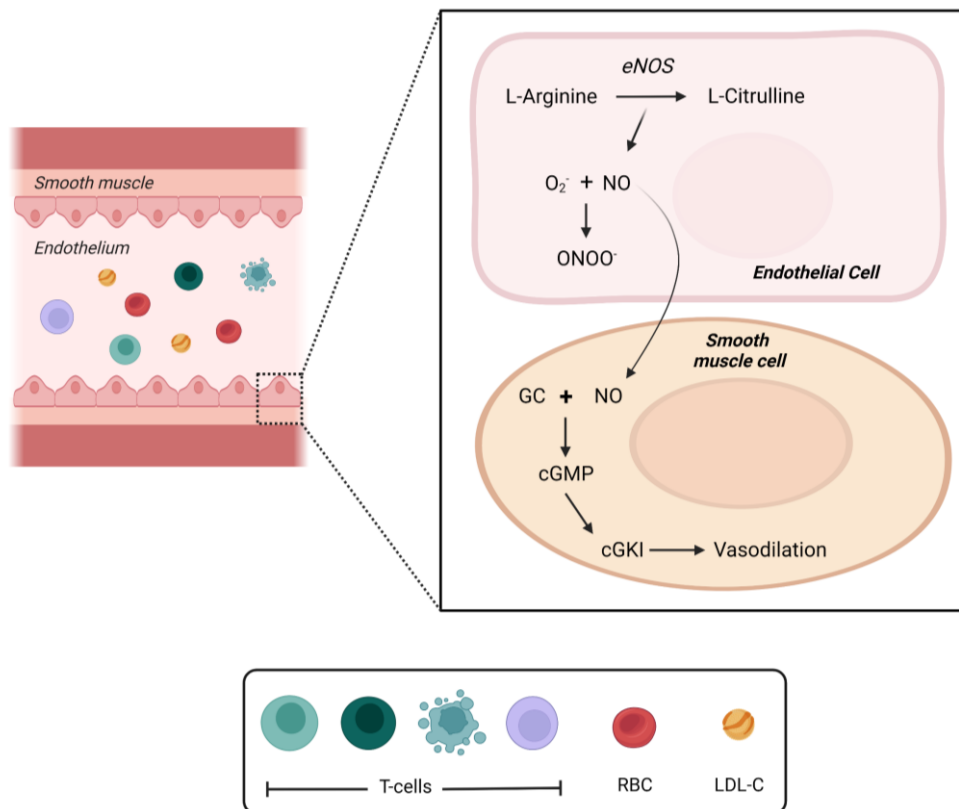


**Figure 1.6.** Muscular Artery Cross-Section and Endothelial Nitric Oxide Production. Created with BioRender.com. Abbreviations: eNOS, endothelial nitric oxide synthase; NO, nitric oxide; GC, guanylyl cyclase; cGMP, cyclic guanosine monophosphate; cGKI, (cGMP)-dependent protein kinase type I; T-cells, T-lymphocytes; RBC, red blood cell; & LDL-C, low-density lipoprotein-cholesterol.

This review will be focused on the role of the endothelium in modulating CVR. The endothelium is a semipermeable single-cell monolayer lining all blood vessels that interacts with the vascular smooth muscle to control several important physiologic functions that maintain vascular homeostasis (Figure 1.6)<sup>98,99</sup> This section will focus on the ability of the endothelium to regulate vascular tone and blood flow in the brain. In this regard, the endothelium plays a critical role in regulating cerebral blood flow and CVR<sup>100</sup>. The endothelium can become dysfunctional, which can result in aberrant cerebrovascular function<sup>100</sup>. Endothelial dysfunction is generally

accepted to be caused by an imbalance of endogenous vasodilators to vasoconstrictors, and is characterized by impaired endothelial-dependent vasodilatory capacity of the blood vessel <sup>101,102</sup>. Nitric oxide (NO) is a major endogenously produced free radical that acts as a vasodilator <sup>99,102</sup>. NO is synthesized by an enzyme called NO synthase (NOS) <sup>99</sup>. There are three NOS enzyme isoforms which include endothelial NOS (eNOS), inducible NOS, and neuronal NOS <sup>99</sup>. In the endothelium, eNOS oxidizes L-arginine to L-citrulline, resulting in the synthesis and release of NO (Figure 1.6) <sup>99</sup>. NO induces vasodilation via the guanylyl cyclase (GC) and cyclic guanosine monophosphate (cGMP)-dependent protein kinase type I (cGKI) pathway <sup>103</sup>. After being synthesized in the endothelium, NO diffuses into the vascular smooth muscle where it interacts with GC to generate cGMP <sup>103</sup>. cGKI is stimulated because of the increased cGMP concentration, resulting in the relaxation of the vascular smooth muscle <sup>103</sup>.

While the extent that NO contributes to sustained CVR is debated, NO appears to be necessary for shear-mediated dilation of larger cerebral vessels <sup>97,104</sup>. Additionally, the production of NO by the endothelium seems to be necessary for maintaining cerebral blood flow <sup>100</sup>. The breath-hold stimulus is also relevant to AD, because people with AD exhibit significantly lower CVR to a 30-second breath-hold <sup>105,106</sup>.

Endothelial dysfunction increases with age, due to an age-related decrease in NO bioavailability and other factors such as reduced L-arginine availability <sup>102</sup>. The decrease in NO bioavailability is caused by the reaction between NO and superoxide radical ( $O_2^-$ ) to form peroxynitrite ( $ONOO^-$ ), or by the reduced abundance and/or uncoupling of eNOS, in addition to other factors <sup>101,102,107</sup>. Normally, the endogenous

antioxidant defense system scavenges for ROS to maintain homeostasis; however, when the concentration of ROS exceeds the capacity of the antioxidant defense system, then this results in oxidative stress<sup>108</sup>. Antioxidants can reduce ROS in multiple ways. Antioxidants will first try to prevent the formation of ROS<sup>109</sup>. An antioxidant like glutathione peroxidase will reduce hydrogen peroxide to water, as an example<sup>109</sup>. Antioxidants will also scavenge for existing ROS and degrade and remove oxidized proteins to prevent their accumulation<sup>109</sup>. ROS have unpaired electrons in the outer valence and oxidize other molecules when they accept electrons, causing other molecules to become unstable<sup>109</sup>. Thus, one way in which antioxidants scavenge for ROS is by reducing them by donating an unpaired electron to ROS to stabilize them<sup>108,109</sup>. As a result, the ROS can no longer act as oxidants.

Nicotinamide adenine dinucleotide phosphate (NADPH) oxidase (NOX) enzymes are major sources of ROS generation<sup>102</sup> via the transfer of electrons to oxygen and the generation of O<sub>2</sub><sup>-</sup> and other ROS downstream of this<sup>110</sup>. NOX activity has been shown to be deleterious for endothelial function, and reducing NOX activity improves endothelial function<sup>102</sup>. The mitochondria are also major sources of ROS generation, with mtROS also being major contributors to endothelial dysfunction<sup>102</sup>. Likewise, reducing mtROS improves endothelial function<sup>102</sup>. There is also evidence that oxidative stress may contribute to inflammaging<sup>102</sup>. Importantly, oxidative stress and the loss of NO impairs cerebrovascular endothelial function and vessel dilation<sup>111</sup>. There are other pathways that contribute to oxidative stress; however, they are outside the scope of this review<sup>102</sup>. In addition to oxidative stress, inflammation also contributes to endothelial dysfunction<sup>102</sup>. Pro-inflammatory cytokines such as interferon- $\gamma$  (INF- $\gamma$ )<sup>112</sup>, tumor necrosis factor- $\alpha$  (TNF- $\alpha$ )<sup>113,114</sup>, interleukin-6 (IL-6)

<sup>114,115</sup> , and interleukin-17 (IL-17) <sup>116</sup> contribute to endothelial dysfunction by altering NO bio-availability and increasing ROS. Whereas anti-inflammatory cytokines, such as interleukin-10 (IL-10) are protective of endothelial function by reducing ROS and the activity of other pro-inflammatory cytokines <sup>117,118</sup> .

## **1.5 The Role of Lymphocytes in Regulating Vascular Function**

### **1.5.1 The Role of B-cells in Regulating Vascular Function**

B-cells have been shown to be important regulators vascular function in age-related cardiac and vascular diseases including hypertension, atherosclerosis, vascular disease, heart failure <sup>119-124</sup> . B-cells may also play a role in regulating endothelial function. For example, Xia et al., 2021 have shown that removing B-cells induced endothelial dysfunction in healthy mice, and that adoptive transfer of naïve B-cells restored endothelial function <sup>63</sup> . The protection conferred by B-cells was thought to be caused by their ability to regulate neutrophil number <sup>63</sup> . However, B-cells may not be entirely protective of endothelium.

B-cells may induce endothelial dysfunction via the secretion of autoantibodies <sup>63</sup> . For example, patients with idiopathic pulmonary hypertension exhibited increased B-cell produced anti-endothelial cell autoantibodies <sup>125</sup> . Patients with peripheral artery disease had increased concentrations of anti-endothelial cell autoantibodies, relative to healthy controls, and endothelial function was lower in those with higher concentrations of autoantibodies <sup>126</sup> . Additionally, patients with Wegener's granulomatosis and systemic lupus erythematosus had elevated concentrations of anti-endothelial cell autoantibodies, resulting in endothelial activation and a pro-

inflammatory phenotype<sup>127,128</sup>. B-cell secreted antibodies have also been shown to reduce endothelial NO production and induce endothelial apoptosis<sup>129,130</sup>.

Additionally, B-cell antibodies in the serum from people infected with the SARS-COV2 virus may also drive endothelial activation and dysfunction<sup>131</sup>. Despite these data, there is a greater preponderance of evidence demonstrating T-cells are important regulators of vascular function. Thus, this study will only focus on the interaction between T-cells and the vasculature.

### **1.5.2 The Role of T-cells in Regulating Vascular Function**

T-cells are important regulators of cardiovascular function in humans. Aberrant T-cell function can result in a pro-inflammatory phenotype that contributes to CVD<sup>34-36</sup>. As previously discussed, the mitochondria in T-cells are essential for regulating normal T-cell function<sup>3,42</sup>. For instance, impaired CD4<sup>+</sup> mitochondrial function led to increased production and secretion of pro-inflammatory cytokines, such as INF- $\gamma$ , TNF- $\alpha$ , and IL-6<sup>42</sup>. As previously discussed, inflammation contributes to impaired endothelial function. Indeed, a large body of animal literature exists to show that T-cells modulate endothelial function via increased inflammation and oxidative stress. Thus, the following section will discuss the role that T-cells play in regulating endothelial function.

Guzik et al., (2007) showed that mice bred to lack both B-and T-cells (RAG1<sup>-/-</sup>) are protected from angiotensin-II induced (ANG-II) endothelial dysfunction<sup>132</sup>. ANG-II induces hypertension through multiple mechanisms, including increased vasoconstriction, oxidative stress, sympathetic activity, and renal sodium reabsorption<sup>133,134</sup>. Additionally, these knockout mice had significantly lower aortic superoxide

production in response to ANG-II and desoxycorticosterone acetate (DOCA)-salt infusion compared to control mice<sup>132</sup>. The DOCA-salt hypertension model is ANG-II independent and induces hypertension via aldosterone mediated sodium reabsorption and by increasing oxidative stress, in addition to other mechanisms<sup>135</sup>. Further experiments showed that the observed endothelial protection was caused specifically by T-cell depletion. In this regard, T-cell adoptive transfer into RAG1<sup>-/-</sup> mice treated with ANG-II restored the aortic production of superoxide, and abolished the endothelial protection conferred by lymphocyte depletion<sup>132</sup>. However, the adoptive transfer of B-cells had no effect on aortic O<sub>2</sub><sup>-</sup> production<sup>132</sup>. In addition to the production of O<sub>2</sub><sup>-</sup>, T-cell mediated inflammation may also have contributed to the ANG-II induced endothelial dysfunction. ANG-II infusions increased T-cell O<sub>2</sub><sup>-</sup> production, and *in vitro* T-cell activation significantly increased TNF- $\alpha$  concentrations<sup>132</sup>. Blocking the TNF- $\alpha$  receptor *in vivo* prevented the hypertensive (HT) response and increased aortic O<sub>2</sub><sup>-</sup> production in response to ANG-II<sup>132</sup>. T-cell activation to ANG-II was only increased when T-cells were co-incubated with ANG-II and anti-CD3, and this effect was negated with the addition of an NADPH oxidase inhibitor<sup>132</sup>.

The effect of T-cells on endothelial function may be dependent on the T-cell subtype. For instance, Guzik et al., (2007) found in mice that the number of CD4<sup>+</sup> T<sub>EFF</sub> was increased in the ANG-II mouse model of hypertension<sup>132</sup>. In this regard, Barhoumi et al., (2011) found in mice that the adoptive transfer of CD4<sup>+</sup> T<sub>REG</sub> in mice protected the endothelium from ANG-II more so than the adoptive transfer of CD4<sup>+</sup> T<sub>EFF</sub><sup>136</sup>. This protection was likely provided via the production of NO, as the infusion of NG-nitro-L-arginine methyl ester (L-NAME) abolished the dilatory response to acetylcholine following the adoptive transfer of either cell type<sup>136</sup>. L-NAME works by

blocking NO production by inhibiting the three NOS isoforms<sup>137</sup>. The adoptive transfer of only CD4<sup>+</sup> T<sub>REG</sub> also prevented increases in vascular cell adhesion molecule 1<sup>136</sup>, a marker of endothelial dysfunction<sup>138</sup>. Importantly, the adoptive transfer of CD4<sup>+</sup> T<sub>REG</sub>, but not CD4<sup>+</sup> T<sub>EFF</sub>, prevented increases in oxidative stress in cardiac tissue in response to ANG-II, as evidenced by the reduced NADPH oxidase activity<sup>136</sup>. This may explain why the adoptive transfer of CD4<sup>+</sup> T<sub>REG</sub> promoted greater endothelial protection compared to CD4<sup>+</sup> T<sub>EFF</sub>.

Barhoumi et al., (2011) also showed that the adoptive transfer of only CD4<sup>+</sup> T<sub>REG</sub> may also reduce inflammation in response to ANG-II. The adoptive transfer of CD4<sup>+</sup> T<sub>REG</sub> prevented a significant increase in circulating inflammation, as evidenced by reduced inflammatory cytokines produced in response to ANG-II<sup>136</sup>. In accordance with these data, Kassan et al., (2011) showed that endothelial function was preserved in ANG-II hypertension in mesenteric arteries that were incubated with media conditioned by CD4<sup>+</sup> T<sub>REG</sub>, but not control media<sup>139</sup>. This protection is conferred specifically by CD4<sup>+</sup> T<sub>REG</sub>, as the same effect was not seen when the arteries were incubated with conditioned with CD4<sup>-</sup> T-cells<sup>139</sup>. These results were also seen in coronary arteries of ANG-II HT mice, where the adoptive transfer of CD4<sup>+</sup> T<sub>REG</sub> preserved endothelial function in an NO-dependent manner<sup>140</sup>. The HT mice that received the adoptive transfer of CD4<sup>+</sup> T<sub>REG</sub> had preserved eNOS activation, as evidenced by preserved phosphorylated eNOS<sup>140</sup>. These HT mice also had elevated concentrations of cardiac TNF- $\alpha$  and increased expression of ICAM and vascular cell adhesion molecule in the coronary arteries, which were not elevated in mice that received the CD4<sup>+</sup> T<sub>REG</sub> adoptive transfer<sup>140</sup>. Radwan et al., (2019) confirmed the endothelial protective role that CD4<sup>+</sup> T<sub>REG</sub> play in hypertension. They showed that the

adoptive transfer of CD4<sup>+</sup> T<sub>REG</sub> in ANG-II HT mice preserved mesenteric resistance artery endothelial function <sup>141</sup>. This was likely due to an upregulation of NADPH isoforms NOX2 and NOX4 <sup>142</sup> and increased NADPH oxidase activity in mesenteric resistance arteries from the HT mice, which was attenuated with the adoptive transfer of CD4<sup>+</sup> T<sub>REG</sub> <sup>141</sup>. The adoptive transfer of CD4<sup>+</sup> T<sub>REG</sub> also preserved eNOS and AKT activity <sup>141</sup>, the latter of which is a protein that is critical for vascular function (e.g., vasodilation) <sup>143</sup>. The adoptive transfer of CD4<sup>+</sup> T<sub>REG</sub> also protect mesenteric artery endothelial function in an NO-dependent manner in an aldosterone model of mice hypertension <sup>144</sup>.

CD4<sup>+</sup> T<sub>REG</sub> adoptive transfer also prevented increases in NADPH oxidase in the aorta and the heart of the mice <sup>144</sup>, although the adoptive transfer was not able to prevent against increases in vascular cell adhesion molecule 1 <sup>144</sup>.

CD4<sup>+</sup> T<sub>REG</sub> may confer their protection via the production of anti-inflammatory cytokine IL-10. The HT mice that received the adoptive transfer of CD4<sup>+</sup> T<sub>REG</sub> had preserved plasma IL-10, whereas plasma IL-10 concentrations were reduced in the HT mice that did not receive the adoptive transfer <sup>140</sup>. Furthermore, blocking IL-10 in mesenteric arteries from HT mice that were incubated with the CD4<sup>+</sup> T<sub>REG</sub> conditioned media with IL-10 specific antibodies or receptor blockage abolished the protective effect, and this also elevated NADPH oxidase activity <sup>139</sup>. Additionally, treating mesenteric resistance arteries from HT mice with IL-10 significantly reduced NADPH oxidase activity after at least 30-minutes <sup>139</sup>. These results were confirmed *in vivo*. ANG-II HT mice that were treated with IL-10 for 2-weeks had preserved mesenteric endothelial function in an NO-dependent manner <sup>139</sup>. The mesenteric arteries from HT mice that received the IL-10 treatment also had significantly lower NADPH oxidase

activity and increased eNOS activation <sup>139</sup>. Additionally, Radwan et al., 2019 showed that mesenteric arteries from HT mice had decreased IL-10 and increased TNF- $\alpha$  and IL-6, and mice that received the adoptive transfer with CD4<sup>+</sup> T<sub>REG</sub> were protected from these changes <sup>141</sup>.

CD8<sup>+</sup> T<sub>C</sub> have also been shown to negatively affect endothelial function and blood pressure. In this regard, knocking out CD8<sup>+</sup> T<sub>C</sub> in ANG-II HT mice preserved endothelial function, whereas knocking out CD4<sup>+</sup> T<sub>H</sub> did not <sup>145</sup>. Additionally, CD4<sup>-/-</sup>, but not CD8<sup>-/-</sup> mice exhibited a HT response to ANG-II infusion <sup>145</sup>. In middle-aged adults humans (aged 51.6  $\pm$  11.2 years, mean  $\pm$  STD), it has also been shown that HT patients have elevated concentrations of senescent CD8<sup>+</sup> T<sub>C</sub>, and CD8<sup>+</sup> T<sub>C</sub> were more likely to produce pro-inflammatory cytokines TNF- $\alpha$  and IFN- $\gamma$  <sup>146</sup>. Additionally, a higher proportion of senescent CD8<sup>+</sup> T<sub>C</sub> was associated with increased arterial stiffness in middle-aged adults humans (aged 59.4  $\pm$  11.7 years, mean  $\pm$  STD), and these cells secreted a greater amount of INF- $\gamma$  and TNF- $\alpha$  when stimulated <sup>147</sup>. RAG1<sup>-/-</sup> mice that had pan T-cells (both CD4<sup>+</sup> and CD8<sup>+</sup>) or CD8<sup>+</sup> T<sub>C</sub> T-cells adoptively transferred had a significantly elevated systolic and diastolic blood pressure response to ANG-II <sup>145</sup>. Whereas, the RAG1<sup>-/-</sup> mice that received the adoptive transfer of CD4<sup>+</sup> T<sub>REG</sub> did not exhibit a blood pressure response to ANG-II, similar to that of the control mice that did not receive an adoptive transfer of cells <sup>145</sup>. Furthermore, the adoptive transfer of CD4<sup>+</sup> T<sub>REG</sub> in wild-type mice abolished the HT response in response to ANG-II <sup>145</sup>. While CD4<sup>+</sup> T<sub>REG</sub> might be protective under most circumstances, some CD4<sup>+</sup> T<sub>H</sub> cells subsets may contribute to hypertension. For instance, HT adults had significantly elevated proportions of TH1 and TH17 T-cells, that was accompanied by increased concentrations of IL17 and INF- $\gamma$  <sup>148</sup>. Many other studies have shown that

either knocking out pan lymphocytes (RAG1<sup>-/-</sup>) in mice or rats<sup>132,149</sup>, removing functional lymphocytes in mice (e.g., severe combined immunodeficiency, SCID), or the adoptive transfer of CD4<sup>+</sup> T<sub>REG</sub><sup>136,140,150</sup>, but not CD4<sup>+</sup> T<sub>EFF</sub> in mice preserves blood pressure<sup>136,144</sup>, likely via IL-10<sup>139</sup>. It should be noted that some studies did not observe a protective effect of the adoptive T-cell transfer on blood pressure, although this may be due to the number of adoptive transfers that the mice received<sup>141,151</sup>.

Thus, the evidence seems to indicate that CD4<sup>+</sup> T<sub>H</sub>, specifically CD4<sup>+</sup> T<sub>REG</sub> are protective of the endothelium, whereas CD8<sup>+</sup> T<sub>C</sub> and CD4<sup>+</sup> T<sub>EFF</sub>, such as TH1 and TH17 CD4<sup>+</sup> T<sub>H</sub> may be damaging to the endothelium. These effects on the endothelium are likely mediated by changes in oxidative stress, inflammation, and NO production, amongst others. This makes sense considering that CD8<sup>+</sup> T<sub>C</sub> and certain CD4<sup>+</sup> T<sub>EFF</sub> subtypes (TH1 & TH17) are more pro-inflammatory than the immunosuppressive CD4<sup>+</sup> T<sub>REG</sub><sup>152</sup>. Despite this, whether the effect on the endothelium is inherent to the type of T-cell or whether the function of the cell is altered via other factors has not been fully elucidated. Radwan et al., (2019) showed that processes such as autophagy and apoptosis may regulate CD4<sup>+</sup> T<sub>REG</sub> function; however, whether other processes such as aging or other cardiometabolic risk factors affect T-cell function and whether these processes also affect other CD4<sup>+</sup> T<sub>H</sub> or CD8<sup>+</sup> T<sub>C</sub> subtypes remains to be elucidated.

### **1.5.2.1 The Effect of Cardiometabolic Risk Factors on T-cell Function and the Implications for Vascular Function**

Stokes, Gurwara, and Granger., (2007) showed that hypercholesterolemia may alter the inflammatory phenotype of T-cells, resulting in impaired endothelial function

<sup>153</sup>. Placing SCID mice on a high cholesterol diet did not induce endothelial dysfunction, as it did in the wild-type mice <sup>153</sup>. However, the injection of T-cells from wild-type into SCID mice on the high cholesterol diet 10-days before the measurements induced endothelial dysfunction <sup>153</sup>. This dysfunction was likely mediated by the production of INF- $\gamma$  by T-cells <sup>153</sup>. The injection of T-cells from wild-type mice on a high cholesterol diet induced endothelial dysfunction in an INF- $\gamma$ <sup>-/-</sup> mouse model where endothelial function was preserved on a high fat diet <sup>153</sup>.

Zhou, Stemme, & Hansson., (1996) showed that CD4<sup>+</sup> T-cells infiltrated atherosclerotic lesions in atherosclerotic mice (APOE<sup>-/-</sup>) fed a high-fat diet, whereas CD8<sup>+</sup> T<sub>C</sub> did not <sup>154</sup>. As stated earlier, endothelial dysfunction precedes the development of atherosclerosis <sup>66,67</sup>, so while not tested, it is likely these mice developed endothelial dysfunction in tandem with atherosclerosis. These findings were expanded upon in 2000, by Zhou et al., where they found that crossing APOE<sup>-/-</sup> mice with immunodeficient SCID mice, significantly reduced atherosclerotic lesions, compared with control APOE<sup>-/-</sup> mice with functional lymphocytes suggesting that T-cells play an important role in the develop of atherosclerosis in the APOE<sup>-/-</sup> model <sup>155</sup>. Furthermore, the adoptive transfer of CD4<sup>+</sup> T<sub>H</sub> from APOE<sup>-/-</sup> into the APOE<sup>-/-</sup> SCID mice significantly increased the number of atherosclerotic lesions and T-cell infiltration into the lesions <sup>155</sup>. The authors speculate that TH1 CD4<sup>+</sup> T<sub>H</sub> were primarily responsible for the development of the atherosclerotic lesions, because the mice had increased IFN- $\gamma$  concentrations, which is produced by TH1 CD4<sup>+</sup> T<sub>H</sub> <sup>155</sup>. Although IFN- $\gamma$  concentrations were correlated with lesion size and the increase in IFN- $\gamma$  was quite large (~8x), the authors admit that the increase was not significantly different from the APOE<sup>-/-</sup> control mice <sup>155</sup>. Thus, one should be hesitant to conclude

this effect was mediated solely by TH1 CD4<sup>+</sup> T<sub>H</sub>. George et al., (2000) immunized an atherosclerotic mouse model (LDL-receptor deficient mice) against an autoantigen found in atherosclerotic lesions to create T-cells that were reactive to this autoantigen<sup>156</sup>. These activated T-cells were then injected into control LDL-receptor deficient mice that were fed a high-fat diet<sup>156</sup>. The mice injected with the activated T-cells had significantly larger atherosclerotic lesions, compared to the control mice<sup>156</sup>. Importantly, the injection of T-cell depleted lymphocytes did not induce the same atherosclerotic lesion formation<sup>156</sup>. These effects were likely also mediated by TH1 CD4<sup>+</sup> T<sub>H</sub>, as the activated T-cells also secreted more IFN- $\gamma$  compared to the control mice<sup>156</sup>.

Mor et al., (2007) showed that in a model of atherosclerosis, 6-month old mice with atherosclerosis have a significantly lower number of CD4<sup>+</sup> T<sub>REG</sub> cells, compared to 3-month old APOE<sup>-/-</sup> mice<sup>157</sup>. Because oxidized low-density lipoprotein cholesterol (oxLDL-C) is a primary cause of atherosclerosis<sup>158</sup>, the authors tested whether oxLDL-C affects T-cell number. They found that treating T-cells from APOE<sup>-/-</sup> mice with oxLDL-C significantly reduced CD4<sup>+</sup> T<sub>REG</sub>, but not CD4<sup>+</sup> T<sub>EFF</sub> number<sup>157</sup>. The ability of CD4<sup>+</sup> T<sub>REG</sub> cell to regulate the activity of cytotoxic immune cells, such as CD4<sup>+</sup> T<sub>EFF</sub> was also reduced following the treatment with oxLDL-C in T-cells from APOE<sup>-/-</sup>, but not wild-type mice<sup>157</sup>. Lastly, the authors found that the adoptive transfer of CD4<sup>+</sup> T<sub>REG</sub> from APOE<sup>-/-</sup> mice led to a significant reduction in atherosclerosis, while this same effect was not shown with the adoptive transfer of CD4<sup>+</sup> T<sub>EFF</sub><sup>157</sup>. Importantly, the reduction in atherosclerosis might have been mediated by the production of IL-10 from CD4<sup>+</sup> T<sub>REG</sub> cell<sup>157</sup>.

Following the consumption of a high-fructose solution for 4-weeks, DAHL salt-sensitive HT rats had significantly increased the proportion of TH17 T-cells and increased IL-17 concentrations, compared to control salt-sensitive rats. Whereas, salt-resistant normotensive rats had a significantly higher proportion of CD4<sup>+</sup> T<sub>REG</sub> and significantly lower concentration of IL-17<sup>159</sup>, compared to control salt-sensitive rats. Both the control and fructose fed salt resistant rats had higher concentrations of IL-10, which may indicate that IL-10 is protective against hypertension<sup>159</sup>. Injecting activated TH17 T-cells from DAHL salt-sensitive rats fed a high-fructose solution significantly increased blood pressure in DAHL salt-sensitive rats, compared with the injection of TH17 T-cells from salt sensitive rats that received tap water<sup>159</sup>. The injection of TH17 T-cells from HT DAHL rats fed a high fructose solution did not elicit a HT response in the salt-resistant rats<sup>159</sup>. Although, the concentration of IL17 was increased in both salt-sensitive and salt-resistant rats that received the injection of TH17 T-cells from HT DAHL rats given a high fructose solution<sup>159</sup>. The concentration of IL-10 was significantly higher in the salt-resistant rats, compared to the salt-sensitive rats<sup>159</sup>. Additionally, salt-sensitive rats that received the injection of TH17 T-cells from HT DAHL rats given a high fructose solution had significantly higher proportion of TH17 cells, compared to salt-sensitive rats that received the injection of control TH17 T-cells<sup>159</sup>.

In addition to atherosclerotic risk factors, non-modifiable cardiometabolic risk factors such as aging also affect T-cell function, which is detrimental to the vasculature. Trott et al., (2021) and Kim et al., (2021) showed that aging in animal models is detrimental to vascular function by altering T-cell function<sup>160,161</sup>. Kim et al., (2021) investigated the role that TH17 CD4<sup>+</sup> T<sub>EFF</sub> in the development of spontaneous

HT (SHR) in rats <sup>161</sup>. At 15-weeks, the spontaneously HT rats (SHR) had significantly elevated blood pressure compared to the control rats <sup>161</sup>. The SHR rats also had a greater proportion of TH17 CD4<sup>+</sup> T<sub>EFF</sub>, and a lower proportion of CD4<sup>+</sup> T<sub>REG</sub> at 15-weeks, compared to the control rats <sup>161</sup>. Kim et al., (2021) then injected both young SHR and control rats with TH17 CD4<sup>+</sup> T<sub>EFF</sub> from adult SHR to determine whether TH17 CD4<sup>+</sup> T<sub>EFF</sub> can induce HT in young rats <sup>161</sup>. The injection of TH17 CD4<sup>+</sup> T<sub>EFF</sub> into young SHR rats induced HT and increased TH17 CD4<sup>+</sup> T<sub>EFF</sub> and CD4<sup>+</sup> T<sub>REG</sub>, compared to the vehicle control <sup>161</sup>. There was no change in blood pressure in the young control rats, despite an increase in TH17 CD4<sup>+</sup> T<sub>EFF</sub> <sup>161</sup>. Trott et al., (2021) showed that T-cells also regulate vascular aging and age-related endothelial dysfunction. Compared to young mice, old mice had an increased proportion of INF- $\gamma$  producing CD4<sup>+</sup> T<sub>H</sub> and CD8<sup>+</sup> T<sub>C</sub> infiltrating aorta <sup>160</sup>. The old mice also exhibited an increased proportion of TNF- $\alpha$  producing CD8<sup>+</sup>, but not CD4<sup>+</sup> T<sub>H</sub> accumulating in the aorta, compared to young control mice <sup>160</sup>. Importantly, the aged mice had a greater proportion of immunosenescent CD8<sup>+</sup> cells, whereas the young mice did not <sup>160</sup>.

Next the authors depleted pan T-cells from young and old mice using anti-CD3 F(ab')<sub>2</sub> fragments compared to a vehicle control (e.g, matched regimen of isotype control F(ab')<sub>2</sub> fragments) <sup>160</sup>. Endothelial function was significantly impaired in the mesenteric resistance arteries from old mice, and the depletion of pan T-cells preserved endothelial function in the old mice, but there was no effect in the arteries from the young mice <sup>160</sup>. This preservation was found to be NO-dependent, as the treatment with L-NAME abolished the protective effect of the pan T-cell depletion <sup>160</sup>. The protective effect of the T-cell depletion with aging was also likely due to a decrease in superoxide, as the treatment with the superoxide scavenger 4-hydroxy-

2,2,6,6-tetramethylpiperidine-1-oxyl (TEMPOL) improved endothelial function in the old control mice, but not the old pan T-cell depleted mice<sup>160</sup>. TEMPOL improves NO bioavailability by decreasing oxidative stress<sup>162</sup>. Importantly, the co-treatment of the mesenteric arteries from old control mice with L-NAME and TEMPOL showed that scavenging for superoxide improved endothelial function in an NO-dependent manner, because the co-treatment abolished the protection conferred by the TEMPOL treatment<sup>160</sup>. Lastly, the authors showed that old RAG1<sup>-/-</sup> mice have preserved endothelial function, compared to old control mice<sup>160</sup>. This was likely because NO bioavailability in the RAG1<sup>-/-</sup> mice was preserved with age<sup>160</sup>. But, as the authors point out, RAG1<sup>-/-</sup> mice also lack B-cells, so the possibility that B-cell depletion also contributed to the preservation of endothelial function cannot be discounted<sup>160</sup>.

While some studies have shown that cerebrovascular function is correlated with peripheral endothelial function<sup>163,164</sup> in specific populations in humans, the preponderance of evidences seems to indicate that cerebrovascular function is not correlated to peripheral endothelial function.<sup>165-169</sup> However, despite these data, considering vasodilation in both arteries are mediated to some extent by endothelial NO<sup>97,170,171</sup>, it is likely that T-cells may influence cerebrovascular endothelial function by regulating NO bioavailability, inflammation, and oxidative stress. Indeed, Lulita et al., (2019) showed that the adoptive transfer of CD4<sup>+</sup> T<sub>REG</sub> preserved cerebrovascular endothelial function and prevented systemic inflammation (e.g., TNF- $\alpha$  & IL-6) and increased cerebral superoxide and TH1 responses in ANG-II HT mice<sup>39</sup>. These effects were likely, in part, mediated by IL-10, as transferring CD4<sup>+</sup> T<sub>REG</sub> from IL-10 deficient mice into ANG-II HT mice did not result in preserved cerebrovascular endothelial function<sup>39</sup>. Furthermore, transferring IL-10<sup>-/-</sup> CD4<sup>+</sup> T<sub>REG</sub>, resulted in an

increase in pro-inflammatory cytokines and TH1 activity in ANG-II HT mice<sup>39</sup>. Although, the infusion of IL-10 in ANG-II HT mice did not preserve cerebrovascular endothelial function, thus the protective effect of CD4<sup>+</sup> T<sub>REG</sub> is likely mediated by a combination of factors<sup>39</sup>. T-cells have also been shown to be modulators of other cerebrovascular disorders. For instance, CD4<sup>+</sup> T<sub>REG</sub> were shown to be protective against brain damage in a mouse model of ischemic stroke by reducing the disruption of the BBB and inflammation and regulating the function of other leukocytes<sup>40,41</sup>. Some of these protective effects may be conferred by CD4<sup>+</sup> T<sub>REG</sub> production of IL-10, but more so in later stages of ischemia<sup>40,41</sup>. Despite these data, more studies are needed examining the role of T-cells and cerebrovascular function, especially in humans.

## **1.6 Summary**

Animal literature has shown that lymphocytes in adaptive immune system (e.g., B-cells and T-cells) are a regulator of vascular function. A larger body of literature exists to show that T-cells are greater regulators of vascular function, compared to B-cells. For instance, aging and LDL-C can induce T-cell metabolic dysfunction, resulting in a pro-inflammatory phenotype that can cause vascular dysfunction in animal models. While no direct evidence exists in humans to show that T-cells regulate vascular function, the large body of literature in animal models makes this likely and worth investigating. Additionally, whether T-cells are related to cerebrovascular function in humans and whether higher physiologic concentrations of LDL-C impair human CD4<sup>+</sup> and CD8<sup>+</sup> T-cell function are not known. Thus, in humans it would seem plausible that the accumulation of cardiometabolic risk factors

(e.g., elevated LDL-C) in combination with advancing age would cause T-cells to become more dysfunctional (e.g., increased activation, senescence, and mitochondrial dysfunction). Dysfunctional T-cells, in turn, become more pro-inflammatory and produce more ROS, both of which contribute to vascular dysfunction and increase risk for cardio- and cerebrovascular diseases. Considering that endogenous LDL-C concentrations begin to peak in mid-life<sup>57,58</sup>, and midlife cardiometabolic risk factors<sup>18-22</sup> and cerebrovascular dysfunction<sup>9-16</sup> are both strong predictors of late-life AD, it is important to study T-cell dysfunction in the context of mid-life cardiometabolic aging for the prevention of AD. Thus, T-cells may be a novel therapeutic target for the prevention and/or treatment of AD<sup>32,33</sup>.

## Chapter 2

### THE ASSOCIATION BETWEEN T-CELL AND CEREBROVASCULAR FUNCTION IN MID-LIFE ADULTS.

#### 2.1 Introduction

6.7 million Americans have been diagnosed with Alzheimer's disease (AD) in 2023, and this number is expected to increase by more than 50% in 2060<sup>172</sup>. Impaired cerebral blood flow and cerebral blood flow regulation (i.e., cerebrovascular dysfunction) is associated with and a risk factor for Alzheimer's Disease<sup>9-16</sup>. Age-related processes such as inflammation and oxidative stress contribute to cerebrovascular dysfunction<sup>173,174</sup>. Aging is associated with a chronic state of low-grade, sterile inflammation beginning in mid-life, termed inflammaging<sup>24-26</sup>. Adaptive immune cells such as T-lymphocytes (T-cells) are implicated in the development of inflammaging<sup>28,29</sup> and the pathogenesis of AD<sup>32,33</sup>, which has implications for cerebrovascular function. Various animal models have shown that T-cells are important for regulating cerebrovascular function by modulating inflammation and oxidative stress<sup>39-41</sup>. While CD8<sup>+</sup> T-cells are deleterious for vascular function<sup>145,160,175,176</sup>, CD4<sup>+</sup> T-cells have been shown to be protective of cerebrovascular function. For example, injecting hypertensive mice with regulatory CD4<sup>+</sup> T-cells (CD4<sup>+</sup> T<sub>REG</sub>) prevented decreases in cerebrovascular function and increases in systemic inflammation (e.g., TNF- $\alpha$  & IL-6) and cerebral superoxide and inflammatory T-cell responses<sup>39</sup>. Injection of CD4<sup>+</sup> T<sub>REG</sub> also protected against blood brain barrier damage and inflammation in a mouse model of ischemic stroke, in part by regulating the responses of other immune cells<sup>40,41</sup>.

T-cells become dysfunctional with aging resulting in a pro-inflammatory phenotype due to factors such as mitochondrial dysfunction<sup>28,177</sup>, and shifts in metabolic function can dictate the inflammatory phenotype of the cell<sup>3,28</sup>. For instance, a shift towards oxidative phosphorylation promotes an anti-inflammatory phenotype; whereas a shift towards glycolysis promotes a pro-inflammatory phenotype<sup>3,28</sup>. Mitochondrial dysfunction contributes to oxidative stress through the generation of reactive oxygen species (ROS), a process which exacerbates inflammation<sup>102</sup>. Mitochondrial function can be assessed by measuring mitochondrial respiration using extracellular flux analysis (Seahorse Real-Time Cell Metabolic Analysis, Agilent). In healthy-controls and patients with early stage heart failure, mitochondrial respiration in peripheral blood mononuclear cells (PBMCs) containing T-cells has been negatively associated with blood pressure and markers of inflammation<sup>48</sup>, and data from our lab suggests a potential negative relation between multiple measures of PBMC mitochondrial respiration and systolic blood pressure<sup>49</sup>.

To our knowledge no studies have investigated the interaction between T-cell mitochondrial respiration and cerebrovascular function in humans. The purpose of this study was to determine whether T-cell mitochondrial respiration was predictive of cerebrovascular function in middle-aged adults. We hypothesized that higher CD4<sup>+</sup> and CD8<sup>+</sup> T-cell OCR and metabolic efficiency would be associated with higher cerebrovascular function, and that higher CD4<sup>+</sup> and CD8<sup>+</sup> T-cell ECAR would be associated with lower cerebrovascular function.

## **2.2 Materials and Methods**

### **2.2.1 Participant Recruitment**

Twenty mid-life adults (aged 50-64 years) with normal endogenous LDL-C concentrations (<150 mg/dL) were recruited. All procedures and protocols used were consistent with the standards set by the latest revisions of the Declaration of Helsinki 1975 (as revised in 1983) and were approved by the Institutional Review Board at the University of Delaware (1753416-6). The study rationale, procedures, risks, and benefits were explained to the participants, and their written or electronic informed consent (REDCap) was obtained before enrollment. Participants were instructed to fast for  $\geq 12$ -hours, to refrain from vigorous aerobic exercise and alcohol for 24-hours, and to refrain from taking over the counter anti-inflammatory medications for 48-hours before each study visit. No study visit took place within 14-days of receiving a vaccination to avoid the influence of any acute inflammatory responses. Participants were not excluded based on race or ethnic background. Participants for this study were recruited through university mailing lists, the Nurse Managed Primary Care Center (NMPCC) study participant registry at the University of Delaware, and by advertising with businesses in the Newark, DE area.

All participants were nonsmokers and free from acute infection (e.g., influenza, COVID-19), systemic medical illness (e.g., CVD, cancer, renal failure), or autoimmune disease (e.g., multiple sclerosis, Type 1 diabetes). Participants were excluded if they did not have normal clinical blood markers and or if they were taking medications likely to affect endogenous lipid concentrations (e.g., statins) or inflammation (e.g., NSAIDs & corticosteroids). Participants were included if they had endogenous LDL-C concentrations  $\leq 150$  mg/dL but were not excluded for other

abnormal blood lipid markers (e.g., high-density lipoprotein, triglycerides, total cholesterol, etc). Participants also completed a medical history questionnaire to determine eligibility.

### **2.2.2 Questionnaires**

Participants were asked to complete a series of questionnaires that were used for screening and as potential co-variables as part of the statistical analyses. Following this, participants completed a sleep questionnaire (Pittsburgh Sleep Quality Index; PSQI)<sup>178</sup> because sleep can affect T-cell populations<sup>179,180</sup> and vascular function<sup>181</sup>. Subjective sleep data are reported as the global sleep score and individual component scores including subjective sleep quality, sleep latency, sleep duration, habitual sleep efficiency, sleep disturbances, use of sleep medications, and daytime dysfunction, which were calculated using the methods described elsewhere<sup>178</sup>. Physical activity was assessed using the Modifiable Activity Questionnaire<sup>182</sup> due its association with mitochondrial function in various cell types, including T-cells<sup>183–185</sup>. Participants were asked to describe any work-related physical activity and report the duration and frequency of all leisure activities performed more than 10 times in the past year. Weekly leisure and work metabolic equivalent (MET) minutes were then calculated using the 2011 Compendium of Physical Activities<sup>186</sup> to determine the participants leisure MET minutes per week. The leisure and work-related MET hours per week were totaled to determine the participants total MET hours per week. Physical activity outcomes were reported as MET hours per week.

Participants were then asked to complete an adapted version of a recent infection questionnaire<sup>187</sup> because antigen stimulation induces metabolic changes in T-cells<sup>84–86</sup>. Participants were asked if they experienced any symptoms for various

types of infections, including general, upper, and lower respiratory, gastro-intestinal, genital, and other types of infections in the past 14 days that lasted longer than 24 hours. If a participant did experience a symptom for any of those categories, then they were the severity (e.g., mild, moderate, or severe) of that symptom. An infection was defined as symptoms lasting for more than 24 hours that participants thought were caused by a recent infection. Finally, a COVID-19 history form was administered to control for previous infection with the SARS-CoV-2 virus, as patients diagnosed with COVID-19 have been reported to have lower PBMC mitochondrial respiration<sup>188</sup> and vascular function<sup>189</sup>. Participants were asked about whether they have previously tested positive for COVID-19, and, if so, they were asked when they last experienced symptoms and to rate the extent to which each symptom interfered with their daily activities on a likert scale of 1-5 (e.g., not at all, a little bit, somewhat, quite a bit, and very much). Participants were then asked how long each symptom lasted, and to rate the severity of their symptoms at their worst (e.g., mild, moderate, severe, and very severe) and the overall interference with performing daily activities (e.g., not a lot, a little bit, somewhat, quite a bit, and very much). These variables were converted to numerical ordinal data on a scale of 1-4, with 4 being the most severe or interfering, respectively. Participants were also asked information about SARS-CoV-2 vaccination status, including the dates of vaccination and the manufacturer of each vaccine.

### **2.2.3 Blood Draw**

Participants were sat in Fowler's position in a stretcher for the blood draw. Blood was drawn from the antecubital vein by a research nurse or a trained member of the research team. 64 mL of blood was drawn for the measures of T-cell mitochondrial respiration in Chapters 2 & 3. An additional 10 mL was drawn for clinical labs that

were processed by LabCorp, including a complete blood count with differential, a comprehensive metabolic panel, and a lipid panel.

#### **2.2.4 Blood Pressure**

Participants rested in semi-recumbent position quietly for 5-minutes with the lights dim and the ambient room temperature at  $22.5 \pm 1.4^{\circ}\text{C}$  (Mean  $\pm$  SD). Blood pressure was measured in the non-dominant arm using a semi-automated oscillometric sphygmomanometer validated by the British Hypertension Society<sup>190</sup> (SunTech ADView 2, SunTech Medical). Multiple recordings were taken until three values were obtained that were within 5 mmHg of one another. The three blood pressures were then averaged to determine resting blood pressure. Two minutes of rest were given between each blood pressure measurement.

#### **2.2.5 Anthropometric Measurements**

Participant height (cm) and mass (kg) were measured using a physician's scale (Health-o-Meter Physician Digital Scale) and were used to calculate body mass index (BMI) using the equation  $\text{BMI} = \text{Weight (kg)} / [\text{Height (cm)}]^2$ .

#### **2.2.6 Peripheral Blood Mononuclear Cell Isolation**

Peripheral blood mononuclear cells (PBMCs) were isolated from whole blood using density gradient centrifugation with SepMate™ -50 PBMC Isolation Tubes (Stemcell Technologies, #8540). Briefly, Sepmate™ tubes were filled with 15 mL histopaque 1077 (Sigma-Aldrich, #SD10771A) and warmed in a  $37^{\circ}\text{C}$  water bath for 10-minutes. Whole blood was diluted 1:1 with 1X phosphate buffered saline (PBS; Corning #21-040-CM) supplemented with 2% fetal bovine serum (FBS; Sigma-Aldrich, # F2442-50ML). Diluted whole blood was pipetted equally on top of pre-

warmed histopaque 1077 in the Sepmate™ tubes. The Sepmate™ tubes were centrifuged at 1200 x G for 10-minutes at room temperature with the acceleration and brake on the highest setting. The top layer was decanted from each Sepmate™ tube into separate fresh 50 mL conical tubes (Corning, #430829). The cell pellet was washed once with 1X PBS and 2% FBS, and the red blood cells were removed using eBioscience™ 1X RBC Lysis Buffer (ThermoFisher, #00-4333-57). The cell pellet was resuspended in the lysis buffer, placed on ice for 5-minutes, and then washed with 1X PBS with 2% FBS. The cells were counted using the Thermo Fisher Countess II Automated Cell Counter and one Countess™ Cell Counting Chamber Slide (ThermoFisher, # C10228), and prepared for the positive T-cell separation.

### **2.2.7 Positive T-cell Separation**

CD4<sup>+</sup> and CD8<sup>+</sup> T-cells were separated from PBMCs using positive magnetic bead separation with the QuadroMACS™ separator (Miltenyi Biotec, #130-091-051) and LS columns (Miltenyi Biotec, #130-042-401). CD8<sup>+</sup> T-cells were separated from the PBMCs using human CD8 MicroBeads (Miltenyi Biotec, #130-045-201) following manufactures protocol and were extracted first because they are less numerous than CD4<sup>+</sup> T-cells in healthy adults <sup>191</sup>. CD4<sup>+</sup> were then isolated from the unlabeled cellular effluent using Human CD4 MicroBeads (Miltenyi BioTec, #130-045-101) per the manufacturers protocol. CD4<sup>+</sup> and CD8<sup>+</sup> T-cells were resuspended in CTS™ AIM-V™ Medium, without phenol red, without antibiotics (ThermoFisher, #A3830801) supplemented with 1x antibiotic-antimycotic (ThermoFisher, #15240062). The cells were placed in the incubator to rest overnight for the assessment of mitochondrial respiration.

### 2.2.8 T-cell Mitochondrial Respirometry

Extracellular flux analysis was used to measure CD4<sup>+</sup> and CD8<sup>+</sup> T-cell mitochondrial respiration using the Seahorse XF Cell Mito Stress Test Kit (Agilent, #103015-100) with the Seahorse XFe96 Analyzer (Agilent) as previously described<sup>49</sup>. Oxygen consumption rate (OCR) was measured at baseline and following three serial injections of 1.5 mM oligomycin, 2 mM carbonyl cyanide-4 (trifluoromethoxy) phenylhydrazone (FCCP), and 0.5 mM rotenone and antimycin A to determine basal and maximal respiration, spare respiratory capacity, coupling efficiency, ATP-linked O<sub>2</sub> consumption, proton leak, and non-mitochondrial O<sub>2</sub> consumption (Fig. 2.1). 2 mM FCCP concentration was determined via FCCP titration experiment. 2 mM was found to produce the greatest increase in respiration without a subsequent decrease (Supplementary Figure 1.1A). In addition to OCR, extracellular acidification rate (ECAR) was calculated as a qualitative measure of glycolysis. The definitions and calculations of the variables obtained from the Mito Stress Test can be found in Appendix A. Prior to the assay cells were resuspended in Seahorse XF RPMI medium, Ph 7.4 (Agilent, # 103576-100) supplemented with 10 mM glucose (Agilent, #103577-100), 1 mM sodium pyruvate (Agilent, #103578-100), and 2 mM glutamine (Agilent, #103579-100), respectively. The cells were seeded into the center 60 wells, as the outer wells are at a greater risk of evaporation<sup>192</sup>. This seeding density was pre-determined from a seeding density titration experiment. There was no difference between a seeding density of 300,000 cells/well and 400,000 cells/well (Supplementary figure 1.1B). Thus, to reduce the amount of blood required, a seeding density of 300,000 cells/well was used.

To account for cellular loss during washes, the seeding density was increased by 5% for a final seeding density of 315,000 cells/well in a final volume of 180

mL/well. 180 mL of XF RPMI assay medium was then added to each empty well and the four background wells. The plate was then centrifuged for 2 minutes at 300 x G. Following the centrifugation, the plate was placed in the non-CO<sub>2</sub> incubator for 45 minutes, while the XFe96 sensor cartridge calibrated in the XFe96 Analyzer. Mitochondrial respiration was then measured using Agilent's Seahorse XF Cell Mito Stress Test protocol. Once the assay was completed, the plate was imaged with transmitted using the ImageXpress Pico Automated Cell Imaging System (Molecular Devices). A 1.92 mm<sup>2</sup> Z-stacking image in three planes (-10 to 0 μM) of the center of each well was taken using transmitted light and the cells within that area were counted. Optimal focus (focus offset = -13 Mm) and exposure (exposure time = 4 ms) settings were determined prior to these experiments (Data not shown). Additionally, Z-stacking focus step (5 mM) and projection calculations (fluorescent = maximum & TL = best plane) were also determined prior to these experiments (Data not shown). The center of each well was chosen because measurement of OCR is primarily driven by the cells in the center of the well. The total cell count within each well was then calculated by multiplying the number of cells/mm<sup>2</sup> by the total area of the well (11.40 mm<sup>2</sup>). If confluency in the well was not uniform, then this was noted and considered when interpreting the OCR results.

Data were analyzed using Agilent's online software (Seahorse Analytics). First the oxygen consumption rate (OCR), extracellular acidification rate (ECAR), O<sub>2</sub> concentration, and Ph were assessed in the background wells. Background wells were removed if they had OCR < -20 pmol/min or > -20 pmol/min, ECAR >5 mpH/min, O<sub>2</sub> concentration < 140 mmHg or > 160 mmHg, or a Ph < 6.8 or > 7.8. The O<sub>2</sub> concentration and Ph were then assessed for each sample well. A well was removed if

the starting O<sub>2</sub> concentration was < 100 mmHg and/or if the O<sub>2</sub> concentration drops below 45 mmHg throughout the assay. If the Ph for any sample well is < 6.8 or > 7.8, then that well was removed. Lastly, the OCR for each sample well was assessed. Any well with a negative OCR was removed, as this is non-physiologic. Additionally, if basal respiration was less than 20 pmol/min, a sample well does not respond appropriately to each compound injection, or if there was a known methodological issue (e.g., known pipetting error), then that well was also removed. Respiration in each well was then normalized to the calculated total cell count within each well with a scaling factor of 10000. While no cells were seeded into the background wells, to ensure that each well was treated similarly, the background wells were also imaged using the ImageXpress Pico Automated Cell Imaging System cell count protocol and then normalized to the cell count after background well data quality had been assessed. Mitochondrial OCR was expressed as pmol/min/10,000 cells, and ECAR was expressed as mpH/min/10,000 cells.

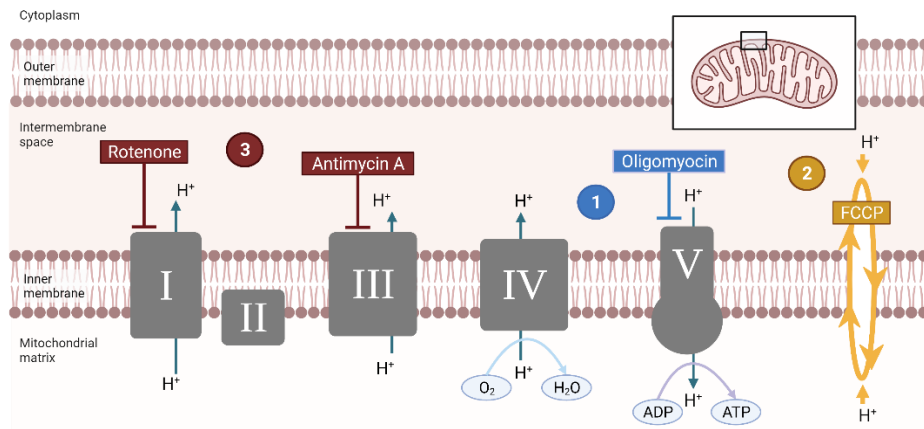


**Figure 2.1.** Agilent Seahorse XF Cell Mito Stress Test Adapted from the Seahorse XF Cell Mito Stress Test Kit User Guide.

### 2.2.9 Measuring Cerebrovascular Reactivity

Cerebrovascular function was assessed by measuring the cerebrovascular reactivity (CVR) of the middle cerebral artery (MCA) to a 30-second breath-hold. CVR was defined as the change in middle-cerebral artery velocity (MCAv) in response to arterial partial pressure of carbon dioxide (CO<sub>2</sub>; hypercapnia) caused by the breath-hold. MCAv was measured using transcranial doppler ultrasound (Transcranial Ultrasound System, Spencer Technologies), and it will be normalized to beat-beat mean reconstructed brachial arterial pressure (Finapres® NOVA, Finapres Medical Systems) to obtain cerebrovascular conductance (MCA<sub>CVC</sub>). The brachial arterial pressure was reconstructed using beat-to-beat finger arterial pressure which was calibrated by taking two brachial blood pressure measurements on the contralateral arm. Heart rate and etCO<sub>2</sub> were also monitored through the test via 3-lead ECG (Finapres® NOVA, Finapres Medical Systems), and the CapStar-100 End-tidal CO<sub>2</sub> Monitor (CWE Incorporated), respectively. All aspects of the protocol were explained to the participants prior to assessment and were given the opportunity to ask any questions. Participants were asked to rest quietly for 1 minute, and at the 50-

second mark were given a 10-second countdown after which they were asked to perform an end inspiratory breath-hold for a maximum of 30-seconds (Fig. 2.2). If a participant was not able to hold their breath for 30 seconds, then this was noted and accounted for in the analysis. After the breath-hold, participants were asked to resume normal breathing at a self-selected pace and rest quietly for an additional minute. The 1-minute rest period in the beginning of the test was considered the baseline. The instructions during the test were given using PsychoPy® Builder (University of Nottingham, v2020.1.3) <sup>193,194</sup>. CVR was calculated as the breath-hold index (BHI) using  $MCA_v$  and  $MCA_{cvc}$ , when applicable (see below).

1.  $MCA_v BHI (\% \Delta s^{-1}) = [(peak\ hyperemia\ MCA_v - average\ baseline\ MCA_v) / (average\ baseline\ MCA_v) \times 100] / breath\text{-}hold\ time$
2.  $MCA_{cvc} BHI (\% \Delta s^{-1}) = [(peak\ hyperemia\ MCA_{cvc} - average\ baseline\ MCA_{cvc}) / (average\ baseline\ MCA_{cvc}) \times 100] / breath\text{-}hold\ time$

All physiologic CVR data were collected using PowerLab (ADInstruments, PL3516 PowerLab 16/35) and Labchart (ADInstruments, #v8.1.13). Raw  $etCO_2$  (%) was converted to its absolute value by dividing the raw input as a percentage for a given respiratory cycle by 100 and then multiplied by the atmospheric pressure in a separate LabChart channel. To obtain breath-breath  $etCO_2$ , the absolute  $etCO_2$  data was converted to a cyclic measure using the maximum absolute  $etCO_2$  for each respiratory cycle. To account for sampling delay, the  $etCO_2$  channels were shifted to match the start and end times of the breath-hold. Maximum, minimum, and mean  $MCA_v$  was extracted in LabChart for each cardiac cycle using a 3-lead ECG to

determine the R-R interval. The data was then plotted and analyzed using Microsoft Excel (Version 2212). Beat-to-beat reconstructed MAP was used to calculate the beat-to-beat change in MAP. An automated brachial arterial pressure reading was taken for a baseline measurement of MAP at the start of the test and was then corrected for the beat-to-beat change in MAP throughout each cardiac cycle during the test. The absolute change in MAP,  $\text{etCO}_2$ , cardiac output (Q), and total peripheral resistance (TPR) from average at baseline to peak during hyperemia was also calculated. The data were plotted and reviewed to ensure data quality. Any non-physiologic data point was removed and then interpolated from a previous point. Any concerns during the data collection were noted and then considered when reviewing the raw data.

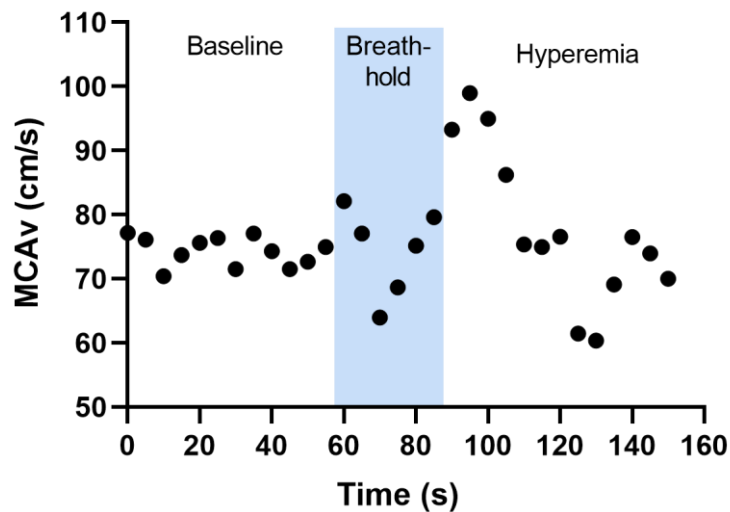


**Figure 2.2.** Breath-Hold Protocol. The figure is a representative tracing of middle cerebral artery blood flow velocity (MCAv) response to a 30-second breath-hold protocol.

### 2.2.10 Statistical Analysis

Before any analyses were carried out, descriptive statistics were generated for each of the variables of interest to determine if there were any inconsistencies or problematic values worth quality checking. Values or distributions that appeared to be beyond the realm of possibility (e.g., negative blood pressure values) were cross-referenced with any existing paper records and corrected as needed. If such values could not be corrected, they were either dropped (if clearly impossible) or retained in their current form. Outliers were identified using the robust regression and outlier removal method (ROUT). Additionally, those that appeared non-physiologic were removed.

To determine if a relationship existed between T-cell mitochondrial function and BHI, we employed uni-variate linear regressions – one model for each unique pairing of T-cell mitochondrial respiration measures and BHI measures. We tested whether the data was normally distributed using the Shapiro-Wilk test. Mediation analyses were performed to determine whether changes in MAP mediated relations between significant measures of mitochondrial respiration and glycolysis and cerebrovascular reactivity. Spearman correlations were performed to assess the relationship between significant measures of mitochondrial respiration and glycolysis and cardiovascular and hemodynamic measurements during the breath-hold assessment.

A total sample size of  $N = 20$  provided us with at least 80% power to detect a large effect ( $f^2 = 0.35$ ) in each of the models while providing for the inclusion of up to three co-variates (one of which may be dichotomous with an approximately even split). Correlations were performed between BHI measures and any potential co-variates (e.g., sleep, physical activity, clinical blood chemistry). Any significantly associated co-variates will be included in the linear regression. All correlations and linear regressions

were carried out using GraphPad Prism 9 (GraphPad Prism 9.4.1.681), and mediation analyses were performed using Jamovi 2.3.21.  $\alpha$  was set at 0.05.

## **2.3 Results**

### *Descriptive Statistics*

Twenty middle-aged adults ( $58 \pm 5$  years) were recruited for this study. Characteristics for the participants can be found in table 2.1 below. Participants were overweight <sup>195</sup>, with elevated blood pressure <sup>196</sup>, but had normal resting heart rate <sup>197</sup>. The participants were all Caucasian and did not identify as Hispanic or Latino. A more diverse cohort was initially recruited but had to either be excluded due to screen failure, withdrew from the study, or were outliers in statistical analyses.

**Table 2.1. Participant Characteristics**

<b>N=20</b>	<b>Mean ± SD</b>	<b>Min-Max</b>
Age, years	58 ± 5	51 – 64
Sex, Male/Female	5/15	-
Height, cm	167.8 ± 9.7	149.4 – 186.0
Mass, kg	71.6 ± 17.7	43.1 – 103.0
BMI, kg/m <sup>2</sup>	25.2 ± 4.4	18.3 – 32.2
<i>Resting Central Hemodynamics</i>		
SBP, mmHg	120 ± 9	104 – 138
DBP, mmHg	73 ± 6	61 – 82
MAP, mmHg	88 ± 6	75 – 97
PP, mmHg	48 ± 8	36 – 69
HR, bpm	60 ± 8	46 – 84

**Table 2.1.** Descriptive Statistics. Abbreviations: BMI, body mass index; SBP, systolic blood pressure; DBP, diastolic blood pressure; MAP, mean arterial pressure; PP, pulse pressure; HR, heart rate; & bpm, beats-per-minute.

Participants had normal total cholesterol, high-density lipoprotein cholesterol (HDL-C), LDL-C, very low-density lipoprotein cholesterol (VLDL-C), triglycerides, and fasting blood glucose (Table 2.2). Participants did not show signs of any ongoing infection, indicated by the normal leukocyte populations (Table 2.2).

**Table 2.2. Clinical Blood Chemistry**

<b>N=20</b>	<b>Mean ± SD</b>	<b>Min-Max</b>
<i>Metabolic Health</i>		
Total cholesterol, mg/dL	194 ± 27	140 - 236
HDL-C, mg/dL	70 ± 23	35 – 117
LDL-C, mg/dL	110 ± 23	69 – 149
VLDL-C, mg/dL	16 ± 11	7 – 49
Triglycerides, mg/dL	86 ± 64	39 – 279
Blood glucose, mg/dL	91 ± 8	73 – 104
<i>Leukocyte Count</i>		
WBC count, 1.0 x 10 <sup>3</sup> cells/uL	6.9 ± 10.5	2.9 – 51.0
Monocytes, 1.0 x 10 <sup>3</sup> cells/μL	0.4 ± 0.1	0.3 – 0.7
Lymphocytes, 1.0 x 10 <sup>3</sup> cells/μL	1.6 ± 0.7	0.8 – 4.1
Neutrophils, 1.0 x 10 <sup>3</sup> cells/μL	2.4 ± 0.8	1.2 – 4.1
Basophils, 1.0 x 10 <sup>3</sup> cells/μL	0.0 ± 0.0	0.0 – 0.0
Eosinophils, 1.0 x 10 <sup>3</sup> cells/μL	0.1 ± 0.1	0.0 – 0.4

**Table 2.2.** Clinical Blood Chemistry. Abbreviations: HDL-C, high-density lipoprotein cholesterol; LDL-C, low-density lipoprotein cholesterol; VLDL-C, very low-density lipoprotein cholesterol; & WBC, white blood cell.

The participants enrolled in this study were physically active, achieving well-above the American College of Sports Medicine recommended 500-1000 MET·min·wk of exercise (Table 2.2)<sup>198</sup>. Participants also had healthy sleep behavior, as they also had relatively low global sleep scores<sup>178</sup> and achieved the recommended amount of sleep set by the American Academy of Sleep Medicine and Sleep Research Society (Table 2.3)<sup>199</sup>.

**Table 2.3. Lifestyle, Health, and Behavioral Factors**

<b>N=20</b>	<b>Mean ± SD</b>	<b>Min-Max</b>
<i>Medications</i>		
Anti-depressants, <b>N</b> (%)	5 (25)	-
Blood pressure, <b>N</b> (%)	3 (15)	-
Thyroid, <b>N</b> (%)	3 (15)	-
Antihistamine, <b>N</b> (%)	1 (5)	-
Corticosteroid, <b>N</b> (%)	1 (5)	-
<i>Medical Conditions</i>		
Hypertension, <b>N</b> (%)	3 (15)	-
Skin cancer remission >10 years, <b>N</b> (%)	1 (5)	-
Depression, <b>N</b> (%)	2 (10)	-
<i>Exercise &amp; Physical Activity</i>		
Leisure exercise, MET/min/wk	2,220 ± 2,040	0 – 7,440
Work physical activity, MET/min/wk	1,920 ± 2,820	0 – 9,900
Total physical activity, MET/min/wk	4,140 ± 3,180	360 – 9,900
<i>Pittsburgh Sleep Quality Index</i>		
Subjective sleep quality, a.u.	0.9 ± 0.7	0.0 – 2.0
Sleep latency, a.u.	0.9 ± 0.7	0.0 – 3.0
Sleep duration, a.u.	0.7 ± 0.6	0.0 – 2.0
Sleep efficiency, a.u.	0.5 ± 0.8	0.0 – 3.0
Sleep disturbance, a.u.	1.2 ± 0.4	1.0 – 2.0
Use of sleeping medications, a.u.	0.7 ± 1.1	0.0 – 3.0
Daytime dysfunction, a.u.	0.3 ± 0.6	0.0 – 2.0
Global sleep score, a.u.	5.0 ± 2.4	1.0 – 10.0
Total sleep duration, hours	7.0 ± 0.9	5.0 – 8.5

**Table 2.3.** Lifestyle, Health, and Behavioral Factors. Sleep components are scored on a likert scale and are totaled for a calculation of the global sleep score. A higher score indicates worse quality. Abbreviations: MET, metabolic equivalent; & a.u., arbitrary units.

### *Cerebrovascular Reactivity*

Cerebrovascular reactivity was measured using a 30-second breath-hold and was reported as BHI calculated using the  $MCA_v$  or  $MCA_{CVC}$ . We were unable to obtain beat-to-beat blood pressure on one participant. The MCA was insonated at an average depth of  $51 \pm 6$  mm (mean  $\pm$  SD) with an average power of  $97 \pm 9$  a.u. (mean  $\pm$  SD). As expected, the 30-second breath-hold elicited a robust cerebral blood flow response (Tables 2.4 & 2.5), in addition to a percent increase in MAP and the partial pressure of end-tidal  $CO_2$  (Table 2.5). All participants were able to hold their breath for the entire 30-second period.

**Table 2.4. Baseline Physiologic Cerebrovascular Reactivity Data**

	<i>Baseline</i>	<i>Hyperemia</i>	<b>p</b>	<b>N</b>
	<b>Mean ± SD</b>	<b>Mean ± SD</b>		
Average HR, bpm	63.2 ± 8.6	62.4 ± 7.8	0.55	20
Peak HR, bpm	71.3 ± 9.3	74.6 ± 10.5	0.024	20
Average MAP, mmHg	95 ± 10	94 ± 9	0.11	19
Peak MAP, mmHg	106 ± 12	108 ± 11	0.52	19
Average Q, L/min	3.42 ± 1.13	3.39 ± 1.06	0.94	19
Peak Q, L/min	-	4.01 ± 1.32	-	19
Average TPR, mmHg*s/ml	2.34 ± 1.05	2.34 ± 1.00	0.77	19
Peak TPR, mmHg*s/ml	-	3.03 ± 1.12	-	19
Average EtCO <sub>2</sub> , mmHg	46.6 ± 11.4	47.6 ± 10.6	0.11	20
Peak EtCO <sub>2</sub> , mmHg	-	54.32 ± 12.90	-	20
Average MCAv, cm/s	53.17 ± 12.39	52.39 ± 12.34	0.35	20
Peak MCAv, cm/s	60.80 ± 13.87	66.69 ± 15.61	<0.0001	20
Average MCA <sub>cvc</sub> , cm/s/mmHg	0.58 ± 0.15	0.57 ± 0.15	0.95	19
Peak MCA <sub>cvc</sub> , cm/s/mmHg	0.65 ± 0.16	0.68 ± 0.18	0.0032	19
Average MCA PI, a.u.	0.81 ± 0.12	0.85 ± 0.11	<0.0001	20

**Table 2.4.** Baseline Physiologic Cerebrovascular Reactivity Data. Abbreviations: HR, heart rate; bpm, beats-per-minute; MAP, mean arterial pressure; etCO<sub>2</sub>, end-tidal carbon dioxide; MCAv, middle cerebral artery velocity; MCA<sub>cvc</sub>, middle cerebral artery cerebrovascular conductance; PI, pulsatility index.

**Table 2.5. Cerebrovascular Reactivity Responses**

	Mean ± STD	N
MCA <sub>v</sub> BHI, %Δ s <sup>-1</sup>	0.86 ± 0.35	20
MCA <sub>cvc</sub> BHI, %Δ s <sup>-1</sup>	0.61 ± 0.22	19
ΔMAP, mmHg	13.54 ± 9.23	19
ΔetCO <sub>2</sub> , mmHg	7.68 ± 5.38	20
ΔQ, L/min	0.59 ± 0.47	19
ΔTPR, mmHg*s/ml	0.69 ± 0.41	19

**Table 2.5.** Cerebrovascular Reactivity Responses. The percent change in MAP and etCO<sub>2</sub> from peak hyperemia to baseline were calculated. Abbreviations: MCA<sub>v</sub>, middle cerebral artery velocity; BHI, breath-hold index; MCA<sub>cvc</sub>, middle cerebral artery cerebrovascular conductance; MAP, mean arterial pressure; Q, cardiac output; & TPR, total peripheral resistance.

#### *Mitochondrial Respiration and Glycolysis vs. Cerebrovascular Reactivity*

Spearman correlations were first performed to determine whether any demographic, clinical blood markers, medications, medical conditions, physical activity, sleep, previous infection, or COVID-19 infection and vaccination variables were associated with BHI to be used as co-variates in multi-linear regressions. No co-variates were significantly associated with BHI calculated using MCA<sub>v</sub> or MCA<sub>cvc</sub>, thus linear regression models only included OCR and ECAR measures with either BHI calculation. No measure of CD4<sup>+</sup> OCR or ECAR were predictive of MCA<sub>v</sub> BHI (Table 2.6), and higher CD8<sup>+</sup> basal OCR was predictive of lower MCA<sub>v</sub> BHI ( $\beta=-0.59$ ,  $R^2=0.27$ ,  $P=0.019$ ). Higher CD8<sup>+</sup> basal ( $\beta=-2.20$ ,  $R^2=0.29$ ,  $P=0.015$ ) and maximum ECAR ( $\beta=-0.50$ ,  $R^2=0.24$ ,  $P=0.29$ ) were predictive of lower MCA<sub>v</sub> BHI. These models were no longer significant after controlling BHI for MAP expressed as MCA<sub>cvc</sub> (Table 2.7). No other measure of CD8<sup>+</sup> T-cell OCR or ECAR were

associated with either BHI calculation (Tables 2.6 & 2.7). These data indicate that higher basal CD8<sup>+</sup>, but not CD4<sup>+</sup> oxidative and glycolytic energetic demand are associated with decreased cerebrovascular function. These associations are abolished after correcting for changes in MAP.

Because the relation between CD8<sup>+</sup> T-cell basal OCR and basal and maximal ECAR was abolished after controlling for the MAP response to the breath-hold, an exploratory analysis was performed to see whether the change in MAP (pressor response) mediates the relation between CD8<sup>+</sup> T-cell bioenergetics and MCAv BHI. Indeed, we found that the pressor response mediated the relation between CD8<sup>+</sup> T-cell basal (Figure 2.3B) and maximal ECAR (Figure 2.3C) and approached significance for CD8<sup>+</sup> T-cell basal OCR (Figure 2.3A). To further investigate this association, we first assessed whether the blunted pressor response was related to a higher baseline MAP or a lower peak MAP. Baseline and peak MAP during the breath-hold were correlated with the absolute change in MAP in response to the breath-hold. Although these relations were not statistically significant, there appeared to be a negative association between baseline MAP and the pressor response ( $R=-0.44$ ,  $P=0.061$ ) and a positive association between peak MAP and the pressor response ( $R=0.45$ ,  $P=0.060$ ). CD8<sup>+</sup> bioenergetics were then correlated with baseline MAP and peak MAP. CD8<sup>+</sup> basal OCR was not associated with baseline MAP ( $R=0.16$ ,  $P=0.51$ ) or peak MAP ( $R=-0.15$ ,  $P=0.53$ ). CD8<sup>+</sup> maximal ECAR was also not associated with baseline MAP ( $R=-0.023$ ,  $P=0.93$ ) or peak MAP ( $R=-0.37$ ,  $P=0.12$ ). However, basal CD8<sup>+</sup> ECAR was positively associated with baseline MAP ( $R=0.64$ ,  $P=0.0031$ ), but not peak MAP ( $R=0.071$ ,  $P=0.77$ ). Thus, it appears that individuals with a higher baseline MAP and

lower peak MAP have a lower pressor response to the breath-hold. Additionally, it appears that higher CD8<sup>+</sup> basal glycolysis is related to a greater baseline MAP.

Because MAP is determined by cardiac output (Q) and total peripheral resistance (TPR), we also investigated whether Q or TPR were related to the pressor response and whether CD8<sup>+</sup> bioenergetics were related to Q or TPR, using the Modelflow method (Finapres). The pressor response was not related to the absolute change in Q (R=0.015, P=0.95) or TPR (R=0.37, P=0.12) during the breath-hold, nor baseline (R=-0.31, P=0.19) or peak Q (R=-0.28, P=0.24) or baseline TPR (R=0.34, P=.16). However, there was a positive relation between the pressor response and peak TPR (R=0.49, P=0.033) during the breath-hold. We then sought to determine whether CD8<sup>+</sup> bioenergetics were correlated with peak TPR and the absolute change in TPR during hyperemia. CD8<sup>+</sup> basal ECAR (Figure 2.4) was negatively correlated with peak TPR (R=-0.58, P=0.0099) and the absolute change in TPR (r=-0.50, p=0.028) suggesting that greater CD8<sup>+</sup> T-cell glycolytic metabolism is affecting the peripheral vasoconstriction during the breath-hold. No significant correlations were observed between maximal ECAR or basal OCR with either peak or the absolute change in TPR. These data suggest that individuals with a greater capacity to vasoconstrict during a breath-hold have a greater pressor response. Additionally, these measures of TPR appear to be related to CD8<sup>+</sup> basal glycolysis, where higher basal glycolysis was associated with a lower peak and absolute change in TPR.

**Table 2.6. CD4<sup>+</sup> Mitochondrial Respiration and Glycolysis vs. Cerebrovascular Reactivity**

	$\beta$	R <sup>2</sup>	P-value	N
<i>MCA<sub>v</sub> BHI</i>				
CD4 <sup>+</sup> Basal OCR	-0.16	0.020	0.56	20
CD4 <sup>+</sup> Proton leak OCR	0.018	0.00015	0.96	20
CD4 <sup>+</sup> Maximum OCR	-0.021	0.034	0.43	20
CD4 <sup>+</sup> SRC OCR	-0.022	0.035	0.43	20
CD4 <sup>+</sup> Non-mitochondrial OCR	-0.16	0.027	0.49	20
CD4 <sup>+</sup> ATP-Linked OCR	-0.15	0.046	0.37	20
CD4 <sup>+</sup> Coupling Efficiency	0.00072	0.0045	0.78	20
CD4 <sup>+</sup> Basal ECAR	-0.35	0.030	0.46	20
CD4 <sup>+</sup> Maximum ECAR	-0.22	0.073	0.25	20
CD4 <sup>+</sup> Basal OCR/ECAR Ratio	-0.024	0.0028	0.82	20
CD4 <sup>+</sup> Maximum OCR/ECAR Ratio	-0.036	0.015	0.61	20
<i>MCA<sub>CVC</sub> BHI</i>				
CD4 <sup>+</sup> Basal OCR	-0.11	0.036	0.44	19
CD4 <sup>+</sup> Proton leak OCR	0.34	0.13	0.13	19
CD4 <sup>+</sup> Maximum OCR	-0.012	0.031	0.47	19
CD4 <sup>+</sup> SRC OCR	-0.013	0.029	0.49	19
CD4 <sup>+</sup> Non-mitochondrial OCR	-0.056	0.0086	0.71	19
CD4 <sup>+</sup> ATP-linked OCR	-0.14	0.098	0.19	19
CD4 <sup>+</sup> Coupling efficiency	-0.0025	0.14	0.12	19
CD4 <sup>+</sup> Basal ECAR	0.28	0.048	0.37	19
CD4 <sup>+</sup> Maximum ECAR	-0.067	0.017	0.60	19
CD4 <sup>+</sup> Basal OCR/ECAR Ratio	-0.060	0.042	0.40	19
CD4 <sup>+</sup> Maximum OCR/ECAR Ratio	-0.045	0.060	0.31	19

**Table 2.6.** CD4<sup>+</sup> Mitochondrial Respiration and Glycolysis vs. Cerebrovascular Reactivity. Data were analyzed using linear regressions. Abbreviations: MCA<sub>v</sub>, middle cerebral artery velocity; BHI, breath-hold index; OCR, oxygen consumption rate; SRC, spare respiratory capacity; & ECAR, extracellular acidification rate.

**Table 2.7. CD8<sup>+</sup> Mitochondrial Respiration and Glycolysis vs. Cerebrovascular Reactivity**

	$\beta$	R <sup>2</sup>	P-value	N
<i>MCA<sub>v</sub> BHI</i>				
CD8 <sup>+</sup> Basal OCR	-0.59	0.27	0.019*	20
CD8 <sup>+</sup> Proton leak OCR	-0.017	0.00014	0.96	20
CD8 <sup>+</sup> Maximum OCR	-0.044	0.10	0.17	20
CD8 <sup>+</sup> SRC OCR	-0.042	0.077	0.24	20
CD8 <sup>+</sup> Non-mitochondrial OCR	-0.51	0.15	0.098	20
CD8 <sup>+</sup> ATP-linked OCR	-0.30	0.13	0.11	20
CD8 <sup>+</sup> Coupling efficiency	0.0044	0.14	0.10	20
CD8 <sup>+</sup> Basal ECAR	-2.20	0.29	0.015*	20
CD8 <sup>+</sup> Maximum ECAR	-0.50	0.24	0.029*	20
CD8 <sup>+</sup> Basal OCR/ECAR Ratio	-0.11	0.057	0.31	20
CD8 <sup>+</sup> Maximum OCR/ECAR Ratio	-0.062	0.033	0.44	20
<i>MCA<sub>cvc</sub> BHI</i>				
CD8 <sup>+</sup> Basal OCR	-0.16	0.049	0.36	19
CD8 <sup>+</sup> Proton leak OCR	0.33	0.12	0.14	19
CD8 <sup>+</sup> Maximum OCR	-0.0023	0.00071	0.91	19
CD8 <sup>+</sup> SRC OCR	0.00004 5	0.00000 023	0.999	19
CD8 <sup>+</sup> Non-mitochondrial OCR	-0.27	0.11	0.17	19
CD8 <sup>+</sup> ATP-linked OCR	-0.18	0.12	0.14	19
CD8 <sup>+</sup> Coupling efficiency	-0.0017	0.049	0.36	19
CD8 <sup>+</sup> Basal ECAR	-0.024	0.00008 9	0.97	19
CD8 <sup>+</sup> Maximum ECAR	-0.076	0.014	0.63	19
CD8 <sup>+</sup> Basal OCR/ECAR Ratio	-0.084	0.081	0.24	19
CD8 <sup>+</sup> Maximum OCR/ECAR Ratio	-0.00037	0.00000 29	0.99	19

**Table 2.7.** CD8<sup>+</sup> Mitochondrial Respiration and Glycolysis vs. Cerebrovascular Reactivity. Data were analyzed using linear regressions. Significant models are in red font.

Abbreviations: MCAv, middle cerebral artery velocity; BHI, breath-hold index; OCR, oxygen consumption rate; SRC, spare respiratory capacity; & ECAR, extracellular acidification rate.

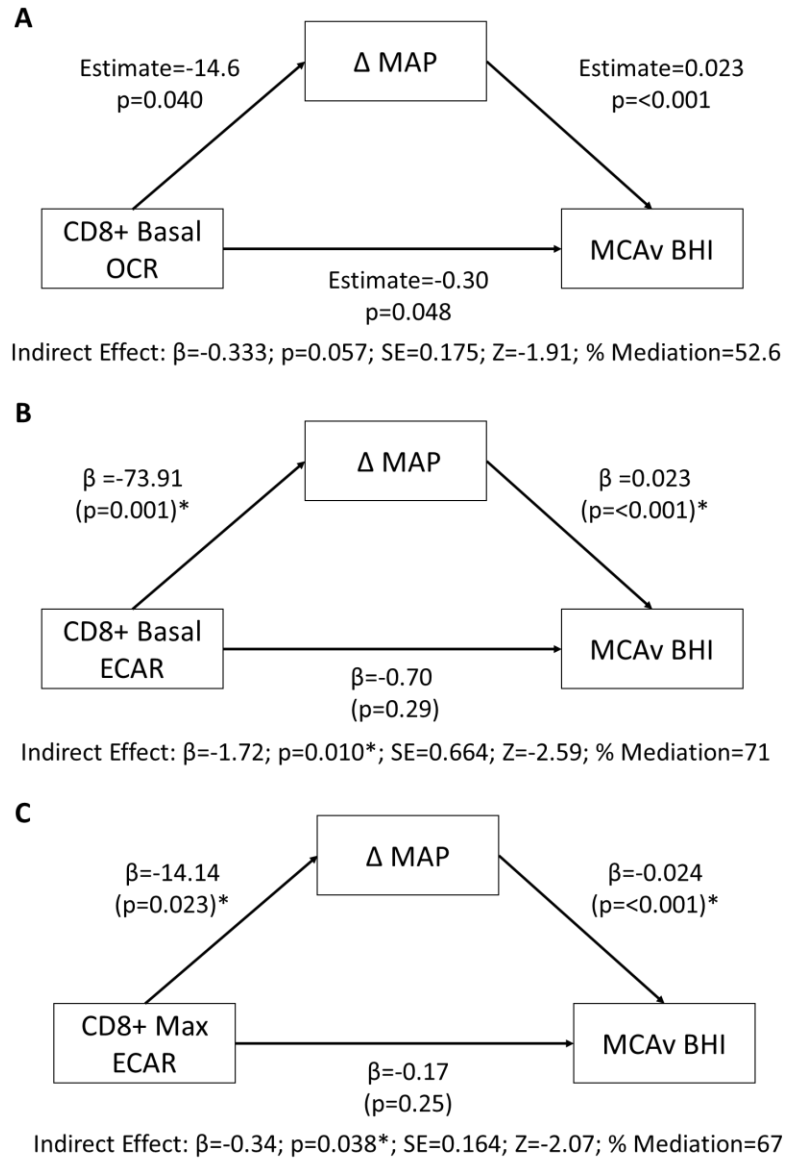


**Figure 2.3.** Mediation Analysis. Data were analyzed using a Mediation Analysis in Jamovi 2.3.21. Abbreviations: OCR; oxygen consumption rate; ECAR, extracellular acidification rate; MAP, mean arterial pressure; MCAv, middle cerebral artery velocity; & BHI, breath-hold index.

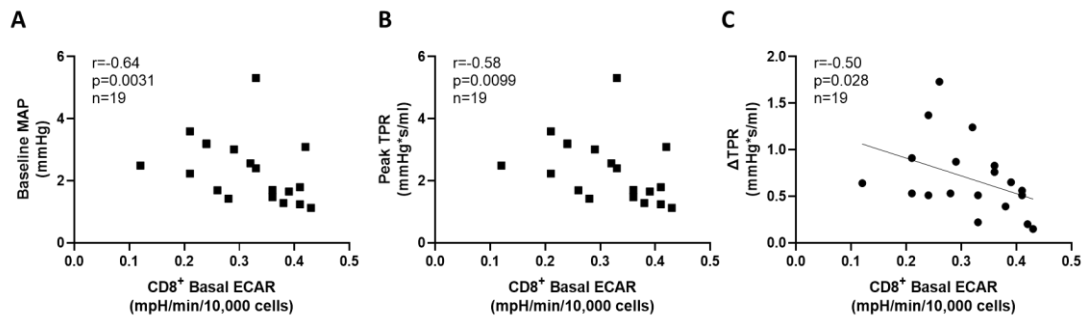


**Figure 2.4.** Spearman correlations. Spearman correlations between basal glycolysis and baseline MAP (A), peak TPR (B), and the absolute change in TPR during hyperemia (C). Absolute change in TPR was calculated by subtracting the average value during the baseline from the peak value during hyperemia after the breath-hold. Abbreviations: ECAR, extracellular acidification rate; MAP, mean arterial pressure; & TPR, total peripheral resistance.

## 2.4 Discussion

We hypothesized that higher CD4<sup>+</sup> and CD8<sup>+</sup> T-cell OCR would be predictive of higher MCA BHI, whereas lower CD4<sup>+</sup> and CD8<sup>+</sup> T-cell ECAR would be predictive of lower BHI. Contrary to our hypothesis, CD4<sup>+</sup> T-cell bioenergetics were not associated with MCA BHI and, unexpectedly, CD8<sup>+</sup> T-cell basal OCR was inversely associated with lower MCA BHI. However, in accordance with our hypothesis, higher CD8<sup>+</sup> T-cell basal and maximum ECAR were associated with lower MCA BHI, which may suggest that CD8<sup>+</sup> T-cell ECAR influences the cerebrovascular response to the breath-hold. However, this association was abolished after correcting for beat-to-beat MAP (e.g., MCA<sub>CVC</sub>), suggesting CD8<sup>+</sup> ECAR may be related to the pressor response to the breath-hold. Indeed, mediation analyses showed that a lower pressor response mediated the relation between CD8<sup>+</sup> ECAR and MCA BHI.

In animal models, CD4<sup>+</sup> T-cells are important regulators of cerebrovascular function by reducing inflammation and oxidative stress<sup>39-41</sup>. Mitochondrial respiration

in CD4<sup>+</sup> T-cells is important for maintaining low basal inflammation and preventing oxidative stress and widespread physiologic dysfunction<sup>3,28,42,83,102</sup>. The participants in this study were generally healthy, and their leukocyte counts were normal. Elevated leukocytes, such as white blood cells are related to elevated systemic inflammation<sup>200,201</sup>. Thus, while not directly measured, it is possible that their basal inflammation was not elevated, and that CD4<sup>+</sup> T-cell bioenergetics may become more important in regulating cerebrovascular function in unhealthier populations with greater basal inflammation. Additionally, we measured mitochondrial respiration and glycolysis in pan CD4<sup>+</sup> T-cells, and not individual subpopulations which have been shown to exert differential effects on the vasculature. For instance, CD4<sup>+</sup> T<sub>REG</sub> cells, in particular, have been shown to be protective of cerebrovascular function in animal models of increased inflammation and oxidative stress<sup>39-41</sup>, while other subpopulations of pro-inflammatory CD4<sup>+</sup> T-cells (e.g., CD4<sup>+</sup> T<sub>EFF</sub>) are detrimental to cerebrovascular<sup>39</sup> and vascular function<sup>132,161,202</sup>. Therefore, measuring mitochondrial respiration and glycolysis in these subpopulations might be more sensitive predictors of cerebrovascular function in healthy populations.

The observation that higher CD8<sup>+</sup> T-cell basal respiration is predictive of lower MCAv BHI is unexpected, considering that CD8<sup>+</sup> T-cells are typically more proinflammatory and have been shown to be deleterious for vascular function under conditions of reduced oxidative metabolism, such as what occurs during acute infection<sup>145</sup>. Thus, we hypothesized that higher mitochondrial respiration would be associated with a less inflammatory phenotype and preserved vascular function<sup>3,28</sup>. However, our observation that higher CD8<sup>+</sup> basal and maximal ECAR were associated

with lower MCAv BHI is consistent with our hypothesis and potentially explained by greater T-cell activation <sup>3,71</sup>, as activated cells rely more on aerobic glycolysis <sup>3,84,85</sup>.

In addition to a well-defined metabolic shift towards greater aerobic glycolysis, during T-cell activation, there is also an increase in oxidative phosphorylation, which may explain why we observed an inverse association between basal OCR and BHI in our study <sup>84,86</sup>. Aging is associated with an increase in effector and effector memory T-cell populations <sup>28,72,73</sup>, and CD8<sup>+</sup> T-cells exhibit a greater shift towards effector memory T-cells compared to CD4<sup>+</sup> T-cells and earlier in life <sup>74</sup>. Thus, basal OCR may reflect an increase in the overall energetic demand of CD8<sup>+</sup> T-cells and be higher in individuals with more glycolytic effector and effector memory CD8<sup>+</sup> T-cells. In the present study, we measured mitochondrial respiration and glycolysis in pan CD8<sup>+</sup> T-cells and therefore were unable to assess energy metabolism in effector or effector memory T-cells individually, so this hypothesis cannot be confirmed.

It is also important to note that, after correcting for beat-to-beat changes in MAP, none of the measured indices of CD8<sup>+</sup> T-cell OCR or ECAR were associated with cerebrovascular function. Our exploratory analysis indicated that the change in MAP (e.g., pressor response) in response to the breath-hold test mediates the relation between CD8<sup>+</sup> T-cell ECAR and MCAv BHI, with higher CD8<sup>+</sup> T-cell basal and maximal ECAR associated with a reduced MAP response to the breath-hold test. Thus, glycolytic CD8<sup>+</sup> T-cells (possibly reflective of greater T-cell activation) may blunt the pressor response to hypercapnia. This may be due to the fact that CD8<sup>+</sup> are pro-inflammatory and cytotoxic <sup>152</sup> and more detrimental to blood pressure regulation than CD4<sup>+</sup> T-helper cells <sup>145</sup>.

Several prior studies have shown that a single breath-hold increases blood pressure<sup>203–207</sup> as a result of increased sympathetic activity, which results from combined responses of and between arterial baroreceptors and chemoreceptors<sup>204,207–209</sup>. Interestingly, we found that higher CD8<sup>+</sup> basal ECAR was negatively associated with the peak and absolute change TPR during the breath-hold, which may reflect a decrease in sympathetic activity. It should be noted that sympathetic activity was not directly measured in our study and the relation between sympathetic activity and TPR appears somewhat dependent on sex and fitness level<sup>210,211</sup>, thus this potential mechanism warrants further investigation. However, there was no effect of sex or fitness on cerebrovascular reactivity in our data set (data not shown). Additionally, whether T-cell bioenergetics relate to the baroreceptor or chemoreceptor sensitivity during the breath-hold also requires further elucidation.

There are limitations that should be considered when interpreting these data. We did not have an equal proportion of males and females in the study, so we are unable to adequately assess whether sex differences exist. Additionally, our measure of glycolysis (ECAR) is qualitative and not quantitative, thus does not offer an exact estimate of glycolysis. Future studies should utilize assays more specific for glycolysis (e.g., XF Glycolysis Stress Test, #103020-100). Lastly, a breath-hold is just one method that can be used to assess CVR. Future studies are needed to determine the association between T-cell metabolism and other methods of CVR (e.g., transient shear-mediated and sustained hypercapnia)<sup>212</sup>.

In conclusion CD4<sup>+</sup> mitochondrial bioenergetics were not associated with the MCA cerebrovascular responses to the breath-hold test, while higher CD8<sup>+</sup> basal OCR and basal and maximal ECAR were associated with a lower MCA BHI. These

associations were abolished after correcting for the change in blood pressure during the breath-hold test, suggesting that CD8<sup>+</sup> T-cell bioenergetics may influence the blood pressure response during a breath-hold, possibly via decreased sympathetic activity. Future studies should explore the effect of T-cell bioenergetics on cerebrovascular function and sympathetic activity by measuring mitochondrial respiration and glycolysis in sub-populations of CD4<sup>+</sup> and CD8<sup>+</sup> T-cells in healthy adults and adults sub-clinical and clinical disease.

## Chapter 3

### THE EFFECT OF EXOGENOUS LOW-DENSITY LIPOPROTEIN CHOLESTEROL ON T-CELL FUNCTION

#### 3.1 Introduction

Aging is associated with an increase in chronic, sterile, low-grade inflammation termed “inflammaging”<sup>24–26,213</sup>. Inflammaging increases the risk for developing age-related conditions such as cardiovascular disease (CVD) and AD<sup>24–26,213–216</sup>. Adaptive immune cells (e.g., T-lymphocytes, T-cells) are thought to be a major source of inflammaging<sup>27–29</sup>. With aging, T-cells become dysfunctional and shift towards a pro-inflammatory phenotype<sup>28,37,38</sup>, as a result of impaired mitochondrial function and cellular senescence<sup>3,28</sup>. Impairments in mitochondrial function, such as mitochondrial respiration can increase oxidative stress<sup>45</sup>, resulting in a pro-inflammatory phenotype that drives early T-cell senescence<sup>3,28,46,47</sup>. For instance, impairing mitochondrial respiration in T-cells from young mice induced premature aging, as well as widespread senescence and physiological dysfunction<sup>42</sup>.

While there is clear evidence linking T-cells function to inflammation, the factors contributing to impaired T-cell function with aging are not entirely understood. Coinciding with inflammaging, endogenous blood low-density lipoprotein cholesterol (LDL-C) also increases with age and peaks in mid-life<sup>57,58</sup>. We and others have shown that blood LDL-C<sup>57</sup>, has been linked to lower mitochondrial respiration in human peripheral blood mononuclear cells<sup>48,49</sup>. Additionally, treating T-cells with exogenous LDL-C decreased mitochondrial function<sup>75</sup>, and has also been shown to induce mitochondrial dysfunction in other immune cells, such as macrophages<sup>50</sup>. There is also evidence to suggest that LDL-C and apolipoprotein B-100 (apoB), the LDL-particle (LDL-P) responsible for carrying LDL-C, can act as a “neo-antigen” for

T-cells<sup>51-53</sup>, possibly resulting in their repetitive activation. Repetitive activation can lead to cellular senescence overtime, and shifts T-cells to a more pro-inflammatory state<sup>28,37,38,54-56</sup>.

Therefore, the purpose of this study was to determine whether elevated exogenous LDL-C impairs CD4<sup>+</sup> and CD8<sup>+</sup> T-cell function collected from middle-aged (50-64 adults). We hypothesized that treatment with a high concentration of exogenous LDL-C would decrease mitochondrial respiration, and increase mitochondrial damage (e.g., proton leak), inflammation (e.g., intracellular inflammatory cytokine production & non-mitochondrial respiration), activation, and senescence compared to treatment with low LDL-C in CD4<sup>+</sup> and CD8<sup>+</sup> T-cells.

## **3.2 Materials and Methods**

### **3.2.1 Participant Recruitment**

Eighteen mid-life adults (aged 50-64 years) with endogenous LDL-C concentrations (<150 mg/dL) were recruited for this study. All procedures and protocols used were approved by the Institutional Review board at the University of Delaware (1753416-6) and are compliant with the standards set by the latest revisions of the Declaration of Helsinki 1975 (as revised in 1983). Before enrollment the rationale, procedures, risks, and benefits of taking part in the study were explained to the participants. Written or electronic informed consent was also obtained prior to enrollment. Participants were asked to refrain from vigorous aerobic exercise and alcohol consumption for 24-hours and taking over-the-counter anti-inflammatory medications for 48-hours and were also asked to fast for at least 12-hours prior to each study visit. Study visits were also scheduled at least 14-days after a vaccination to

account for any acute changes in immune function. Participants were brought in for two study visits. The first visit was for the assessment of T-cell mitochondrial respiration using extracellular flux analysis, and the second was for the assessment of T-cell function using flow cytometry.

Participants of all races and ethnic backgrounds were allowed to participate in this study. Study participants were recruited by advertising with businesses in the Newark, DE area, and by using university mailing lists and the Nurse Managed Primary Care Center (NMPCC) study participant registry at the University of Delaware. All participants were generally healthy (e.g., nonsmokers & free from systemic medical illness) and did not experience an acute infection (e.g., influenza, COVID-19) within 14 days prior to study enrollment. Participants were recruited if they had endogenous LDL-C concentrations  $\leq 150$  mg/dL but were not excluded for other abnormal blood lipid markers (e.g., high-density lipoprotein, triglycerides, total cholesterol, etc). Participants were excluded if they had a systemic medical illness (e.g., CVD, cancer, renal failure), or autoimmune disease (e.g., multiple sclerosis, Type 1 diabetes). Participants were also excluded if clinical blood markers were abnormal ( $\pm 2.5$ x the upper or lower limit) or if they were taking medications that affected inflammation (e.g., NSAIDs & corticosteroids) or endogenous lipid concentrations (e.g., statins).

### **3.2.2 Questionnaires**

A series of questionnaires were administered for determining participant eligibility and as control variables for statistical analysis (when applicable). Participants were asked to complete a medical history questionnaire, sleep questionnaire (Pittsburgh Sleep Quality Index), physical activity questionnaire, recent

infections questionnaire, and a COVID-19 screening questionnaire. Variables such as sleep, physical activity, and acute infections can affect T-cell populations<sup>179,180</sup>, vascular function<sup>181</sup>, LDL-C concentrations<sup>217</sup>, and cellular metabolism<sup>84,86,183–185</sup>.

### **3.2.3 Blood Draw**

Participants sat on a stretcher in a semi-recumbent position. A trained member of our research team or a trained research nurse performed the blood draw on two separate visits. For the first visit, 64 mL of blood was taken for measures of T-cell mitochondrial respiration using extracellular flux analysis, and for the second visit 48 mL of blood was drawn for measures of T-cell function via flow cytometry. Control cells in the mitochondrial respiration experiments without the treatment of exogenous LDL-C were used for the analyses performed in Chapter 2. Cells treated with both the low (100 mg/dL) and high (200 mg/dL) concentration of exogenous LDL-C will be discussed here in Chapter 3. Additionally, 10 mL was drawn for the analysis of clinical labs including a complete blood count with differential, a comprehensive metabolic panel, and a lipid panel. The clinical samples were processed by LabCorp.

### **3.2.4 Blood Pressure**

Participants rested quietly in semi-recumbent position for 5 minutes. The lights were dim, and the ambient room temperature was  $22.4 \pm 1.3^{\circ}\text{C}$  for the Seahorse experimental visits and  $22.5 \pm 1.3^{\circ}\text{C}$  during the flow cytometry experimental visits. Using a semi-automated oscillometric sphygmomanometer validated by the British Hypertension Society<sup>190</sup> (SunTech ADView 2, SunTech Medical) blood pressure was measured in the non-dominant arm. Continuous blood pressure measurements were taken until we obtained three values within 5 mmHg of one another with 2-minutes of

rest in-between in measurement. These three blood pressure values were then averaged for the calculation of resting blood pressure.

### **3.2.5 Height and Weight**

A physician's scale (Health o Meter Physician Digital Scale) was used to measure participant height (cm) and body mass (kg). Body mass index was calculated using height and body mass because obesity influences mitochondrial function<sup>218</sup>. The equation for calculating BMI can be found below.

$$BMI = Mass (kg) / [Height (cm)]^2$$

### **3.2.6 Peripheral Blood Mononuclear Cell Isolation**

Density gradient centrifugation was performed to isolate peripheral blood mononuclear cells (PBMCs) from whole blood SepMate™ -50 PBMC Isolation Tubes (Stemcell Technologies, #8540) for the separation of T-cells for the Seahorse and flow cytometry experiments. 15 mL histopaque 1077 (Sigma-Aldrich, #SD10771A) was pipetted into Sepmate™ tubes and pre-warmed for 10-minutes in a 37°C water bath. 1X phosphate buffered saline (PBS; Corning #21-040-CM) supplemented with 2% fetal bovine serum (FBS; Sigma-Aldrich, # F2442-50ML) was used to dilute the whole blood 1:1. The diluted whole blood was then pipetted into the Sepmate™ tubes containing the pre-warmed histopaque 1077. The Sepmate™ tubes were centrifuged for 10-minutes at room temperature at 1200 x G. The cells were then washed with 1X PBS with 2% FBS and centrifuged for 8-minutes at 300 x G. The red blood cells were then removed by resuspending the cell pellet in eBioscience™ 1X RBC Lysis Buffer (ThermoFisher, #00-4333-57) for 5-minutes on ice. The cells were then washed again, counted using the Thermo Fisher Countess II Automated Cell Counter and one

Countess™ Cell Counting Chamber Slide (ThermoFisher, # C10228), and prepared for either the positive T-cell separation (Seahorse) or the negative pan T-cell separation (Flow cytometry).

### **3.2.7 Positive T-cell Separation and LDL-C Treatment**

To measure the effect of LDL-C on mitochondrial respiration, positive magnetic bead separation with the QuadroMACS™ separator (Miltenyi Biotec, #130-091-051) and LS columns (Miltenyi Biotec, #130-042-401) were used to separate CD4<sup>+</sup> and CD8<sup>+</sup> T-cells from PBMCs. Positive selection was first performed to isolate CD8<sup>+</sup> T-cells using Human CD8 MicroBeads (Miltenyi Biotec, #130-045-201) following the protocol provided by the manufacturer, because they are a smaller proportion of pan T-cells<sup>191</sup>. Following CD8<sup>+</sup> T-cell separation, CD4<sup>+</sup> T-cells in the effluent were labeled using Human CD4 MicroBeads (Miltenyi BioTec, #130-045-101) per the manufacturers protocol. The cells were then resuspended in CTS™ AIM-V™ Medium, without phenol red, without antibiotics (ThermoFisher, #A3830801) supplemented with 1x antibiotic-antimycotic (ThermoFisher, #15240062) and treated with LDL-C.

Due to issues with LDL particle (LDL-P) availability, the LDL-P had to be obtained from two different vendors (StemCell, #02698 & Lee BioSolutions, #360-10), resulting in slightly different LDL-C treatment concentrations. Additionally, the LDL-C concentration reported by the manufacturer varied from what was measured from an independent organization (IDEXX BioAnalytics, Columbia, MO). We originally aimed to treat the cells with 100 mg/dL and 200 mg/dL; however, based on the LDL-C concentration measured, the cells were treated with a low ( $66 \pm 6.6$  mg/dL)

and high ( $133 \pm 13.6$  mg/dL) concentration of LDL-C for 20 hours in a 37°C cell culture incubator with 5% CO<sub>2</sub>.

### **3.2.8 T-cell Mitochondrial Respirometry**

CD4<sup>+</sup> and CD8<sup>+</sup> T-cell mitochondrial respiration with extracellular flux analysis using the Seahorse XFe96 Analyzer (Agilent) and the Seahorse XF Cell Mito Stress Test Kit (Agilent, #103015-100). The Seahorse analyzer measures oxygen consumption rate before and after a series of injections that manipulate the electron transport chain. These injections allow for the calculation of basal and maximal respiration, spare respiratory capacity, coupling efficiency, ATP-linked O<sub>2</sub> consumption, proton leak, and non-mitochondrial O<sub>2</sub> consumption. The compounds consist of 1.5 μM oligomycin, 2 μM carbonyl cyanide-4 (trifluoromethoxy) phenylhydrazone (FCCP), and 0.5 μM rotenone and antimycin A. The day before the assay, the XFe96 sensor cartridge was filled with 200 μL Seahorse XF Calibrant Solution (Agilent, #100840-000) and placed in a non-CO<sub>2</sub> incubator at 37°C overnight. Seahorse XF RPMI medium, pH 7.4 (Agilent, # 103576-100) was supplemented with 10 mM glucose (Agilent, #103577-100), 1 mM sodium pyruvate (Agilent, #103578-100), and 2 mM glutamine (Agilent, #103579-100). The cells were then washed and resuspended in the complete medium (XF RPMI). The cells were then seeded into separate wells at a density of 315,000 cells/well in 180 μL. To prevent evaporation, the inner 60-wells were used<sup>192</sup>. The plate was centrifuged at 300 x G for 2 minutes.

The XFe96 sensor cartridge calibrated in the XFe96 Analyzer, while the cells were buffered in a non-CO<sub>2</sub> incubator for 45 minutes. Agilent's Seahorse XF Cell Mito Stress Test protocol was used to analyze mitochondrial respiration. The plate was imaged with transmitted light using the ImageXpress Pico Automated Cell Imaging

System (Molecular Devices) to normalize the respiration data in each well to the total seeding density. The total cell count of the well was then extrapolated based on the seeding density within the 1.92 mm<sup>2</sup> area of each well. The Seahorse data was analyzed using Agilent's online software (Seahorse Analytics). The wells were normalized to the total cell count with a scaling factor of 10000 and mitochondrial respiration was expressed as pmol/min/10,000 cells/well and glycolysis was expressed as mpH/min/10,000 cells/well. The definitions and calculations for each measure of mitochondrial respiration or glycolysis can be found in Appendix A. The background wells were also imaged and normalized to ensure all wells were treated consistently, despite not containing any cells.

### **3.2.9 Negative T-cell Separation and LDL-C Treatment**

Pan T-cells were separated from PBMCs using negative magnetic bead separation for flow cytometry experiments using the Pan T-cell Biotin Antibody Cocktail (Miltenyi Biotek, #130-096-535) and the Pan T-cell Microbead Cocktail (Miltenyi Biotek, #130-096-535) per the manufacturers protocol. The pan T-cells cells were then resuspended in CTS™ AIM-V™ Medium, without phenol red, without antibiotics (ThermoFisher, #A3830801) supplemented with 1x antibiotic-antimycotic (ThermoFisher, #15240062). For the T-cell dysfunction experiment, the samples the samples were treated with a low (71 mg/dL) and high (142 mg/dL) concentration of LDL-C (StemCell, #02698) for 20 hours. The LDL-C concentration in the LDL particles (LDL-P) were assessed by IDEXX BioAnalytics (Columbia, MO). As previously mentioned, the LDL-C concentrations measured varied from the concentrations provided by the manufacturer. Reported is the actual concentration the cells were treated with based on the IDEXX measurement. The cells were then placed

in a 37°C cell culture incubator with 5% CO<sub>2</sub>. For the intracellular cytokine experiment the cells were first treated with 2 μM monensin (Biolegend, #420701), a compound that blocks the transport of cytokines from the medial to trans cisternae for 24-hours<sup>219</sup>, and then treated with low (71 mg/dL) and high (142 mg/dL) concentration of LDL-C for 20 hours. Additionally, a subset of the samples was also treated with Cell Activation Cocktail (without Brefeldin A; Biolegend, #423301), per the manufacturer instructions for 12-hours. These samples were used as positive controls for cytokine production. Unstained controls were present for both flow cytometry experiments.

### **3.2.10 Flow Cytometry Experiments**

For the T-cell dysfunction experiment, samples incubated with 1 μm MitoSOX™ (PE Texas Red; Thermofisher, #M36008) for 30-minutes in a 37°C water bath in the dark. MitoSOX™ is a fluorogenic dye that specifically targets mitochondrial superoxide in T-cells<sup>220-222</sup>. The concentration was determined from preliminary experiments (Data not shown). The samples were then washed with flow buffer (1X PBS + 0.5% FBS) and stained with 1 μm BODIPY™ 493/503 (FITC; Invitrogen, #D3922) for 15-minutes at room temperature in the dark. The concentration was determined from preliminary experiments (data not shown). The samples were then washed and stained with the antibody cocktail for 30-minutes at room temperature in the dark.

For the intracellular cytokine experiment, the samples were first incubated with 1:1000 Zombie Red™ (561nm 610/20BP; Biolegend, 423109) for 10-minutes at room temperature in the dark. The samples were then washed with flow buffer and stained with the surface marker antibody cocktail for 15-minutes at room temperature in the

dark. Samples were washed and incubated with Cyto-Fast™ Fix Perm Solution for 20-minutes at room temperature in the dark (Biolegend, #426803), and then washed three times with 1x Cyto-Fast™ Perm Wash Solution (Biolegend, #426803) per the manufacturers protocol. Samples were then incubated with intracellular cytokine antibody cocktail for 20-minutes in the dark at room temperature.

The samples were analyzed using a BD FACSAria Fusion High Speed Cell Sorter. Samples were analyzed for 20,000 events. To correct for fluorescence spillover, compensation control experiments were performed (Data not shown). The compensation corrections were used in all experiments. The gating strategy for identifying CD3<sup>+</sup>, CD4<sup>+</sup>, and CD8<sup>+</sup> cells for both flow cytometry experiments can be found in figure 3.1 below. To define positive populations, the unstained untreated sample was used as the negative control for CD3<sup>+</sup> T-cells and viability dyes. CD4<sup>+</sup> was plotted against CD8<sup>+</sup>, and a threshold of 10<sup>3</sup> was used to define CD4<sup>+</sup> and CD8<sup>+</sup> T-cells. The surface marker-stained sample was only stained for CD3<sup>+</sup>, CD4<sup>+</sup>, and CD8<sup>+</sup> T-cells, and was used as a negative control for MitoSOX, BODIPY, CD69<sup>+</sup>, and inflammatory cytokines. For the T-cell dysfunction experiment, the effect of LDL-C on mitochondrial superoxide, intracellular lipids, T-cell activation, and T-cell senescent populations was assessed. The fully-stained sample was stained with all of the markers of interest for each experiment.

To assess the effect of LDL-C on mitochondrial superoxide, the percent of PE Texas Red MitoSOX™ positive CD4<sup>+</sup> and CD8<sup>+</sup> T-cells were plotted on a contour plot. To determine whether the LDL-C treatment increased intracellular lipids, the percent of FITC BODIPY™ 493/503 positive CD4<sup>+</sup> and CD8<sup>+</sup> T-cells were plotted on a contour plot. Finally, to determine the effect of LDL-C on T-cell activation, the

percentage of APC-Cy7 CD69<sup>+</sup> CD4<sup>+</sup> and CD8<sup>+</sup> T-cells were plotted on a contour plot. A double-positive gating strategy was used to define activated cells. As mentioned, the surface marker-stained sample was used to define CD69<sup>+</sup> cells, and the fully stained untreated sample was used to define CD69<sup>++</sup> cells vs. CD69<sup>+</sup>. Activated cells are those that are CD69<sup>++</sup>. To determine the effect of LDL-C on changes in CD4<sup>+</sup> and CD8<sup>+</sup> senescent T-cell populations, CD45RA was plotted against CD27. A threshold of 10<sup>3</sup> was used to identify positive populations for CD45RA vs. CD27. Naïve T-cells were identified as CD45RA<sup>+</sup> CD27<sup>+</sup>, central memory T-cells were identified as CD45RA<sup>-</sup> CD27<sup>+</sup>, effector memory T-cells were identified as CD45RA<sup>-</sup> CD27<sup>-</sup> and terminally differentiated were identified as CD45RA<sup>+</sup> CD27<sup>-</sup>. Although all T-cell populations contain senescent cells (e.g., β-galactosidase)<sup>223</sup>, effector memory and terminally differentiated T-cell populations contain the greatest proportion of senescent T-cells<sup>28,78,223</sup>. Additionally, terminally differentiated cells express a pro-inflammatory, senescent phenotype, and contain the greatest proportion of senescent cells<sup>28,78,223</sup>. Thus, for this study, terminally differentiated T-cells will be considered senescent.

For the intracellular cytokine experiment, the effect of LDL-C on intracellular cytokines was assessed. The same gating strategy was used to define live, CD3<sup>+</sup>, CD4<sup>+</sup> and CD8<sup>+</sup> T-cells (Figure 3.2). The surface marker-stained sample was used to define the negative inflammatory cytokine populations. Flow cytometry analysis was performed using FCS Express™ Flow Cytometry Software (De Nova Software, Pasadena, CA, version 7.16.0047). The percentage of each positive inflammatory cytokine listed in table 3 were plotted on a contour plot. These protocols were developed with the assistance of the University of Delaware's Flow Cytometry Core.

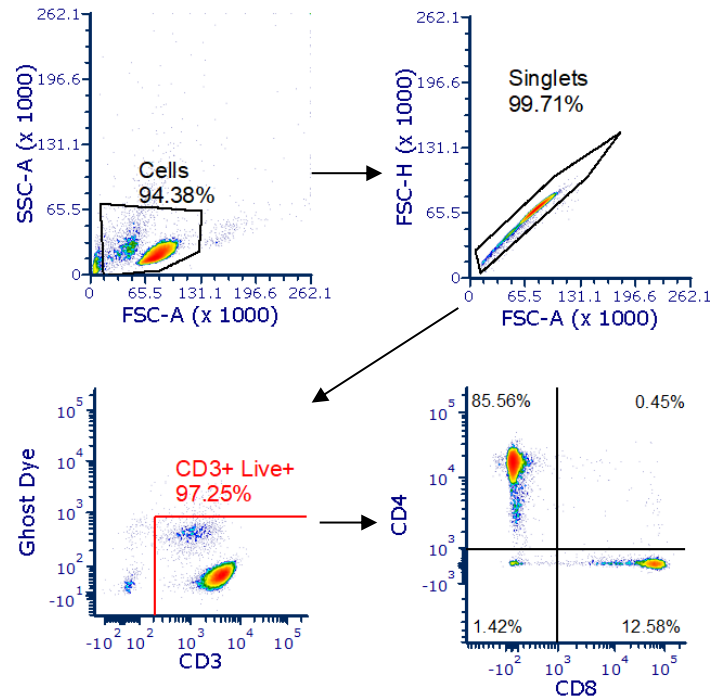


**Figure 3.1.** Representative Gating Strategy. The figure is a representation of the gating strategy used to identify CD3<sup>+</sup>, CD4<sup>+</sup>, and CD8<sup>+</sup> T-cells for both flow cytometry experiments. The only difference is the viability dye used in each experiment. In T-cell dysfunction experiment, Ghost Dye Violet 510 was used, and in the intracellular cytokine experiment, Zombie Red™ was used. For either experiment, live cells were identified as the populations negative for either viability dye.

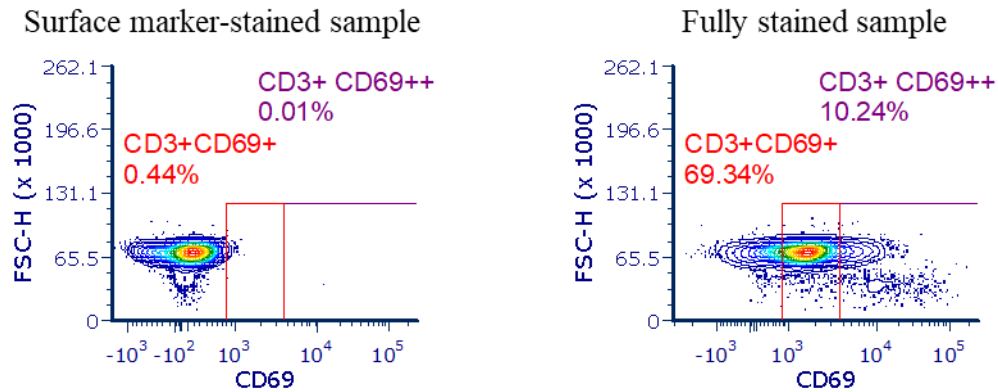


**Figure 3.2.** Gating strategy for CD69 marker. The figure is a representation of the gating strategy used to identify CD69<sup>+</sup> and CD69<sup>++</sup> T-cells. CD69<sup>++</sup> were considered activated.

### 3.2.11 Statistical Analysis

To assess data quality for any inconsistencies or problematic data, descriptive statistics were first performed for each variable. Any non-physiologic or impossible values were cross-referenced with existing records and corrected. Values that could not be corrected were either dropped or left in the analysis if there was sufficient rationale to do so. The robust regression and outlier removal method (ROUT) was used to define and remove outliers.

To assess the impact of cholesterol treatment level (high vs. low) on T-cell function, we used the Wilcoxon signed-rank test – one test for each measure of T-cell function. The Wilcoxon signed-rank test was also used to assess the differential effect of LDL-C on CD4<sup>+</sup> vs. CD8<sup>+</sup> T-cells. This test is 95% as powerful as the T-test when the data are drawn from normally distributed populations, and it can also accommodate non-normal scenarios at the relatively small sample sizes that this study hopes to recruit. An of  $n^* = 14$  allowed us to detect a large effect ( $d = 0.85$ ) for each of the tests described with 80% power. Spearman correlations matrices were used to determine the association between changes in measures of T-cell function between high and low LDL-C

treatment.  $\alpha$  was set at 0.05. GraphPad Prism 9 (GraphPad Prism 9.4.1.681) was used for all statistical analyses.

### 3.3 Results

Eighteen middle-aged ( $59 \pm 5$  years; 5 male, 13 female) participants were recruited for the study. Participants were generally healthy with normal BMI <sup>195</sup> and resting heart rate <sup>197</sup>, and exhibited elevated blood pressure (Table 3.1) <sup>196</sup>. Participants blood lipids were also normal with only slightly elevated LDL-C concentration, as would be expected with aging. However, the participant's LDL-C concentrations were well below our exclusion of 150 mg/dL. Participants leukocyte counts were also normal (Table 3.2).

**Table 3.1. Participant Characteristics**

<b>N=18</b>	<b>Mean <math>\pm</math> SD</b>	<b>Min-Max</b>
Age, years	$59 \pm 5$	52 – 64
Sex, Male/Female	5/13	-
Height, cm	$167.9 \pm 10.3$	149.4 – 182.4
Mass, kg	$71.0 \pm 18.4$	43.1 – 98.7
BMI, kg/m <sup>2</sup>	$24.9 \pm 4.5$	18.3 – 32.2
<i>Resting Central Hemodynamics</i>		
SBP, mmHg	$121 \pm 10$	104 – 138
DBP, mmHg	$73 \pm 6$	61 – 82
MAP, mmHg	$88 \pm 6$	75 – 97
PP, mmHg	$48 \pm 8$	36 – 69
HR, bpm	$60 \pm 8$	46 – 84

**Table 3.1.** Descriptive Statistics. Abbreviations: BMI, body mass index; SBP, systolic blood pressure; DBP, diastolic blood pressure; MAP, mean arterial pressure; PP, pulse pressure; HR, heart rate; & bpm, beats-per-minute.

**Table 3.2 Clinical Blood Chemistry**

<b>N=18</b>	<b>Mean ± SD</b>	<b>Min-Max</b>
<i>Metabolic Health</i>		
Total cholesterol, mg/dL	196 ± 27	140 – 236
HDL-C, mg/dL	71 ± 24	35 – 117
LDL-C, mg/dL	111 ± 23	69 – 149
VLDL-C, mg/dL	17 ± 11	7 – 49
Triglycerides, mg/dL	92 ± 67	39 – 279
Blood glucose, mg/dL	91 ± 9	73 – 102
<i>Leukocyte Count</i>		
WBC count, 1.0 x 10 <sup>3</sup> cells/μL	7.1 ± 11.0	2.9 – 51.0
Monocytes, 1.0 x 10 <sup>3</sup> cells/μL	0.4 ± 0.1	0.3 – 0.7
Lymphocytes, 1.0 x 10 <sup>3</sup> cells/μL	1.6 ± 0.7	0.8 – 4.1
Neutrophils, 1.0 x 10 <sup>3</sup> cells/μL	2.4 ± 0.8	1.2 – 3.5
Basophils, 1.0 x 10 <sup>3</sup> cells/μL	0.0 ± 0.0	0.0 – 0.0
Eosinophils, 1.0 x 10 <sup>3</sup> cells/μL	0.1 ± 0.1.	0.0 – 0.3

**Table 3.2.** Clinical Blood Chemistry. Abbreviations: HDL-C, high-density lipoprotein cholesterol; LDL-C, low-density lipoprotein cholesterol; VLDL-C, very low-density lipoprotein cholesterol; & WBC, white blood cell.

### *The Effect of LDL-C on Mitochondrial Respiration and Glycolysis*

We first assessed whether treatment with higher ( $133 \pm 13.6$  mg/dL), compared to lower ( $66 \pm 6.6$  mg/dL) concentrations of LDL-C impaired bioenergetics in CD4<sup>+</sup> T-cells (Table 3.3). Compared to the low LDL-C condition, the high LDL-C condition lowered basal OCR (low:  $0.75 \pm 0.34$  vs. high:  $0.65 \pm 0.35$  pMol/min/10,000 cells,  $p=0.022$ , Fig. 3.3A), ATP-Linked OCR (low:  $0.84 \pm 0.31$  vs. high:  $0.64 \pm 0.3$ ,  $p<0.0001$ , Fig. 3.3B), non-mitochondrial OCR (low:  $0.87 \pm 0.37$  vs. high:  $0.75 \pm 0.28$ ,  $p=0.030$ , Fig. 3.3C), and increased proton leak (low:  $-0.11 \pm 0.13$  vs. high:  $-0.03 \pm 0.13$ ,  $p=0.018$ , Fig. 3.3D) in CD4<sup>+</sup> T-cells (Table 3.3). There was no effect of LDL-C on CD4<sup>+</sup> maximal OCR, spare respiratory capacity, or coupling efficiency (Table 3.3). One data point for CD4<sup>+</sup> basal OCR had to be removed because it was not physiological. We then assessed whether high LDL-C treatment increased glycolysis in CD4<sup>+</sup> T-cells and found that the ratio of basal OCR/ECAR was decreased (low:  $0.29 \pm 0.79$  vs. high:  $2.16 \pm 0.81$  pH/min/10,000 cells,  $p=$ , Fig. 3.3F) following the treatment with high LDL-C compared to treatment with low LDL-C, indicating CD4<sup>+</sup> T-cells underwent a metabolic switch from oxidative to glycolytic metabolism. High LDL-C treatment also appeared to increase basal ECAR (low:  $0.25 \pm 0.09$  vs. high:  $0.28 \pm 0.12$  pH/min/10,000 cells,  $p=0.054$ , Fig. 3.3E), but this was not statistically significant. There was also no effect of the LDL-C treatment on maximal ECAR or the ratio of maximal OCR/ECAR (Table 3.3).

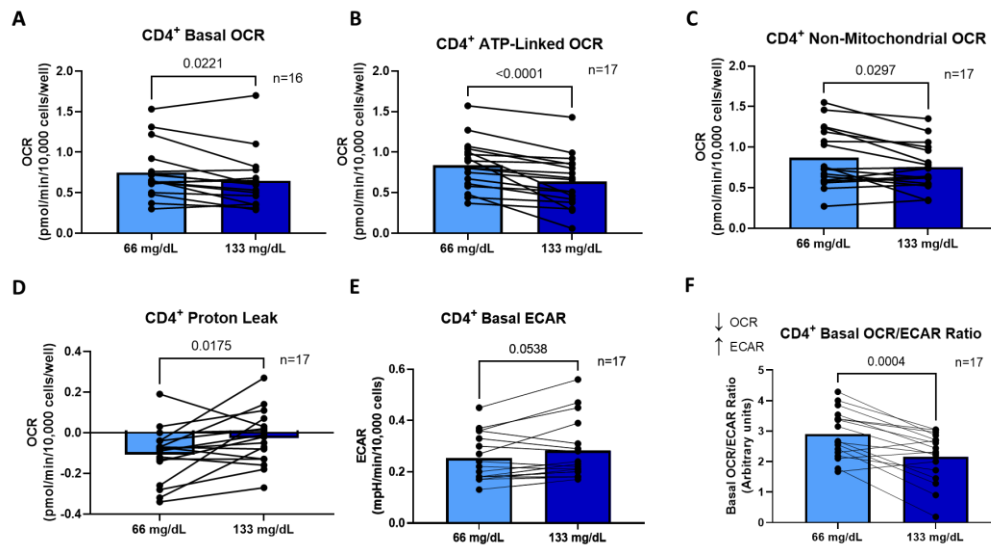


**Figure 3.3.** The Effect Of LDL-C on CD4<sup>+</sup> bioenergetics. CD4<sup>+</sup> T-cells were treated with a low (66 mg/dL) and high (133 mg/dL) for 20 hours and the following measures of mitochondrial respiration and glycolysis were calculated: A) basal OCR, B) ATP-linked OCR, C) non-mitochondrial OCR, D) proton leak, E) basal ECAR, F) the ratio of basal OCR/ECAR. Wilcoxon signed rank tests were used for statistical analysis. Data are presented as mean ± SD. Abbreviations: OCR, oxygen consumption rate; & ECAR, extracellular acidification rate.

**Table 3.3. The Effect of LDL-C on CD4<sup>+</sup> Mitochondrial Respiration and Glycolysis**

	Low LDL-C Mean ± SD	High LDL-C Mean ± SD	p-value	N
Basal OCR, pMol/min/10,000 cells	0.75 ± 0.34	0.65 ± 0.35	0.022	17
Proton leak, pMol/min/10,000 cells	-0.11 ± 0.13	-0.03 ± 0.13	0.018	17
Maximal OCR, pMol/min/10,000 cells	7.01 ± 4.36	6.66 ± 3.84	0.52	17
SRC OCR, pMol/min/10,000 cells	6.28 ± 4.07	6.05 ± 3.53	0.71	17
Non-mitochondrial OCR, pMol/min/10,000 cells	0.87 ± 0.37	0.75 ± 0.28	0.030	17
ATP-linked OCR, pMol/min/10,000 cells	0.84 ± 0.31	0.64 ± 0.3	<0.0001	17
Coupling efficiency, %	122.20 ± 21.90	113.72 ± 33.12	0.25	17
Basal ECAR, mpH/min/10,000 cells	0.25 ± 0.09	0.28 ± 0.12	0.054	17
Maximal ECAR, mpH/min/10,000 cells	1.13 ± 0.55	1.03 ± 0.50	0.15	17
Basal OCR/ECAR ratio, a.u.	2.90 ± 0.79	2.16 ± 0.81	0.0004	17
Maximal OCR/ECAR ratio, a.u.	6.05 ± 1.03	6.19 ± 1.41	0.41	17

**Table 3.3.** The Effect of LDL-C on CD4<sup>+</sup> Mitochondrial Respiration and Glycolysis. Wilcoxon signed rank tests were used to assess the effect of low (66 mg/dL) vs. high (133 mg/dL) LDL-C treatment on measures of mitochondrial respiration and glycolysis in CD4<sup>+</sup> and CD8<sup>+</sup> T-cells. Abbreviations: OCR, oxygen consumption rate; SRC, spare respiratory capacity; ECAR, extracellular acidification rate; & LDL-C, low-density lipoprotein cholesterol.

We next assessed the effect of LDL-C on CD8<sup>+</sup> bioenergetics. Compared with the low LDL-C condition, the higher LDL-C condition impaired ATP-Linked OCR (low: 0.85 ± 0.44 vs. high: 0.64 ± 0.14, p=<0.0024, Fig. 3.4B) and increased proton leak (low: -0.24 ± 0.15 vs. high: -0.11 ± 0.16, p=<0.012, Fig. 3.4D) and appeared to exert a similar effect on CD8<sup>+</sup> basal OCR; however, this was not statistically

significant. The higher LDL-C condition also did not affect non-mitochondrial OCR, maximal OCR, spare respiratory capacity, or coupling efficiency (Table 3.4). One data point had to be removed for CD8<sup>+</sup> coupling efficiency and ATP-linked OCR because they were non-physiologic. Like CD4<sup>+</sup> cells, we found that the higher LDL-C condition increased CD8<sup>+</sup> basal ECAR (low:  $0.20 \pm 0.07$  vs. high:  $0.23 \pm 0.09$ ,  $p <$ , Fig. 3.4B) and lowered the basal ratio of OCR/ECAR (low:  $2.78 \pm 0.84$  vs. high:  $2.05 \pm 0.77$ ,  $p = 0.0001$ , Fig. 3.4B) relative to the low LDL-C condition, indicating a metabolic shift towards glycolysis. There was no effect of higher LDL-C on CD8<sup>+</sup> maximal ECAR or the maximal ratio of OCR/ECAR (Table 3.4).

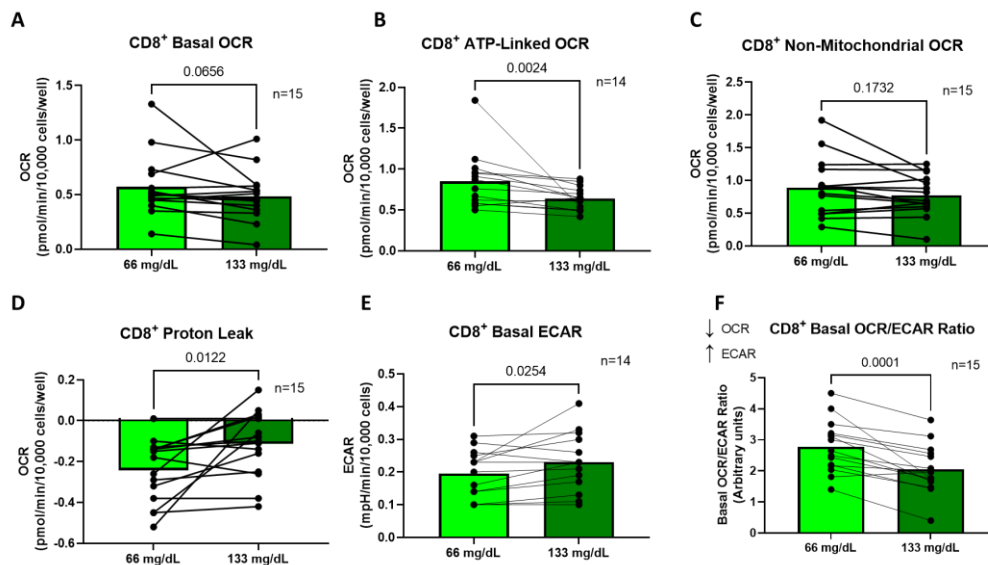


**Figure 3.4.** The Effect Of LDL-C on CD8<sup>+</sup> bioenergetics. CD8<sup>+</sup> T-cells were treated with a low (66 mg/dL) and high (133 mg/dL) for 20 hours and the following measures of mitochondrial respiration and glycolysis were calculated: A) basal OCR, B) ATP-linked OCR, C) non-mitochondrial OCR, D) proton leak, E) basal ECAR, F) the ratio of basal OCR/ECAR. Wilcoxon signed rank tests were used for statistical analysis. Data are presented as mean  $\pm$  SD. Abbreviations: OCR, oxygen consumption rate; & ECAR, extracellular acidification rate.

**Table 3.4. The Effect of LDL-C on CD8<sup>+</sup> Mitochondrial Respiration and Glycolysis**

	Low LDL-C Mean ± SD	High LDL-C Mean ± SD	p-value	N
Basal OCR, pMol/min/10,000 cells	0.57 ± 0.28	0.49 ± 0.23	0.066	15
Proton leak, pMol/min/10,000 cells	-0.24 ± 0.15	-0.11 ± 0.16	0.012	15
Maximal OCR, pMol/min/10,000 cells	7.42 ± 5.25	7.51 ± 3.88	0.37	15
SRC OCR, pMol/min/10,000 cells	6.86 ± 5.07	7.02 ± 3.73	0.39	15
Non-mitochondrial OCR, pMol/min/10,000 cells	0.89 ± 0.44	0.77 ± 0.31	0.17	15
ATP-linked OCR, pMol/min/10,000 cells	0.85 ± 0.35	0.64 ± 0.14	0.0024	14
Coupling efficiency, %	155.89 ± 40.39	113.36 ± 54.54	0.060	14
Basal ECAR, mpH/min/10,000 cells	0.20 ± 0.07	0.23 ± 0.09	0.025	14
Maximal ECAR, mpH/min/10,000 cells	1.02 ± 0.44	1.07 ± 0.46	0.40	14
Basal OCR/ECAR ratio, a.u.	2.78 ± 0.84	2.05 ± 0.77	0.0001	15
Maximal OCR/ECAR ratio, a.u.	6.21 ± 1.09	6.50 ± 1.45	0.23	15

**Table 3.4.** The Effect of LDL-C on CD8<sup>+</sup> Mitochondrial Respiration and Glycolysis. Wilcoxon signed rank tests were used to assess the effect of low (66 mg/dL) vs. high (133 mg/dL) LDL-C treatment on measures of mitochondrial respiration and glycolysis in CD8<sup>+</sup> T-cells. Abbreviations: OCR, oxygen consumption rate; SRC, spare respiratory capacity; ECAR, extracellular acidification rate; & LDL-C, low-density lipoprotein cholesterol.

We then sought to determine whether LDL-C differentially affected CD4<sup>+</sup> vs. CD8<sup>+</sup> bioenergetics. An exploratory analysis was performed by calculating and comparing the percent change between treatment with high and low LDL-C for each measure of OCR and ECAR and compared that was significant in both CD4<sup>+</sup> and CD8<sup>+</sup> T-cells. There was no difference between the effect of high LDL-C treatment on CD4<sup>+</sup> or CD8<sup>+</sup> ATP-linked OCR (CD4<sup>+</sup>: -25.20 ± 23.50 vs. CD8<sup>+</sup>: -18.73 ± 20.02

pMol/min/10,000 cells,  $p=0.86$ ), proton leak ( $CD4^+$ :  $-86.42 \pm 219.25$  vs.  $CD8^+$ :  $-44.55 \pm 60.84$ ,  $p=0.15$ ), or basal ratio of OCR/ECAR ( $CD4^+$ :  $-25.20 \pm 27.70$  vs.  $CD8^+$ :  $-26.60 \pm 20.03$  mpH/min/10,000 cells,  $p=0.42$ ). However, LDL-C seemed to affect basal ECAR to a greater extent in  $CD8^+$  cells compared with  $CD4^+$  cells, as the change in basal ECAR appeared higher after the treatment with high LDL-C ( $CD4$ :  $12.10 \pm 17.52$  vs.  $CD8$ :  $19.21 \pm 25.07\% \Delta$ ,  $p=0.068$ ), although this was not statistically significant.

These data suggest that treatment with a higher concentration of LDL-C impairs  $CD4^+$  and  $CD8^+$  T-cell basal oxidative metabolism and metabolism linked to ATP-production. Additionally, the treatment with a higher concentration of LDL-C appeared to augment  $CD4^+$  and  $CD8^+$  T-cell glycolysis.  $CD8^+$  T-cell glycolytic metabolism may also be more sensitive to LDL-C treatment, as basal ECAR appeared to increase to a greater extent in  $CD8^+$  T-cells, compared to  $CD4^+$  T-cells.

#### *The Effect of LDL-C on T-cell Function*

We next sought to determine the effect of LDL-C on  $CD4^+$  and  $CD8^+$  lipid uptake, mitochondrial reactive oxygen species (mtROS), activation, T-cell differentiation, and senescence (e.g., terminal differentiation). High LDL-C (142 mg/dL) increased intracellular lipid uptake (low:  $81.62 \pm 20.80$  vs. high:  $91.13 \pm 18.17$  % gated from plot,  $p=0.043$ , Fig 3.5A), mtROS (low:  $11.23 \pm 7.12$  vs. high:  $36.04 \pm 35.43$ ,  $p=0.0026$ , Fig 3.5B), and activation (low:  $6.78 \pm 5.77$  vs. high:  $19.16 \pm 20.51$ ,  $p=0.0093$ , Fig 3.5C), compared to treatment with low LDL-C (72 mg/dL) in  $CD4^+$  T-cells. Because LDL-C increased activation, we also investigated T-cell differentiation following LDL-C treatment. High LDL-C did not alter  $CD4^+$  naïve populations (low:

32.02 ± 13.81 vs. high: 30.98 ± 14.15, p=0.28, Fig 3.5D), but decreased the proportion of CD4<sup>+</sup> central memory T-cells (low: 49.55 ± 10.83 vs. high: 42.31 ± 9.01, p=0.0001, Fig 3.5E) and increased the proportion of CD4<sup>+</sup> effector memory (low: 17.39 ± 7.79 vs. high: 24.31 ± 11.46, p=, Fig 3.5F) and terminally differentiated (low: 1.04 ± 1.40 vs. high: 2.40 ± 2.52, p=, Fig 3.5G) T-cells.

Treatment with high LDL-C also increased CD8<sup>+</sup> T-cell lipid uptake (low: 72.92 ± 28.24 vs. high: 89.95 ± 14.67 % gated from plot, p=0.0085, Fig 3.6A), mitochondrial ROS (low: 4.90 ± 5.35 vs. high: 20.17 ± 22.19 , p=0.0024, Fig 3.6B) compared with low LDL-C. Similar to CD4<sup>+</sup> T-cells, the treatment with LDL-C increased activation (low: 12.75 ± 11.73 vs. high: 27.91 ± 26.87, p=0.0009, Fig 3.6C) in CD8<sup>+</sup> T-cells. We then investigated the effect of high LDL-C treatment on CD8<sup>+</sup> T-cell differentiation and found significantly decreased naïve (low: 37.83 ± 15.56 vs. high: 33.28 ± 16.58, p=0.010, Fig 3.6D), central memory (low: 33.71 ± 12.73 vs. high: 30.08 ± 11.75, p=, Fig 3.6D), and increased effector memory (low: 14.56 ± 7.10 vs. high: 21.36 ± 8.98, p=, Fig 3.6E) and senescence (e.g., terminally differentiated) (low: 13.01 ± 7.78 vs. high: 14.86 ± 8.10, p=, Fig 3.6F) in CD8<sup>+</sup> T-cells. Importantly, there was only a small reduction in CD3<sup>+</sup> viability following treatment with high LDL-C, compared with low LDL-C (low: 92.9 vs. 88.8%, p=0.0092).

We then performed an exploratory analysis to assess whether LDL-C differentially effected CD4<sup>+</sup> and CD8<sup>+</sup> T-cell function by calculating the percent change in lipid uptake, mtROS, activation, and T-cell differentiation from treatment with high and low LDL-C in CD4<sup>+</sup> and CD8<sup>+</sup> T-cells. Treatment with high LDL-C increased intracellular lipid uptake (CD4: 16.74 ± 34.45 vs. CD8: 46.57 ± 74.79%Δ, p=0.034) and appeared to increase mtROS (CD4: 234.52 ± 314.28 vs. CD8: 321.03 ±

376.05  $p=0.068$ ) to a greater extent in CD8<sup>+</sup> compared to CD4<sup>+</sup> T-cells. Although, the difference in mtROS production in response to high LDL-C was not statistically significant between CD4<sup>+</sup> vs. CD8<sup>+</sup> T-cells. There was also no differential effect of LDL-C on CD4<sup>+</sup> and CD8<sup>+</sup> T-cell activation (CD4:  $205.7 \pm 293.3$  vs. CD8:  $123.2 \pm 161.9$ ,  $p=0.47$ ). Additionally, treatment with high LDL-C significantly increased senescent CD4<sup>+</sup> T-cells to a greater extent compared to CD8<sup>+</sup> T-cells (CD4:  $291.39 \pm 480.78$  vs. CD8:  $18.57 \pm 32.33$ ,  $p=0.0015$ ). There was no differential effect of LDL-C on CD4<sup>+</sup> or CD8<sup>+</sup> central (CD4:  $-13.54 \pm 12.70$  vs. CD8:  $10.09 \pm 12.19$   $p=0.59$ ) or effector (CD4:  $48.99 \pm 71.91$  vs. CD8:  $61.02 \pm 80.63$ ,  $p=0.30$ ) memory populations.

Treatment with LDL-C increased intracellular lipids and mtROS in CD4<sup>+</sup> and CD8<sup>+</sup> T-cells. Although, CD8<sup>+</sup> T-cells appear to be more sensitive to lipid uptake and mtROS production following treatment with higher LDL-C. Additionally, higher LDL-C treatment increased activation in CD4<sup>+</sup> and CD8<sup>+</sup> T-cells, decreased the proportion of CD8<sup>+</sup> naïve T-cells and CD4<sup>+</sup> and CD8<sup>+</sup> central memory T-cells, and increased CD4<sup>+</sup> and CD8<sup>+</sup> effector memory and senescent T-cell populations. CD4<sup>+</sup> T-cells appear to be more susceptible to undergo senescence following treatment with high LDL-C.

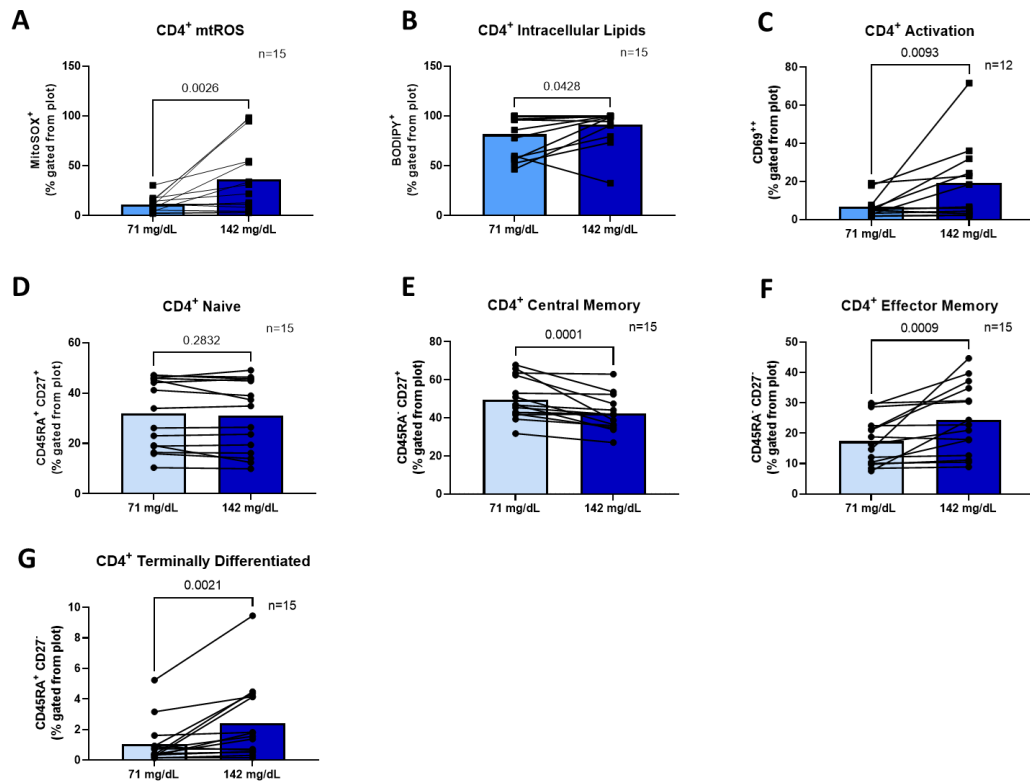


**Figure 3.5.** The Effect Of LDL-C on CD4<sup>+</sup> T-cell Function. CD4<sup>+</sup> and CD8<sup>+</sup> were treated with a low (71 mg/dL) and high (142 mg/dL) concentration of LDL-C for 20 hours. The following variables were measured in CD4<sup>+</sup> using flow cytometry: A) intracellular lipids, B) mtROS, C) T-cell activation, D) central memory populations, E) effector memory populations, & F) terminally differentiated populations. Wilcoxon signed-rank tests were used for statistical analyses. Data are presented as mean  $\pm$  SD. Abbreviations: mtROS, mitochondrial reactive oxygen species.

### *The Effect of LDL-C on T-cell Intracellular Cytokines*

Because we saw a shift in mitochondrial bioenergetics, activation status, and T-cell populations towards a pro-inflammatory phenotype, we also assessed the effect of LDL-C on inflammatory cytokine production in CD4<sup>+</sup> and CD8<sup>+</sup> T-cells. We found that production of pro-inflammatory cytokines IL-6 (low:  $72.49 \pm 21.47$  vs. high:  $77.19 \pm 22.42\%$  gated from plot,  $p=0.0092$ , Fig. 3.7B) and IL-1 $\beta$  (low:  $7.73 \pm 9.59$  vs.

high:  $16.60 \pm 25.85$ ,  $p=0.0056$ , Fig. 3.7C) were increased in CD4<sup>+</sup> T-cells following treatment with high LDL-C. This was coupled with an increase in intracellular anti-inflammatory cytokine IL-10 (low:  $5.13 \pm 9.21$  vs. high:  $12.28 \pm 19.96$ ,  $p=0.0013$ , Fig 3.7A). The pro-inflammatory cytokine IL-17A also appeared to increase following the treatment with high LDL-C (low:  $0.63 \pm 1.30$  vs. high:  $0.97 \pm 1.79$ ,  $p=0.081$ ), however this was not statistically significant. There was no effect of the high LDL-C treatment on INF- $\gamma$  (low:  $4.14 \pm 5.48$  vs. high:  $4.06 \pm 4.77$ ,  $p=0.58$ ) or TNF- $\alpha$  (low:  $26.20 \pm 15.79$  vs. high:  $28.00 \pm 15.47$ ,  $p=0.26$ ).

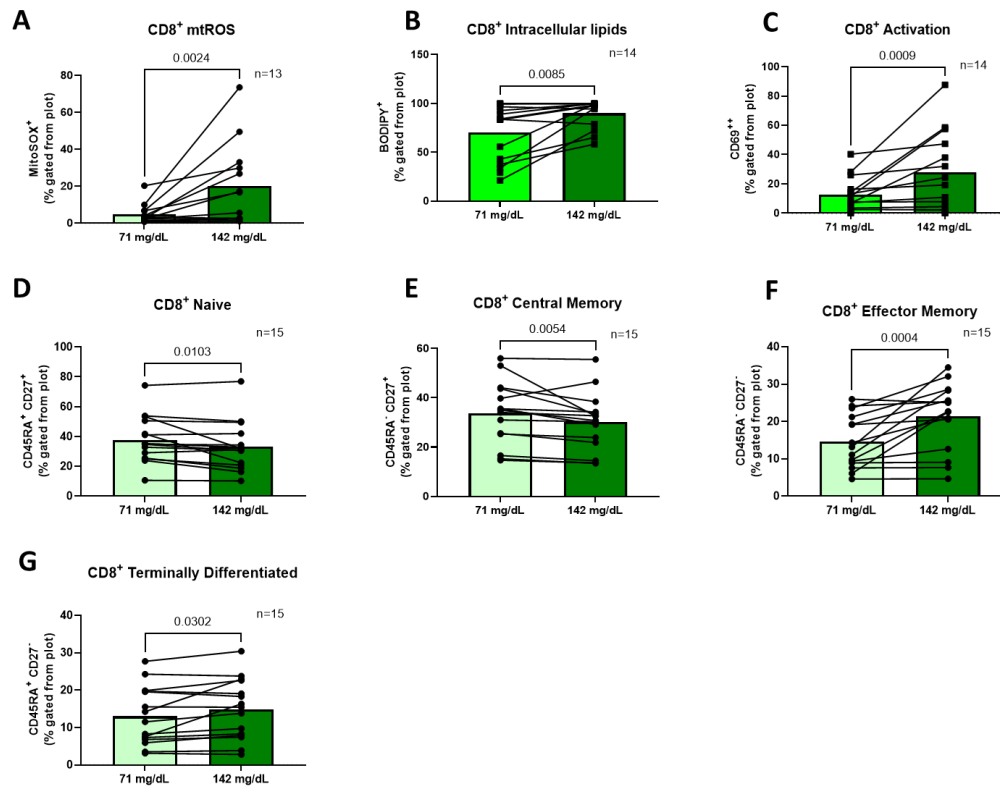


**Figure 3.6.** The Effect Of LDL-C on CD8<sup>+</sup> T-cell Function. CD4<sup>+</sup> and CD8<sup>+</sup> were treated with a low (71 mg/dL) and high (142 mg/dL) concentration of LDL-C for 20 hours. The following variables were measured in CD8<sup>+</sup> using flow cytometry: A) intracellular lipids, B) mtROS, C) T-cell activation, D) central memory populations, E) effector memory populations, & F) terminally differentiated populations. Wilcoxon signed-rank tests were used for statistical

analyses. Data are presented as mean  $\pm$  SD. Abbreviations: mtROS, mitochondrial reactive oxygen species.

Similarly, LDL-C increased intracellular production of pro-inflammatory cytokines IL-6 (low:  $74.48 \pm 25.54$  vs. high:  $78.82 \pm 26.45$  % gated from plot,  $p=0.0044$ , Fig. 3.7E) and IL- $1\beta$  (low:  $11.13 \pm 15.62$  vs. high:  $20.75 \pm 30.02$ ,  $p=0.0151$ , Fig. 3.7F), and increased production of anti-inflammatory cytokine IL-10 (low:  $1.84 \pm 3.00$  vs. high:  $6.94 \pm 10.99$ ,  $p=0.0009$ , Fig. 3.7D). Surprisingly, pro-inflammatory cytokine TNF- $\alpha$  was significantly lower following the treatment with high LDL-C (low:  $11.83 \pm 7.83$  vs. high:  $8.19 \pm 6.64$ ,  $p=0.0076$ ), and appeared to decrease pro-inflammatory cytokine IL-17A (low:  $0.30 \pm 0.41$  vs. high:  $0.22 \pm 0.32$ ,  $p=0.060$ ), although this was not statistically significant. There was no effect of the high LDL-C treatment on CD3<sup>+</sup> viability compared with low LDL-C treatment (low: 92.3 vs. high: 91.6%,  $p=0.71$ )

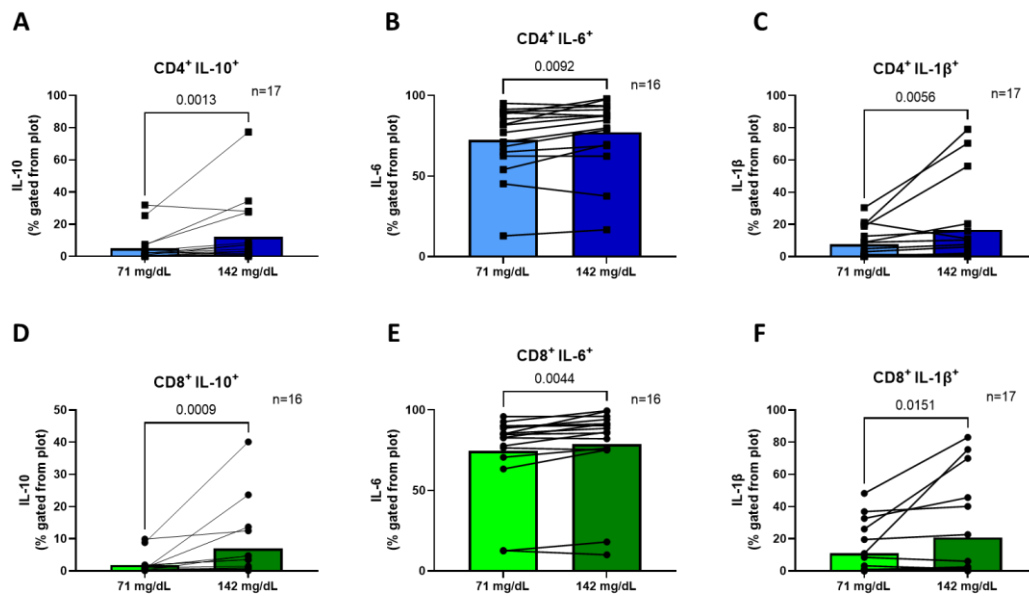


**Figure 3.7.** The Effect Of LDL-C on CD4<sup>+</sup> and CD8<sup>+</sup> T-cell Cytokine Production. CD4<sup>+</sup> and CD8<sup>+</sup> were treated with a low (71 mg/dL) and high (142 mg/dL) concentration of LDL-C for 20 hours. The production of the following intracellular cytokines was measured using flow cytometry: A) CD4<sup>+</sup> IL10, B) CD4<sup>+</sup> IL-6, C) CD4<sup>+</sup> IL-1β, D) CD8<sup>+</sup> IL-10, E) CD8<sup>+</sup> IL-6, & F) CD8<sup>+</sup> IL-1β. Wilcoxon signed-rank tests were used for statistical analyses. Data are presented as mean ± SD.

We then wanted to determine whether treatment with high LDL-C differentially affected cytokine production in CD4<sup>+</sup> and CD8<sup>+</sup> T-cells. As was done previously, we performed an exploratory analysis and calculated and compared the percent change from high to low LDL-C treatment in CD4<sup>+</sup> and CD8<sup>+</sup> T-cells. Treatment with high LDL-C did not differentially affect IL-10 (CD4: 330.47 ± 385.86 vs. CD8: 491.26 ± 972.18%Δ, p=0.30), IL-6 (CD4: 7.76 ± 11.82 vs. CD8: 6.68 ± 13.58%Δ, p=0.36), or IL-1β (CD4: 770.02 ± 2624.77 vs. CD8: 78.75 ± 159.99%Δ, p=0.81).

Treatment with higher LDL-C increased anti-inflammatory cytokine IL-10 and pro-inflammatory cytokines IL-6 and IL-1β in CD4<sup>+</sup> and CD8<sup>+</sup> T-cells. There was no differential effect of LDL-C on CD4<sup>+</sup> or CD8<sup>+</sup> T-cell cytokine production.

*The Interaction Between T-cell Lipid Uptake, Bioenergetics, Dysfunction, and Inflammation.*

Finally, to determine whether the changes in T-cell function were associated with one another, the percentage change in each measure of T-cell function was calculated between the high and low LDL-C conditions, and a Spearman correlation matrix was performed to correlate the changes in each measure of CD4<sup>+</sup> and CD8<sup>+</sup> T-cell function with one another (Fig 3.8A&B).

In CD4<sup>+</sup> T-cells we found that the increase in intracellular lipids was associated with an increase in activation following treatment with high LDL-C (R=0.69, p=0.016), which was associated with increased mtROS (R=0.88, p=0.00033). Although it was not associated with activation, increased basal ECAR was associated with increased mtROS (R=0.61, p=0.24). CD4<sup>+</sup> T-cell activation was also associated with an increase in activated effector memory (R=0.57, p=0.036) and senescent T-cells (R=0.70, p=0.0072). The increase in activation was also associated with increased intracellular IL-10 (R=0.59, P=0.046) and IL-1 $\beta$  production (R=0.97, P=0.0000061). Effector memory and senescent T-cells were also associated with increased IL-6 and IL-1 $\beta$  (Figure 3.8). These data indicate that increases in activation and glycolysis in CD4<sup>+</sup> T-cells may increase oxidative stress and inflammation.

We next assessed whether the changes in CD8<sup>+</sup> T-cell function following the treatment with high LDL-C were associated with one another. Like in CD4<sup>+</sup> T-cells, we found that the increase in CD8<sup>+</sup> basal ECAR in response to LDL-C was also associated with increased CD8<sup>+</sup> T-cell mtROS production (R=0.71, p=0.043), as was the decrease in the ratio of basal OCR/ECAR (R=-0.69, p=0.023). These findings suggest that greater glycolytic activity may promote a greater the production of

mtROS. Additionally, the reduction in CD8<sup>+</sup> basal OCR was associated with increased production of anti-inflammatory cytokine IL-10 (R=0.57, p=0.035) and pro-inflammatory cytokine IL1- $\beta$  (R=0.86, p=0.00028) in CD8<sup>+</sup> T-cells. Thus, the reduction in mitochondrial respiration following the treatment with high LDL-C could increase the inflammatory phenotype of the cell. The increase in activation was also associated with increased effector memory (R=0.85, p=0.00043) and a decrease in naïve T-cell populations (R=-0.71, P=0.0086) which could indicate that the effector memory T-cells are activated because of decreased naïve CD8<sup>+</sup> T-cell populations following treatment with high LDL-C. An increase in CD8<sup>+</sup> mtROS following treatment with high LDL-C was associated with increased activation (R=0.63, p=0.044) and effector memory populations (R=0.76, p=0.031). Like in CD4<sup>+</sup> T-cells, these data indicate that increased T-cell activation or activated effector memory populations increases oxidative stress.

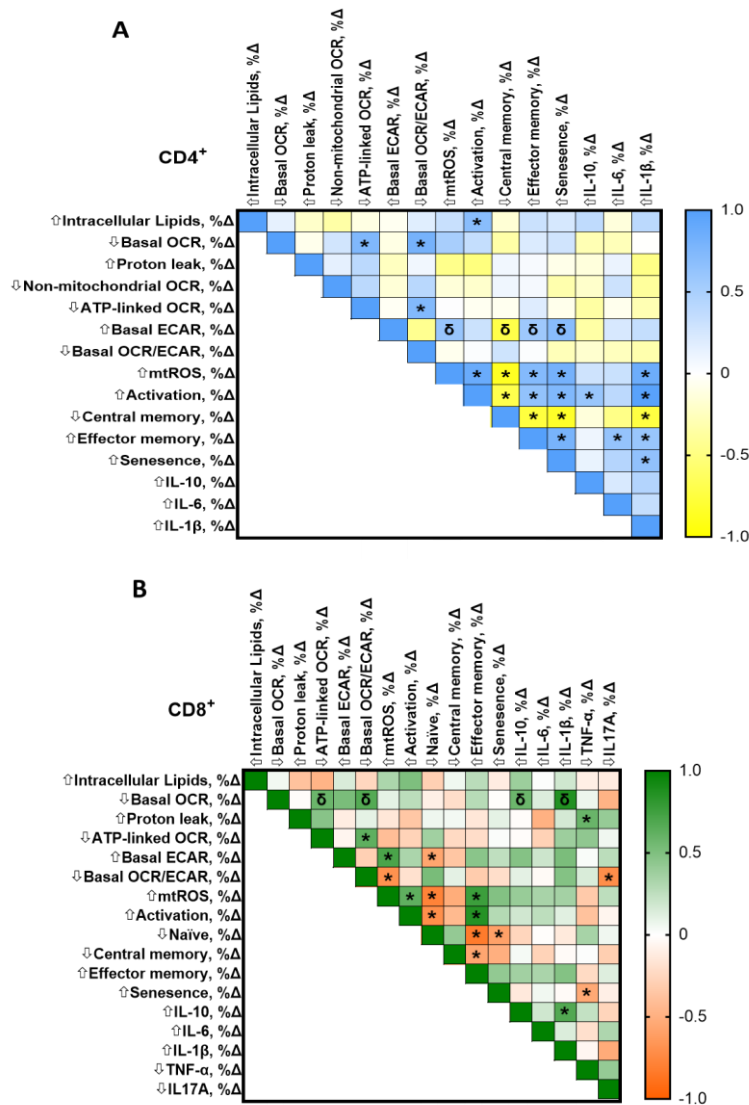


**Figure 3.8.** The Associations Between Measures of CD4<sup>+</sup> and CD8<sup>+</sup> T-cell Function in Response to LDL-C. A) Spearman correlations between the percentage changes in CD4<sup>+</sup> T-cell function following treatment with high compared with low LDL-C. B) Spearman correlations between the percentage changes in CD8<sup>+</sup> T-cell function following treatment with high compared with low LDL-C. \*p<0.05. δ indicates significance p<0.05 for changes in measures of T-cell function that were close to, but not significant (<0.07).

### 3.4 Discussion

We found that exogenous treatment of CD4<sup>+</sup> and CD8<sup>+</sup> T-cells with higher LDL-C induced T-cell activation and impaired mitochondrial respiration, shifting T-cells towards a more glycolytic metabolism. Our data also suggest that T-cell activation and alterations in mitochondrial function may accelerate T-cell differentiation and contribute to T-cell senescence, as evidenced by the observed decrease in the proportion of central memory T-cells, and the increase proportion of effector memory and terminally differentiated T-cells. The highest LDL-C condition also increased mitochondrial oxidative stress and inflammation in both CD4<sup>+</sup> and CD8<sup>+</sup> T-cells, which may have been a result of the impaired mitochondrial function and increased glycolysis, T-cell activation, and/or the shift towards activated effector memory and senescent cells. Collectively, these findings may indicate that the characteristic increase in endogenous LDL-C observed with normal aging<sup>57</sup> may cause accelerated T-cell aging, contributing to the inflammaging phenotype.

When T-cells are activated, they undergo a metabolic shift to quickly produce energy to respond to a pathogen, resulting in increased glycolysis, and to an extent increased oxidative phosphorylation<sup>3,84-86</sup>. Our data support a role for LDL-C in initiating this process, as we found higher LDL-C increased CD4<sup>+</sup> and CD8<sup>+</sup> T-cell activation and this was correlated with increased glycolytic activity and mtROS production. These data are consistent with our hypothesis that LDL-C activates T-cells, impairing oxidative phosphorylation, and shifting T-cells towards glycolytic metabolism, resulting in increased generation of mtROS.

LDL-C has been shown to act as an “neo-antigen” as it is bound to the major histocompatibility complex (MHC) for presentation by antigen-presenting cells (APCs)<sup>51-53</sup>. T-cells that are reactive to LDL-C as a neo-antigen become more pro-

inflammatory, including normally anti-inflammatory CD4<sup>+</sup> regulatory T-cells<sup>52</sup>. APCs were not present in culture with the T-cells; thus, it seems unlikely APCs are presenting LDL-C to T-cells. This seems to suggest that T-cells are activated independently of MHC-antigen presentation to even moderately elevated LDL-C concentrations. This is supported by the observation that there were limited associations between changes in measures of T-cell function and the increase in intracellular lipids following high LDL-C treatment. Despite these data, it is possible that the accumulation of cholesterol in the cell is altering mitochondrial function in other ways, for example by inducing mitochondrial DNA damage, inhibiting the transport of antioxidants into the mitochondria, or decreasing mitochondrial mass<sup>50,75</sup>.

Aging is associated with thymic involution and a reduced T-cell repertoire, resulting in an imbalance of naïve to memory T-cells and an accumulation of senescent T-cells<sup>28</sup>. It is possible that age-related elevations in LDL-C exacerbate these population imbalances and drive increases in senescent T-cells earlier in life. In accordance with this hypothesis, we observed an increase in both CD4<sup>+</sup> and CD8<sup>+</sup> effector memory and terminally differentiated or senescent T-cells, and a decrease in CD4<sup>+</sup> and CD8<sup>+</sup> central memory T-cells and a decrease in CD8<sup>+</sup> naïve T-cells following treatment with high LDL-C. These data may suggest activation of naïve T-cells and re-activation of central memory T-cells and differentiation into effector memory T-cells or, for those cells that have been repetitively activated, a transition to senescence. Indeed, increased activation was associated with a decrease in the proportion of CD4<sup>+</sup> central memory cells and CD8<sup>+</sup> naïve T-cells, and an increased proportion of CD4<sup>+</sup> and CD8<sup>+</sup> effector memory and CD4<sup>+</sup> senescent T-cells. Treatment with LDL-C also increased the proportion of effector memory and

terminally differentiated (senescent) T-cells. This is consistent with a recent publication showing that intracellular cholesterol accumulation modulates the senescent phenotype, and that these cells exhibit increased glycolytic gene expression<sup>224</sup>. Our data suggest that chronically elevated LDL-C concentrations may induce early T-cell aging through repetitive activation, leading to activated and senescent pro-inflammatory T-cells. In this respect, we found that treatment with high LDL-C increased the production of pro-inflammatory cytokines IL-6 and IL-1 $\beta$  and anti-inflammatory cytokine IL-10 in both CD4<sup>+</sup> and CD8<sup>+</sup> T-cells. Thus, preserving mitochondrial function by maintaining low concentrations of LDL-C will be important to prevent the accumulation of glycolytic, pro-inflammatory senescent cells.

We also found that treatment with high LDL-C increased proton leak, which is a marker of mitochondrial damage<sup>225,226</sup> in both CD4<sup>+</sup> and CD8<sup>+</sup> T-cells. LDL-C has been linked to increased mitochondrial damage and decreased mitochondrial respiration in other cells, such as macrophages, in part because of decreased antioxidant capacity, mitochondrial DNA, and mitophagy, and increased mitochondrial oxidative stress<sup>50</sup>, so it is possible these mechanisms are conserved in T-cells. Although, we did not measure T-cell antioxidant capacity, mitochondrial DNA, or mitophagy in this study, mitochondrial oxidative stress did was increased. High LDL-C treatment impaired basal OCR and ATP-linked OCR and augmented proton leak. Our findings are consistent with a previous study showing that treatment with LDL-C in  $\gamma\delta$  T-cells decreased in ATP production, mtDNA, and mitochondrial mass following treatment with LDL-C<sup>75</sup>. However, it is worth noting that they also saw a decrease in ROS, impaired T-cell activation, and impaired INF- $\gamma$  production<sup>75</sup>. This study used a very low concentration of LDL-C (e.g., 10 mg/dL), and it is possible

that T-cells may require a certain concentration of LDL-C for normal physiologic function. This prior study also highlights the importance of the LDL receptor to cellular function, and its relation to cholesterol uptake. Thus, it may be difficult to dissociate the effect of the cellular uptake from the cholesterol in the LDL-P from the interaction between the LDL-P and the membrane receptor.

This study has a few limitations. Many of these mechanisms are integrated (e.g., oxidative stress and mitochondrial respiration), thus it is difficult to determine causality from our present dataset. We were also not able to discern the effects of the LDL-P interacting with the membrane receptor and from the effect of LDL-C itself. As we saw that lipid accumulation was not associated with many markers of T-cell function, it is likely that LDL-P is exerting these effects through its interaction with the membrane receptor. Future studies should consider blocking the LDL-P receptor or depleting cholesterol from the LDL-P to confirm these findings in  $\alpha\beta$  T-cells. We also did not measure functional senescent markers (e.g., senescence-associated  $\beta$ -galactosidase, senescence marker protein-30, p53, or p16) or a quantitative measure of glycolysis, and future studies should incorporate these functional markers of senescence and more exact measures of glycolysis.

To have a representative sampling of middle-aged adults, we recruited participants with a wide range of blood LDL-C concentrations (69-149 mg/dL) that were not on lipid lowering medications. We intended to treat T-cells from these participants at much higher concentrations of LDL-C (e.g., 200 mg/dL); however, discrepancies in reported LDL-C concentrations by the manufacturers led to us treating the cells with lower concentrations than expected. Thus, the “high” LDL-C treatment might not have provided a robust stimulus in participants with “borderline

high” endogenous LDL-C ( $\geq 130$  mg/dL) concentrations<sup>227</sup> that were still below 150 mg/dL. However, despite this discrepancy, these data have important clinical implications. We found that treatment with exogenous LDL-C concentrations that within ranges considered “borderline high” (e.g., 133 mg/dL & 142 mg/dL) appears to induce significant T-cell dysfunction. Additionally, to isolate the direct effect of LDL-C, T-cells were treated with LDL-C in a serum free medium. This media did not any other lipids that are normally found in blood. Thus, it is possible that the interaction between other blood lipids, such as high-density lipoprotein cholesterol (HDL) and T-cells may have yielded different results. Considering that HDL-C can act as an anti-inflammatory<sup>228,229</sup>, future studies should explore the protective role of HDL-C on T-cell function. Our data may indicate that patients who are otherwise healthy but have borderline high LDL-C may be at an increased risk of inflammation and premature immune aging. We also did not have an equal proportion of male and female participants, and future studies should investigate whether sex differences exist in T-cell response to LDL-C.

One strength of our experimental design is that the removal of APCs provided novel evidence that T-cells are activated by LDL-C independent of MHC presentation. However, this strength can also be a weakness because *in vitro* experiments inherently remove some translational impact. It is possible that if PBMCs had been treated with LDL-C that the interaction between T-cells and other mononuclear cells might have yielded different results. Different LDL-C concentrations were used for the Seahorse and flow cytometry experiments, with the concentration for the Seahorse experiment being 9 mg/dL lower. This was caused by an LDL-C shortage from one supplier, causing us to have to use LDL-C from a different supplier towards the end of the

study. It is possible that if a higher concentration had been used for the Seahorse experiments, we might have seen more robust effects of the LDL-C treatment.

In conclusion, exogenous treatment with high concentrations of LDL-C induced age-related dysfunction in T-cells from middle-aged adults. LDL-C treatment impaired basal mitochondrial respiration and ATP-linked respiration and increased glycolytic metabolism in CD4<sup>+</sup> and CD8<sup>+</sup> T-cells. Additionally, LDL-C increased T-cell activation, differentiation, oxidative stress, lipid accumulation, and inflammation. Many of these changes were associated with each other, indicating the relation between changes in T-cell bioenergetics, activation, inflammation, differentiation, and senescence. Furthermore, these data show that LDL-C may be detrimental independent of risk for atherosclerosis, and to prevent inflammation, clinicians may consider early intervention in healthy adults with borderline high LDL-C.

## CONCLUSIONS

### 4.1 Summary

Animal models have shown that T-cells are important modulators of cerebrovascular function by regulating inflammation and oxidative stress<sup>39-41</sup>. Shifts in T-cell metabolism from oxidative to glycolytic can increase inflammation<sup>3,28,42,230</sup> and impaired oxidative metabolism can increase oxidative stress<sup>45,83,231</sup>. We found that T-cell metabolism was predictive of cerebrovascular function in middle-aged adults with glycolytic CD8<sup>+</sup> T-cell metabolism being predictive of lower middle cerebral velocity (MCAv) breath-hold index (BHI). Specifically, changes in CD8<sup>+</sup> T-cell metabolism may alter the sympathetic response and vasoconstriction in response

to the breath-hold, resulting in an impaired pressor response. This was evidenced by the fact that the pressor response mediated the relation between CD8<sup>+</sup> T-cell metabolism and MCAv BHI, and that the peak total peripheral resistance during the breath-hold was negatively correlated with CD8<sup>+</sup> T-cell glycolytic metabolism.

Importantly, factors that contribute to glycolytic T-cell metabolism may induce accelerated cerebrovascular aging via increased inflammation and oxidative stress. In this regard, we showed that treatment with a “high” exogenous concentration of low-density lipoprotein cholesterol (LDL-C) impaired mitochondrial respiration and increased glycolysis and the production of pro-inflammatory cytokines and mitochondrial oxidative stress in CD4<sup>+</sup> and CD8<sup>+</sup> T-cells. We also found that treatment with high LDL-C resulted in T-cell activation and increased the proportion of senescent CD4<sup>+</sup> and CD8<sup>+</sup> T-cells. Changes in many of these measures of T-cell function in response to LDL-C treatment were correlated with each other, indicating how integrated these mechanisms are.

## **4.2 Perspectives**

The concentrations of cholesterol were within physiological ranges and would be considered “borderline high” by clinical standards<sup>227</sup>. These data suggest that even moderately high endogenous LDL-C concentrations can lead to pre-mature immune aging, resulting in elevated inflammation and oxidative stress in otherwise healthy adults. Early interventions should be considered to prevent moderate increases in LDL-C and resulting deleterious changes in T-cell function. This is especially true of CD8<sup>+</sup> T-cells, where even subtle changes in metabolism in healthy adults can result in altered cerebrovascular function. Future studies should explore the regulation of

cerebrovascular function by T-cells in diseased populations with broader ranges of LDL-C. Targeting T-cell metabolism may be a novel therapeutic to combat age-related diseases that result from accelerated immune aging and increased inflammation and oxidative stress, such as AD.

## REFERENCES

1. Punt J, Stranford S, Jones P, Owen J. *Kuby Immunology*. Eighth. New York: W. H. Freeman; 2018.
2. Nsiah-Sefaa A, McKenzie M. Combined defects in oxidative phosphorylation and fatty acid  $\beta$ -oxidation in mitochondrial disease. *Biosci Rep*. 2016;36(2). doi:10.1042/BSR20150295
3. Desdín-Micó G, Soto-Herederó G, Mittelbrunn M. Mitochondrial activity in T cells. *Mitochondrion*. 2018;41:51-57. doi:10.1016/j.mito.2017.10.006
4. Alzheimer's Association. 2022 Alzheimer's disease facts and figures. *Alzheimer's Dement*. 2022;18(4):700-789. doi:10.1002/alz.12638
5. He W, Goodkin D, Kowal P. *An Aging World: 2015.*; 2016. <https://www.census.gov/content/dam/Census/library/publications/2016/demo/p95-16-1.pdf>.
6. Kametani F, Hasegawa M. Reconsideration of Amyloid Hypothesis and Tau Hypothesis in Alzheimer's Disease. *Front Neurosci*. 2018;12. doi:10.3389/fnins.2018.00025
7. Scheffer S, Hermkens DMA, van der Weerd L, de Vries HE, Daemen MJAP. Vascular Hypothesis of Alzheimer Disease. *Arterioscler Thromb Vasc Biol*. 2021;41(4):1265-1283. doi:10.1161/ATVBAHA.120.311911
8. Gonzales MM, Garbarino VR, Pollet E, et al. Biological aging processes underlying cognitive decline and neurodegenerative disease. *J Clin Invest*. 2022;132(10). doi:10.1172/JCI158453
9. Glodzik L, Randall C, Rusinek H, de Leon MJ. Cerebrovascular Reactivity to Carbon Dioxide in Alzheimer's Disease. *J Alzheimer's Dis*. 2013;35(3):427-440. doi:10.3233/JAD-122011
10. Sur S, Lin Z, Li Y, et al. Association of cerebrovascular reactivity and Alzheimer pathologic markers with cognitive performance. *Neurology*. 2020;95(8):e962-e972. doi:10.1212/WNL.0000000000010133
11. Silvestrini M, Pasqualetti P, Baruffaldi R, et al. Cerebrovascular Reactivity and Cognitive Decline in Patients With Alzheimer Disease. *Stroke*. 2006;37(4):1010-1015. doi:10.1161/01.STR.0000206439.62025.97
12. Kim D, Hughes TM, Hugenschmidt CE, et al. Relationship between cerebrovascular reactivity and cognition among people with risk of cognitive

- decline. *Alzheimer's Dement.* 2020;16(S5). doi:10.1002/alz.044578
13. Catchlove SJ, Parrish TB, Chen Y, Macpherson H, Hughes ME, Pipingas A. Regional Cerebrovascular Reactivity and Cognitive Performance in Healthy Aging. *J Exp Neurosci.* 2018;12:117906951878515. doi:10.1177/1179069518785151
  14. Toth P, Tarantini S, Csiszar A, Ungvari Z. Functional vascular contributions to cognitive impairment and dementia: mechanisms and consequences of cerebral autoregulatory dysfunction, endothelial impairment, and neurovascular uncoupling in aging. *Am J Physiol Circ Physiol.* 2017;312(1):H1-H20. doi:10.1152/ajpheart.00581.2016
  15. Di Marco LY, Venneri A, Farkas E, Evans PC, Marzo A, Frangi AF. Vascular dysfunction in the pathogenesis of Alzheimer's disease — A review of endothelium-mediated mechanisms and ensuing vicious circles. *Neurobiol Dis.* 2015;82:593-606. doi:10.1016/j.nbd.2015.08.014
  16. Rius-Pérez S, Tormos AM, Pérez S, Taléns-Visconti R. Vascular pathology: Cause or effect in Alzheimer disease? *Neurol (English Ed.)* 2018;33(2):112-120. doi:10.1016/j.nrleng.2015.07.008
  17. de Bruijn RF, Ikram MA. Cardiovascular risk factors and future risk of Alzheimer's disease. *BMC Med.* 2014;12(1):130. doi:10.1186/s12916-014-0130-5
  18. Malik R, Georgakis MK, Neitzel J, et al. Midlife vascular risk factors and risk of incident dementia: Longitudinal cohort and Mendelian randomization analyses in the UK Biobank. *Alzheimer's Dement.* 2021;17(9):1422-1431. doi:10.1002/alz.12320
  19. Gottesman RF, Schneider ALC, Zhou Y, et al. Association Between Midlife Vascular Risk Factors and Estimated Brain Amyloid Deposition. *JAMA.* 2017;317(14):1443. doi:10.1001/jama.2017.3090
  20. Fayosse A, Nguyen D-P, Dugravot A, et al. Risk prediction models for dementia: role of age and cardiometabolic risk factors. *BMC Med.* 2020;18(1):107. doi:10.1186/s12916-020-01578-x
  21. Lennon MJ, Makkar SR, Crawford JD, Sachdev PS. Midlife Hypertension and Alzheimer's Disease: A Systematic Review and Meta-Analysis. *J Alzheimer's Dis.* 2019;71(1):307-316. doi:10.3233/JAD-190474
  22. Ninomiya T, Ohara T, Hirakawa Y, et al. Midlife and Late-Life Blood Pressure and Dementia in Japanese Elderly. *Hypertension.* 2011;58(1):22-28. doi:10.1161/HYPERTENSIONAHA.110.163055
  23. Shakya S, Bajracharya R, Ledbetter L, Cary MP. The Association Between Cardiometabolic Risk Factors and Frailty in Older Adults: A Systematic Review. Albert SM, ed. *Innov Aging.* 2022;6(5). doi:10.1093/geroni/igac032
  24. Franceschi C, Garagnani P, Parini P, Giuliani C, Santoro A. Inflammaging: a new immune–metabolic viewpoint for age-related diseases. *Nat Rev Endocrinol.* 2018;14(10):576-590. doi:10.1038/s41574-018-0059-4
  25. Ferrucci L, Fabbri E. Inflammaging: chronic inflammation in ageing,

- cardiovascular disease, and frailty. *Nat Rev Cardiol*. 2018;15(9):505-522. doi:10.1038/s41569-018-0064-2
26. Santoro A, Bientinesi E, Monti D. Immunosenescence and inflammaging in the aging process: age-related diseases or longevity? *Ageing Res Rev*. 2021;71:101422. doi:10.1016/j.arr.2021.101422
  27. Macaulay R, Akbar AN, Henson SM. The role of the T cell in age-related inflammation. *Age (Omaha)*. 2013;35(3):563-572. doi:10.1007/s11357-012-9381-2
  28. Mittelbrunn M, Kroemer G. Hallmarks of T cell aging. *Nat Immunol*. 2021;22(6):687-698. doi:10.1038/s41590-021-00927-z
  29. Kroemer G, Zitvogel L. CD4+ T Cells at the Center of Inflammaging. *Cell Metab*. 2020;32(1):4-5. doi:10.1016/j.cmet.2020.04.016
  30. Baruch K, Rosenzweig N, Kertser A, et al. Breaking immune tolerance by targeting Foxp3+ regulatory T cells mitigates Alzheimer's disease pathology. *Nat Commun*. 2015;6(1):7967. doi:10.1038/ncomms8967
  31. Machhi J, Yeapuri P, Lu Y, et al. CD4+ effector T cells accelerate Alzheimer's disease in mice. *J Neuroinflammation*. 2021;18(1):272. doi:10.1186/s12974-021-02308-7
  32. Stojić-Vukanić Z, Hadžibegović S, Nicole O, Nacka-Aleksić M, Leštarević S, Leposavić G. CD8+ T Cell-Mediated Mechanisms Contribute to the Progression of Neurocognitive Impairment in Both Multiple Sclerosis and Alzheimer's Disease? *Front Immunol*. 2020;11. doi:10.3389/fimmu.2020.566225
  33. Dai L, Shen Y. Insights into T-cell dysfunction in Alzheimer's disease. *Ageing Cell*. 2021;20(12). doi:10.1111/accel.13511
  34. Simons KH, de Jong A, Jukema JW, de Vries MR, Arens R, Quax PHA. T cell co-stimulation and co-inhibition in cardiovascular disease: a double-edged sword. *Nat Rev Cardiol*. 2019;16(6):325-343. doi:10.1038/s41569-019-0164-7
  35. Blanton RM, Carrillo-Salinas FJ, Alcaide P. T-cell recruitment to the heart: friendly guests or unwelcome visitors? *Am J Physiol Circ Physiol*. 2019;317(1):H124-H140. doi:10.1152/ajpheart.00028.2019
  36. Ilatovskaya D V., Halade G V., DeLeon-Pennell KY. Adaptive immunity-driven inflammation and cardiovascular disease. *Am J Physiol Circ Physiol*. 2019;317(6):H1254-H1257. doi:10.1152/ajpheart.00642.2019
  37. Elyahu Y, Hekselman I, Eizenberg-Magar I, et al. Aging promotes reorganization of the CD4 T cell landscape toward extreme regulatory and effector phenotypes. *Sci Adv*. 2019;5(8). doi:10.1126/sciadv.aaw8330
  38. Schmitt V, Rink L, Uciechowski P. The Th17/Treg balance is disturbed during aging. *Exp Gerontol*. 2013;48(12):1379-1386. doi:10.1016/j.exger.2013.09.003
  39. Iulita MF, Duchemin S, Vallerand D, et al. CD4 + Regulatory T Lymphocytes Prevent Impaired Cerebral Blood Flow in Angiotensin II-Induced Hypertension. *J Am Heart Assoc*. 2019;8(1). doi:10.1161/JAHA.118.009372
  40. Li P, Gan Y, Sun B-L, et al. Adoptive regulatory T-cell therapy protects against

- cerebral ischemia. *Ann Neurol*. 2013;74(3):458-471. doi:10.1002/ana.23815
41. Liesz A, Suri-Payer E, Veltkamp C, et al. Regulatory T cells are key cerebroprotective immunomodulators in acute experimental stroke. *Nat Med*. 2009;15(2):192-199. doi:10.1038/nm.1927
  42. Desdín-Micó G, Soto-Herederó G, Aranda JF, et al. T cells with dysfunctional mitochondria induce multimorbidity and premature senescence. *Science (80- )*. 2020;368(6497):1371-1376. doi:10.1126/science.aax0860
  43. Bektas A, Schurman SH, Gonzalez-Freire M, et al. Age-associated changes in human CD4+ T cells point to mitochondrial dysfunction consequent to impaired autophagy. *Aging (Albany NY)*. 2019;11(21):9234-9263. doi:10.18632/aging.102438
  44. Ron-Harel N, Notarangelo G, Ghergurovich JM, et al. Defective respiration and one-carbon metabolism contribute to impaired naïve T cell activation in aged mice. *Proc Natl Acad Sci*. 2018;115(52):13347-13352. doi:10.1073/pnas.1804149115
  45. Cui H, Kong Y, Zhang H. Oxidative Stress, Mitochondrial Dysfunction, and Aging. *J Signal Transduct*. 2012;2012:1-13. doi:10.1155/2012/646354
  46. Vasileiou P, Evangelou K, Vlasis K, et al. Mitochondrial Homeostasis and Cellular Senescence. *Cells*. 2019;8(7):686. doi:10.3390/cells8070686
  47. Chapman J, Fielder E, Passos JF. Mitochondrial dysfunction and cell senescence: deciphering a complex relationship. *FEBS Lett*. 2019;593(13):1566-1579. doi:10.1002/1873-3468.13498
  48. Li P, Wang B, Sun F, et al. Mitochondrial respiratory dysfunctions of blood mononuclear cells link with cardiac disturbance in patients with early-stage heart failure. *Sci Rep*. 2015;5(1):10229. doi:10.1038/srep10229
  49. DeConne TM, Muñoz ER, Sanjana F, Hobson JC, Martens CR. Cardiometabolic risk factors are associated with immune cell mitochondrial respiration in humans. *Am J Physiol Circ Physiol*. 2020;319(2):H481-H487. doi:10.1152/ajpheart.00434.2020
  50. Oliveira HCF, Vercesi AE. Mitochondrial bioenergetics and redox dysfunctions in hypercholesterolemia and atherosclerosis. *Mol Aspects Med*. 2020;71:100840. doi:10.1016/j.mam.2019.100840
  51. Hansson GK, Hermansson A. The immune system in atherosclerosis. *Nat Immunol*. 2011;12(3):204-212. doi:10.1038/ni.2001
  52. Wolf D, Gerhardt T, Winkels H, et al. Pathogenic Autoimmunity in Atherosclerosis Evolves From Initially Protective Apolipoprotein B 100 – Reactive CD4 + T-Regulatory Cells. *Circulation*. 2020;142(13):1279-1293. doi:10.1161/CIRCULATIONAHA.119.042863
  53. Hermansson A, Ketelhuth DFJ, Strodthoff D, et al. Inhibition of T cell response to native low-density lipoprotein reduces atherosclerosis. *J Exp Med*. 2010;207(5):1081-1093. doi:10.1084/jem.20092243
  54. Fukushima Y, Minato N, Hattori M. The impact of senescence-associated T cells on immunosenescence and age-related disorders. *Inflamm Regen*.

- 2018;38(1):24. doi:10.1186/s41232-018-0082-9
55. P. Chou J, B. Effros R. T Cell Replicative Senescence in Human Aging. *Curr Pharm Des.* 2013;19(9):1680-1698. doi:10.2174/138161213805219711
  56. Kasakovski D, Xu L, Li Y. T cell senescence and CAR-T cell exhaustion in hematological malignancies. *J Hematol Oncol.* 2018;11(1):91. doi:10.1186/s13045-018-0629-x
  57. Félix-Redondo FJ, Grau M, Fernández-Bergés D. Cholesterol and cardiovascular disease in the elderly. Facts and gaps. *Aging Dis.* 2013;4(3):154-169. <https://www.ncbi.nlm.nih.gov/pmc/articles/PMC3660125/pdf/ad-4-6-154.pdf>.
  58. Downer B, Estus S, Katsumata Y, Fardo D. Longitudinal Trajectories of Cholesterol from Midlife through Late Life according to Apolipoprotein E Allele Status. *Int J Environ Res Public Health.* 2014;11(10):10663-10693. doi:10.3390/ijerph111010663
  59. Araos P, Figueroa S, Amador CA. The Role of Neutrophils in Hypertension. *Int J Mol Sci.* 2020;21(22):8536. doi:10.3390/ijms21228536
  60. Qi H, Yang S, Zhang L. Neutrophil Extracellular Traps and Endothelial Dysfunction in Atherosclerosis and Thrombosis. *Front Immunol.* 2017;8. doi:10.3389/fimmu.2017.00928
  61. Mittal M, Siddiqui MR, Tran K, Reddy SP, Malik AB. Reactive Oxygen Species in Inflammation and Tissue Injury. *Antioxid Redox Signal.* 2014;20(7):1126-1167. doi:10.1089/ars.2012.5149
  62. Soehnlein O. Multiple Roles for Neutrophils in Atherosclerosis. *Circ Res.* 2012;110(6):875-888. doi:10.1161/CIRCRESAHA.111.257535
  63. Xia N, Hasselwander S, Reifenberg G, et al. B Lymphocyte-Deficiency in Mice Causes Vascular Dysfunction by Inducing Neutrophilia. *Biomedicines.* 2021;9(11):1686. doi:10.3390/biomedicines9111686
  64. Gupta RM, Lee-Kim VS, Libby P. The March of Monocytes in Atherosclerosis. *Circ Res.* 2020;126(10):1324-1326. doi:10.1161/CIRCRESAHA.120.316981
  65. Hilgendorf I, Swirski FK, Robbins CS. Monocyte Fate in Atherosclerosis. *Arterioscler Thromb Vasc Biol.* 2015;35(2):272-279. doi:10.1161/ATVBAHA.114.303565
  66. Davignon J, Ganz P. Role of Endothelial Dysfunction in Atherosclerosis. *Circulation.* 2004;109(23\_suppl\_1). doi:10.1161/01.CIR.0000131515.03336.f8
  67. Xu S, Ilyas I, Little PJ, et al. Endothelial Dysfunction in Atherosclerotic Cardiovascular Diseases and Beyond: From Mechanism to Pharmacotherapies. Ma Q, ed. *Pharmacol Rev.* 2021;73(3):924-967. doi:10.1124/pharmrev.120.000096
  68. Golubovskaya V, Wu L. Different Subsets of T Cells, Memory, Effector Functions, and CAR-T Immunotherapy. *Cancers (Basel).* 2016;8(3):36. doi:10.3390/cancers8030036
  69. Kreslavsky T, Gleimer M, Garbe AI, Von Boehmer H.  $\alpha\beta$  versus  $\gamma\delta$  fate choice: counting the T-cell lineages at the branch point. *Immunol Rev.*

- 2010;238(1):169-181. doi:10.1111/j.1600-065X.2010.00947.x
70. Zhao Y, Niu C, Cui J. Gamma-delta ( $\gamma\delta$ ) T cells: friend or foe in cancer development? *J Transl Med.* 2018;16(1):3. doi:10.1186/s12967-017-1378-2
  71. Salam N, Rane S, Das R, et al. T cell ageing: effects of age on development, survival & function. *Indian J Med Res.* 2013;138(5):595-608. doi:24434315
  72. Zhang H, Weyand CM, Goronzy JJ. Hallmarks of the aging T-cell system. *FEBS J.* 2021;288(24):7123-7142. doi:10.1111/febs.15770
  73. Goronzy JJ, Weyand CM. Mechanisms underlying T cell ageing. *Nat Rev Immunol.* 2019;19(9):573-583. doi:10.1038/s41577-019-0180-1
  74. Saule P, Trauet J, Dutriez V, Lekeux V, Dessaint J-P, Labalette M. Accumulation of memory T cells from childhood to old age: Central and effector memory cells in CD4+ versus effector memory and terminally differentiated memory cells in CD8+ compartment. *Mech Ageing Dev.* 2006;127(3):274-281. doi:10.1016/j.mad.2005.11.001
  75. Rodrigues N V., Correia D V., Mensurado S, et al. Low-Density Lipoprotein Uptake Inhibits the Activation and Antitumor Functions of Human V $\gamma$ 9V $\delta$ 2 T Cells. *Cancer Immunol Res.* 2018;6(4):448-457. doi:10.1158/2326-6066.CIR-17-0327
  76. Castella B, Melaccio A, Foglietta M, Riganti C, Massaia M. V $\gamma$ 9V $\delta$ 2 T Cells as Strategic Weapons to Improve the Potency of Immune Checkpoint Blockade and Immune Interventions in Human Myeloma. *Front Oncol.* 2018;8. doi:10.3389/fonc.2018.00508
  77. Holmen Olofsson G, Idorn M, Carnaz Simões AM, et al. V $\gamma$ 9V $\delta$ 2 T Cells Concurrently Kill Cancer Cells and Cross-Present Tumor Antigens. *Front Immunol.* 2021;12. doi:10.3389/fimmu.2021.645131
  78. Xu W, Larbi A. Markers of T Cell Senescence in Humans. *Int J Mol Sci.* 2017;18(8):1742. doi:10.3390/ijms18081742
  79. Vercellino I, Sazanov LA. The assembly, regulation and function of the mitochondrial respiratory chain. *Nat Rev Mol Cell Biol.* 2022;23(2):141-161. doi:10.1038/s41580-021-00415-0
  80. Osellame LD, Blacker TS, Duchon MR. Cellular and molecular mechanisms of mitochondrial function. *Best Pract Res Clin Endocrinol Metab.* 2012;26(6):711-723. doi:10.1016/j.beem.2012.05.003
  81. Zorov DB, Juhaszova M, Sollott SJ. Mitochondrial Reactive Oxygen Species (ROS) and ROS-Induced ROS Release. *Physiol Rev.* 2014;94(3):909-950. doi:10.1152/physrev.00026.2013
  82. Dan Dunn J, Alvarez LA, Zhang X, Soldati T. Reactive oxygen species and mitochondria: A nexus of cellular homeostasis. *Redox Biol.* 2015;6:472-485. doi:10.1016/j.redox.2015.09.005
  83. Murphy MP. How mitochondria produce reactive oxygen species. *Biochem J.* 2009;417(1):1-13. doi:10.1042/BJ20081386
  84. Kornberg MD. The immunologic Warburg effect: Evidence and therapeutic opportunities in autoimmunity. *WIREs Syst Biol Med.* 2020;12(5).

doi:10.1002/wsbm.1486

85. Madden MZ, Rathmell JC. The Complex Integration of T-cell Metabolism and Immunotherapy. *Cancer Discov.* 2021;11(7):1636-1643. doi:10.1158/2159-8290.CD-20-0569
86. Corrado M, Pearce EL. Targeting memory T cell metabolism to improve immunity. *J Clin Invest.* 2022;132(1). doi:10.1172/JCI148546
87. Møller SH, Hsueh P-C, Yu Y-R, Zhang L, Ho P-C. Metabolic programs tailor T cell immunity in viral infection, cancer, and aging. *Cell Metab.* 2022;34(3):378-395. doi:10.1016/j.cmet.2022.02.003
88. Quinn KM, Hussain T, Kraus F, et al. Metabolic characteristics of CD8+ T cell subsets in young and aged individuals are not predictive of functionality. *Nat Commun.* 2020;11(1):2857. doi:10.1038/s41467-020-16633-7
89. Yanes RE, Zhang H, Shen Y, Weyand CM, Goronzy JJ. Metabolic reprogramming in memory CD4 T cell responses of old adults. *Clin Immunol.* 2019;207:58-67. doi:10.1016/j.clim.2019.07.003
90. Callender LA, Carroll EC, Bober EA, Akbar AN, Solito E, Henson SM. Mitochondrial mass governs the extent of human T cell senescence. *Aging Cell.* 2020;19(2). doi:10.1111/accel.13067
91. Larbi A, Dupuis G, Khalil A, Douziech N, Fortin C, Fülöp T. Differential role of lipid rafts in the functions of CD4+ and CD8+ human T lymphocytes with aging. *Cell Signal.* 2006;18(7):1017-1030. doi:10.1016/j.cellsig.2005.08.016
92. Kelleher RJ, Soiza RL. Evidence of endothelial dysfunction in the development of Alzheimer's disease: Is Alzheimer's a vascular disorder? *Am J Cardiovasc Dis.* 2013;3(4):197-226. <http://www.ncbi.nlm.nih.gov/pubmed/24224133>.
93. Love S, Miners JS. Cerebral Hypoperfusion and the Energy Deficit in Alzheimer's Disease. *Brain Pathol.* 2016;26(5):607-617. doi:10.1111/bpa.12401
94. Austin BP, Nair VA, Meier TB, et al. Effects of Hypoperfusion in Alzheimer's Disease. Ashford JW, Rosen A, Adamson M, et al., eds. *J Alzheimer's Dis.* 2011;26(s3):123-133. doi:10.3233/JAD-2011-0010
95. Wolters FJ, Zonneveld HI, Hofman A, et al. Cerebral Perfusion and the Risk of Dementia. *Circulation.* 2017;136(8):719-728. doi:10.1161/CIRCULATIONAHA.117.027448
96. Alwatban M, Murman DL, Bashford G. Cerebrovascular Reactivity Impairment in Preclinical Alzheimer's Disease. *J Neuroimaging.* 2019;29(4):493-498. doi:10.1111/jon.12606
97. Carr JMJR, Caldwell HG, Ainslie PN. Cerebral blood flow, cerebrovascular reactivity and their influence on ventilatory sensitivity. *Exp Physiol.* 2021;106(7):1425-1448. doi:10.1113/EP089446
98. Félétou M. The Endothelium, Part I: Multiple Functions of the Endothelial Cells -- Focus on Endothelium-Derived Vasoactive Mediators. *Colloq Ser Integr Syst Physiol From Mol to Funct.* 2011;3(4):1-306. doi:10.4199/C00031ED1V01Y201105ISP019

99. Cyr AR, Huckaby L V., Shiva SS, Zuckerbraun BS. Nitric Oxide and Endothelial Dysfunction. *Crit Care Clin.* 2020;36(2):307-321. doi:10.1016/j.ccc.2019.12.009
100. Ashby JW, Mack JJ. Endothelial Control of Cerebral Blood Flow. *Am J Pathol.* 2021;191(11):1906-1916. doi:10.1016/j.ajpath.2021.02.023
101. Sun H-J, Wu Z-Y, Nie X-W, Bian J-S. Role of Endothelial Dysfunction in Cardiovascular Diseases: The Link Between Inflammation and Hydrogen Sulfide. *Front Pharmacol.* 2020;10. doi:10.3389/fphar.2019.01568
102. Ungvari Z, Tarantini S, Kiss T, et al. Endothelial dysfunction and angiogenesis impairment in the ageing vasculature. *Nat Rev Cardiol.* 2018;15(9):555-565. doi:10.1038/s41569-018-0030-z
103. Lehnert M, Dobrowinski H, Feil S, Feil R. cGMP Signaling and Vascular Smooth Muscle Cell Plasticity. *J Cardiovasc Dev Dis.* 2018;5(2):20. doi:10.3390/jcdd5020020
104. Hoiland RL, Caldwell HG, Carr JMJR, et al. Nitric oxide contributes to cerebrovascular shear-mediated dilatation but not steady-state cerebrovascular reactivity to carbon dioxide. *J Physiol.* 2022;600(6):1385-1403. doi:10.1113/JP282427
105. Alwatban M, Murman DL, Bashford G. Cerebrovascular Reactivity Impairment in Preclinical Alzheimer ' s Disease. 2019;(Dlm):1-6. doi:10.1111/jon.12606
106. Shim Y, Yoon B, Shim DS, Kim W, An JY, Yang DW. Cognitive correlates of cerebral vasoreactivity on transcranial doppler in older adults. *J Stroke Cerebrovasc Dis.* 2015;24(6):1262-1269. doi:10.1016/j.jstrokecerebrovasdis.2015.01.031
107. Förstermann U, Münzel T. Endothelial Nitric Oxide Synthase in Vascular Disease. *Circulation.* 2006;113(13):1708-1714. doi:10.1161/CIRCULATIONAHA.105.602532
108. Tan BL, Norhaizan ME, Liew W-P-P, Sulaiman Rahman H. Antioxidant and Oxidative Stress: A Mutual Interplay in Age-Related Diseases. *Front Pharmacol.* 2018;9. doi:10.3389/fphar.2018.01162
109. Lobo V, Patil A, Phatak A, Chandra N. Free radicals, antioxidants and functional foods: Impact on human health. *Pharmacogn Rev.* 2010;4(8):118. doi:10.4103/0973-7847.70902
110. Tarafdard A, Pula G. The Role of NADPH Oxidases and Oxidative Stress in Neurodegenerative Disorders. *Int J Mol Sci.* 2018;19(12):3824. doi:10.3390/ijms19123824
111. Freeman LR, Keller JN. Oxidative stress and cerebral endothelial cells: Regulation of the blood–brain-barrier and antioxidant based interventions. *Biochim Biophys Acta - Mol Basis Dis.* 2012;1822(5):822-829. doi:10.1016/j.bbdis.2011.12.009
112. Javanmard SH, Dana N. The effect of interferon  $\gamma$  on endothelial cell nitric oxide production and apoptosis. *Adv Biomed Res.* 2012;1:69. doi:10.4103/2277-9175.102973

113. Zhang H, Park Y, Wu J, et al. Role of TNF- $\alpha$  in vascular dysfunction. *Clin Sci*. 2009;116(3):219-230. doi:10.1042/CS20080196
114. Lee J, Lee S, Zhang H, Hill MA, Zhang C, Park Y. Interaction of IL-6 and TNF- $\alpha$  contributes to endothelial dysfunction in type 2 diabetic mouse hearts. Bader M, ed. *PLoS One*. 2017;12(11):e0187189. doi:10.1371/journal.pone.0187189
115. Hung M-J, Cherng W-J, Hung M-Y, Wu H-T, Pang J-HS. Interleukin-6 inhibits endothelial nitric oxide synthase activation and increases endothelial nitric oxide synthase binding to stabilized caveolin-1 in human vascular endothelial cells. *J Hypertens*. 2010;28(5):940-951. doi:10.1097/HJH.0b013e32833992ef
116. Nguyen H, Chiasson VL, Chatterjee P, Kopriva SE, Young KJ, Mitchell BM. Interleukin-17 causes Rho-kinase-mediated endothelial dysfunction and hypertension. *Cardiovasc Res*. 2013;97(4):696-704. doi:10.1093/cvr/cvs422
117. Gunnett CA, Heistad DD, Berg DJ, Faraci FM. IL-10 deficiency increases superoxide and endothelial dysfunction during inflammation. *Am J Physiol Circ Physiol*. 2000;279(4):H1555-H1562. doi:10.1152/ajpheart.2000.279.4.H1555
118. Kinzenbaw DA, Chu Y, Peña Silva RA, Didion SP, Faraci FM. Interleukin-10 protects against aging-induced endothelial dysfunction. *Physiol Rep*. 2013;1(6):e00149. doi:10.1002/phy2.149
119. Srikakulapu P, McNamara CA. B cells and atherosclerosis. *Am J Physiol Circ Physiol*. 2017;312(5):H1060-H1067. doi:10.1152/ajpheart.00859.2016
120. Adamo L, Rocha-Resende C, Mann DL. The Emerging Role of B Lymphocytes in Cardiovascular Disease. *Annu Rev Immunol*. 2020;38(1):99-121. doi:10.1146/annurev-immunol-042617-053104
121. Hansson GK. The B Cell. *Arterioscler Thromb Vasc Biol*. 2002;22(4):523-524. doi:10.1161/01.ATV.0000015098.68671.1C
122. Tsiantoulas D, Sage AP, Mallat Z, Binder CJ. Targeting B Cells in Atherosclerosis. *Arterioscler Thromb Vasc Biol*. 2015;35(2):296-302. doi:10.1161/ATVBAHA.114.303569
123. Norlander AE, Madhur MS, Harrison DG. The immunology of hypertension. *J Exp Med*. 2018;215(1):21-33. doi:10.1084/jem.20171773
124. Chan CT, Sobey CG, Lieu M, et al. Obligatory Role for B Cells in the Development of Angiotensin II-Dependent Hypertension. *Hypertension*. 2015;66(5):1023-1033. doi:10.1161/HYPERTENSIONAHA.115.05779
125. Blum LK, Cao RRL, Sweatt AJ, et al. Circulating plasmablasts are elevated and produce pathogenic anti-endothelial cell autoantibodies in idiopathic pulmonary arterial hypertension. *Eur J Immunol*. 2018;48(5):874-884. doi:10.1002/eji.201747460
126. Varela C, de Haro J, Bleda S, Esparza L, de Maturana IL, Acin F. Anti-endothelial cell antibodies are associated with peripheral arterial disease and markers of endothelial dysfunction and inflammation. *Interact Cardiovasc Thorac Surg*. 2011;13(5):463-467. doi:10.1510/icvts.2011.275016
127. Yazici ZA, Raschi E, Patel A, et al. Human monoclonal anti-endothelial cell

- IgG-derived from a systemic lupus erythematosus patient binds and activates human endothelium in vitro. *Int Immunol.* 2001;13(3):349-357.  
doi:10.1093/intimm/13.3.349
128. del Papa N, Guidali L, Sironi M, et al. Anti-endothelial cell IgG antibodies from patients with Wegener's granulomatosis bind to human endothelial cells in vitro and induce adhesion molecule expression and cytokine secretion. *Arthritis Rheum.* 1996;39(5):758-766. doi:10.1002/art.1780390507
  129. Lin C-F, Lei H-Y, Shiau A-L, et al. Endothelial Cell Apoptosis Induced by Antibodies Against Dengue Virus Nonstructural Protein 1 Via Production of Nitric Oxide. *J Immunol.* 2002;169(2):657-664.  
doi:10.4049/jimmunol.169.2.657
  130. Lin Y, Lin C, Lei H, et al. Antibody-Mediated Endothelial Cell Damage Via Nitric Oxide. *Curr Pharm Des.* 2004;10(2):213-221.  
doi:10.2174/1381612043453469
  131. Shi H, Zuo Y, Navaz S, et al. Endothelial Cell-Activating Antibodies in COVID-19. *Arthritis Rheumatol.* 2022;74(7):1132-1138. doi:10.1002/art.42094
  132. Guzik TJ, Hoch NE, Brown KA, et al. Role of the T cell in the genesis of angiotensin II-induced hypertension and vascular dysfunction. *J Exp Med.* 2007;204(10):2449-2460. doi:10.1084/jem.20070657
  133. Zimmerman MC, Lazartigues E, Sharma R V., Davisson RL. Hypertension Caused by Angiotensin II Infusion Involves Increased Superoxide Production in the Central Nervous System. *Circ Res.* 2004;95(2):210-216.  
doi:10.1161/01.RES.0000135483.12297.e4
  134. Fyhrquist F, Metsärinne K, Tikkanen I. Role of angiotensin II in blood pressure regulation and in the pathophysiology of cardiovascular disorders. *J Hum Hypertens.* 1995;9 Suppl 5:S19-24.  
<http://www.ncbi.nlm.nih.gov/pubmed/8583476>.
  135. Iyer A, Chan V, Brown L. The DOCA-Salt Hypertensive Rat as a Model of Cardiovascular Oxidative and Inflammatory Stress. *Curr Cardiol Rev.* 2010;6(4):291-297. doi:10.2174/157340310793566109
  136. Barhoumi T, Kasal DA, Li MW, et al. T Regulatory Lymphocytes Prevent Angiotensin II-Induced Hypertension and Vascular Injury. *Hypertension.* 2011;57(3):469-476. doi:10.1161/HYPERTENSIONAHA.110.162941
  137. Wu Z, Yao H, Xu H, et al. Inhibition of eNOS by L-NAME resulting in rat hind limb developmental defects through PFKFB3 mediated angiogenetic pathway. *Sci Rep.* 2020;10(1):16754. doi:10.1038/s41598-020-74011-1
  138. Habas K, Shang L. Alterations in intercellular adhesion molecule 1 (ICAM-1) and vascular cell adhesion molecule 1 (VCAM-1) in human endothelial cells. *Tissue Cell.* 2018;54:139-143. doi:10.1016/j.tice.2018.09.002
  139. Kassan M, Galan M, Partyka M, Trebak M, Matrougui K. Interleukin-10 Released by CD4 + CD25 + Natural Regulatory T Cells Improves Microvascular Endothelial Function Through Inhibition of NADPH Oxidase Activity in Hypertensive Mice. *Arterioscler Thromb Vasc Biol.*

- 2011;31(11):2534-2542. doi:10.1161/ATVBAHA.111.233262
140. Matrougui K, Zakaria AE, Kassan M, et al. Natural Regulatory T Cells Control Coronary Arteriolar Endothelial Dysfunction in Hypertensive Mice. *Am J Pathol.* 2011;178(1):434-441. doi:10.1016/j.ajpath.2010.11.034
  141. Radwan E, Mali V, Haddox S, et al. Treg cells depletion is a mechanism that drives microvascular dysfunction in mice with established hypertension. *Biochim Biophys Acta - Mol Basis Dis.* 2019;1865(2):403-412. doi:10.1016/j.bbadis.2018.10.031
  142. Sirker A, Zhang M, Shah AM. NADPH oxidases in cardiovascular disease: insights from in vivo models and clinical studies. *Basic Res Cardiol.* 2011;106(5):735-747. doi:10.1007/s00395-011-0190-z
  143. Abeyrathna P, Su Y. The critical role of Akt in cardiovascular function. *Vascul Pharmacol.* 2015;74:38-48. doi:10.1016/j.vph.2015.05.008
  144. Kasal DA, Barhoumi T, Li MW, et al. T Regulatory Lymphocytes Prevent Aldosterone-Induced Vascular Injury. *Hypertension.* 2012;59(2):324-330. doi:10.1161/HYPERTENSIONAHA.111.181123
  145. Trott DW, Thabet SR, Kirabo A, et al. Oligoclonal CD8 + T Cells Play a Critical Role in the Development of Hypertension. *Hypertension.* 2014;64(5):1108-1115. doi:10.1161/HYPERTENSIONAHA.114.04147
  146. Youn J-C, Yu HT, Lim BJ, et al. Immunosenescent CD8 + T Cells and C-X-C Chemokine Receptor Type 3 Chemokines Are Increased in Human Hypertension. *Hypertension.* 2013;62(1):126-133. doi:10.1161/HYPERTENSIONAHA.113.00689
  147. Yu HT, Youn J, Kim JH, et al. Arterial Stiffness Is Associated With Cytomegalovirus-Specific Senescent CD8 + T Cells. *J Am Heart Assoc.* 2017;6(9). doi:10.1161/JAHA.117.006535
  148. Ji Q, Cheng G, Ma N, et al. Circulating Th1, Th2, and Th17 Levels in Hypertensive Patients. *Dis Markers.* 2017;2017:1-12. doi:10.1155/2017/7146290
  149. Mattson DL, Lund H, Guo C, Rudemiller N, Geurts AM, Jacob H. Genetic mutation of recombination activating gene 1 in Dahl salt-sensitive rats attenuates hypertension and renal damage. *Am J Physiol Integr Comp Physiol.* 2013;304(6):R407-R414. doi:10.1152/ajpregu.00304.2012
  150. Crowley SD, Song Y-S, Lin EE, Griffiths R, Kim H-S, Ruiz P. Lymphocyte responses exacerbate angiotensin II-dependent hypertension. *Am J Physiol Regul Integr Comp Physiol.* 2010;298(4):R1089-97. doi:10.1152/ajpregu.00373.2009
  151. Kvakani H, Kleinewietfeld M, Qadri F, et al. Regulatory T Cells Ameliorate Angiotensin II-Induced Cardiac Damage. *Circulation.* 2009;119(22):2904-2912. doi:10.1161/CIRCULATIONAHA.108.832782
  152. Dittel BN. CD4 T cells: Balancing the coming and going of autoimmune-mediated inflammation in the CNS. *Brain Behav Immun.* 2008;22(4):421-430. doi:10.1016/j.bbi.2007.11.010

153. Stokes KY, Gurwara S, Granger DN. T-Cell–Derived Interferon- $\gamma$  Contributes to Arteriolar Dysfunction During Acute Hypercholesterolemia. *Arterioscler Thromb Vasc Biol.* 2007;27(9):1998-2004. doi:10.1161/ATVBAHA.107.146449
154. Zhou X, Stemme S, Hansson GK. Evidence for a local immune response in atherosclerosis. CD4<sup>+</sup> T cells infiltrate lesions of apolipoprotein-E-deficient mice. *Am J Pathol.* 1996;149(2):359-366. <http://www.ncbi.nlm.nih.gov/pubmed/8701976>.
155. Zhou X, Nicoletti A, Elhage R, Hansson GK. Transfer of CD4 + T Cells Aggravates Atherosclerosis in Immunodeficient Apolipoprotein E Knockout Mice. *Circulation.* 2000;102(24):2919-2922. doi:10.1161/01.CIR.102.24.2919
156. George J, Harats D, Gilburd B, et al. Adoptive Transfer of  $\beta$  2 -Glycoprotein I–Reactive Lymphocytes Enhances Early Atherosclerosis in LDL Receptor–Deficient Mice. *Circulation.* 2000;102(15):1822-1827. doi:10.1161/01.CIR.102.15.1822
157. Mor A, Planer D, Luboshits G, et al. Role of Naturally Occurring CD4 + CD25 + Regulatory T Cells in Experimental Atherosclerosis. *Arterioscler Thromb Vasc Biol.* 2007;27(4):893-900. doi:10.1161/01.ATV.0000259365.31469.89
158. Poznyak A V., Nikiforov NG, Markin AM, et al. Overview of OxLDL and Its Impact on Cardiovascular Health: Focus on Atherosclerosis. *Front Pharmacol.* 2021;11. doi:10.3389/fphar.2020.613780
159. Lee E, Kim N, Kang J, et al. Activated pathogenic Th17 lymphocytes induce hypertension following high-fructose intake in Dahl salt-sensitive (SS) but not Dahl salt-resistant (SR) rats. *Dis Model Mech.* January 2020. doi:10.1242/dmm.044107
160. Trott DW, Machin DR, Phuong TTT, et al. T cells mediate cell non-autonomous arterial ageing in mice. *J Physiol.* 2021;599(16):3973-3991. doi:10.1113/JP281698
161. Kim JY, Lee E, Koo S, Kim C-W, Kim I. Transfer of Th17 from Adult Spontaneous Hypertensive Rats Accelerates Development of Hypertension in Juvenile Spontaneous Hypertensive Rats. Wada K, ed. *Biomed Res Int.* 2021;2021:1-13. doi:10.1155/2021/6633825
162. Wilcox CS. Effects of tempol and redox-cycling nitroxides in models of oxidative stress. *Pharmacol Ther.* 2010;126(2):119-145. doi:10.1016/j.pharmthera.2010.01.003
163. McCarty N, Freeberg K, Seals D, Craighead D. Cerebrovascular reactivity is related to peripheral endothelial function among healthy postmenopausal women but not midlife and older men. *FASEB J.* 2021;35(S1):fasebj.2021.35.S1.05117. doi:10.1096/fasebj.2021.35.S1.05117
164. Zupan M, Šabović M, Zaletel M, Popovič KŠ, Žvan B. The presence of cerebral and/or systemic endothelial dysfunction in patients with leukoaraiosis - a case control pilot study. *BMC Neurol.* 2015;15(1):158. doi:10.1186/s12883-015-0416-z

165. Carr JMJR, Hoiland RL, Caldwell HG, et al. Internal carotid and brachial artery shear-dependent vasodilator function in young healthy humans. *J Physiol.* 2020;598(23):5333-5350. doi:10.1113/JP280369
166. Palazzo P, Maggio P, Passarelli F, et al. Lack of Correlation Between Cerebral Vasomotor Reactivity and Flow-Mediated Dilation in Subjects Without Vascular Disease. *Ultrasound Med Biol.* 2013;39(1):10-15. doi:10.1016/j.ultrasmedbio.2012.08.022
167. Bailey TG, Klein T, Meneses AL, et al. Cerebrovascular function and its association with systemic artery function and stiffness in older adults with and without mild cognitive impairment. *Eur J Appl Physiol.* 2022;122(8):1843-1856. doi:10.1007/s00421-022-04956-w
168. Pretnar-Oblak J, Sabovic M, Zaletel M. Associations between Systemic and Cerebral Endothelial Impairment Determined by Cerebrovascular Reactivity to <sc>L</sc> -Arginine. *Endothelium.* 2007;14(2):73-80. doi:10.1080/10623320701346692
169. Perko D, Pretnar-Oblak J, Šabovič M, Zaletel M, Žvan B. Associations between cerebral and systemic endothelial function in migraine patients: a post-hoc study. *BMC Neurol.* 2011;11(1):146. doi:10.1186/1471-2377-11-146
170. Thijssen DHJ, Bruno RM, van Mil ACCM, et al. Expert consensus and evidence-based recommendations for the assessment of flow-mediated dilation in humans. *Eur Heart J.* 2019;40(30):2534-2547. doi:10.1093/eurheartj/ehz350
171. Green DJ, Dawson EA, Groenewoud HMM, Jones H, Thijssen DHJ. Is Flow-Mediated Dilation Nitric Oxide Mediated? *Hypertension.* 2014;63(2):376-382. doi:10.1161/HYPERTENSIONAHA.113.02044
172. Alzheimer's Association. 2023 Alzheimer's disease facts and figures. *Alzheimer's Dement.* 2023;19(4):1598-1695. doi:10.1002/alz.13016
173. Finger CE, Moreno-Gonzalez I, Gutierrez A, Moruno-Manchon JF, McCullough LD. Age-related immune alterations and cerebrovascular inflammation. *Mol Psychiatry.* 2022;27(2):803-818. doi:10.1038/s41380-021-01361-1
174. Carvalho C, Moreira PI. Oxidative Stress: A Major Player in Cerebrovascular Alterations Associated to Neurodegenerative Events. *Front Physiol.* 2018;9(July):806. doi:10.3389/fphys.2018.00806
175. Wu J, Saleh MA, Kirabo A, et al. Immune activation caused by vascular oxidation promotes fibrosis and hypertension. *J Clin Invest.* 2015;126(1):50-67. doi:10.1172/JCI80761
176. Kirabo A, Fontana V, de Faria APC, et al. DC isoketal-modified proteins activate T cells and promote hypertension. *J Clin Invest.* 2014;124(10):4642-4656. doi:10.1172/JCI74084
177. Aw D, Silva AB, Palmer DB. Immunosenescence: emerging challenges for an ageing population. *Immunology.* 2007;120(4):435-446. doi:10.1111/j.1365-2567.2007.02555.x
178. Buysse DJ, Reynolds CF, Monk TH, Berman SR, Kupfer DJ. The Pittsburgh

- sleep quality index: A new instrument for psychiatric practice and research. *Psychiatry Res.* 1989;28(2):193-213. doi:10.1016/0165-1781(89)90047-4
179. Bollinger T, Bollinger A, Skrum L, Dimitrov S, Lange T, Solbach W. Sleep-dependent activity of T cells and regulatory T cells. *Clin Exp Immunol.* 2009;155(2):231-238. doi:10.1111/j.1365-2249.2008.03822.x
  180. Said EA, Al-Abri MA, Al-Saidi I, et al. Sleep deprivation alters neutrophil functions and levels of Th1-related chemokines and CD4+ T cells in the blood. *Sleep Breath.* 2019. doi:10.1007/s11325-019-01851-1
  181. Sauvet F, Leftheriotis G, Gomez-Merino D, et al. Effect of acute sleep deprivation on vascular function in healthy subjects. *J Appl Physiol.* 2010;108(1):68-75. doi:10.1152/jappphysiol.00851.2009
  182. KRISKA AM, EDELSTEIN SL, HAMMAN RF, et al. Physical Activity in Individuals at Risk for Diabetes. *Med Sci Sport Exerc.* 2006;38(5):826-832. doi:10.1249/01.mss.0000218138.91812.f9
  183. Distefano G, Standley RA, Zhang X, et al. Physical activity unveils the relationship between mitochondrial energetics, muscle quality, and physical function in older adults. *J Cachexia Sarcopenia Muscle.* 2018;9(2):279-294. doi:10.1002/jcsm.12272
  184. Hedges CP, Woodhead JST, Wang HW, et al. Peripheral blood mononuclear cells do not reflect skeletal muscle mitochondrial function or adaptation to high-intensity interval training in healthy young men. *J Appl Physiol.* 2019;126(2):454-461. doi:10.1152/jappphysiol.00777.2018
  185. Andonian BJ, Koss A, Koves TR, et al. Rheumatoid arthritis T cell and muscle oxidative metabolism associate with exercise-induced changes in cardiorespiratory fitness. *Sci Rep.* 2022;12(1):7450. doi:10.1038/s41598-022-11458-4
  186. AINSWORTH BE, HASKELL WL, HERRMANN SD, et al. 2011 Compendium of Physical Activities. *Med Sci Sport Exerc.* 2011;43(8):1575-1581. doi:10.1249/MSS.0b013e31821ece12
  187. Lain SJ, Roberts CL, Warning J, Vivian-Taylor J, Ford JB. A survey of acute self-reported infections in pregnancy. *BMJ Open.* 2011;1(1):e000083-e000083. doi:10.1136/bmjopen-2011-000083
  188. Ajaz S, McPhail MJ, Singh KK, et al. Mitochondrial metabolic manipulation by SARS-CoV-2 in peripheral blood mononuclear cells of patients with COVID-19. *Am J Physiol Physiol.* 2021;320(1):C57-C65. doi:10.1152/ajpcell.00426.2020
  189. Riou M, Oulehri W, Momas C, et al. Reduced Flow-Mediated Dilatation Is Not Related to COVID-19 Severity Three Months after Hospitalization for SARS-CoV-2 Infection. *J Clin Med.* 2021;10(6):1318. doi:10.3390/jcm10061318
  190. Polo Friz H, Facchetti R, Primitz L, et al. Simultaneous validation of the SunTech 247 diagnostic station blood pressure measurement device according to the British Hypertension Society protocol, the International Protocol and the Association for the Advancement of Medical Instrumentation standards. *Blood*

- Press Monit.* 2009;14(5):222-227. doi:10.1097/MBP.0b013e328330c873
191. McBride JA, Striker R. Imbalance in the game of T cells: What can the CD4/CD8 T-cell ratio tell us about HIV and health? Coyne CB, ed. *PLOS Pathog.* 2017;13(11):e1006624. doi:10.1371/journal.ppat.1006624
  192. Divakaruni AS, Jastroch M. A practical guide for the analysis, standardization and interpretation of oxygen consumption measurements. *Nat Metab.* 2022;4(8):978-994. doi:10.1038/s42255-022-00619-4
  193. Peirce J, Gray JR, Simpson S, et al. PsychoPy2: Experiments in behavior made easy. *Behav Res Methods.* 2019;51(1):195-203. doi:10.3758/s13428-018-01193-y
  194. Brooks J. Peirce, J., & MacAskill, M. (Eds.). Building Experiments in PsychoPy. *Perception.* 2019;48(2):189-190. doi:10.1177/0301006618823976
  195. Weir CB, Jan A. *BMI Classification Percentile And Cut Off Points.*; 2023. <http://www.ncbi.nlm.nih.gov/pubmed/11234459>.
  196. Pk W, Whelton PK, Carey RM, et al. 2017 *ACC/AHA/AAPA/ABC/ACPM/AGS/APhA/ASH/ASPC/NMA/PCNA Guideline for the Prevention, Detection, Evaluation, and Management of High Blood Pressure in Adults.*; 2017. doi:10.1161/HYP.000000000000065/-/DC1.The
  197. American Heart Association. All About Heart Rate (Pulse). <https://www.heart.org/en/health-topics/high-blood-pressure/the-facts-about-high-blood-pressure/all-about-heart-rate-pulse>. Published 2015.
  198. Garber CE, Blissmer B, Deschenes MR, et al. Quantity and Quality of Exercise for Developing and Maintaining Cardiorespiratory, Musculoskeletal, and Neuromotor Fitness in Apparently Healthy Adults. *Med Sci Sport Exerc.* 2011;43(7):1334-1359. doi:10.1249/MSS.0b013e318213fefb
  199. Watson NF, Badr MS, Belenky G, et al. Recommended Amount of Sleep for a Healthy Adult: A Joint Consensus Statement of the American Academy of Sleep Medicine and Sleep Research Society. *Sleep.* June 2015. doi:10.5665/sleep.4716
  200. Chmielewski PP, Strzelec B. Elevated leukocyte count as a harbinger of systemic inflammation, disease progression, and poor prognosis: a review. *Folia Morphol (Warsz).* 2018;77(2):171-178. doi:10.5603/FM.a2017.0101
  201. Wirth MD, Sevoyan M, Hofseth L, Shivappa N, Hurley TG, Hébert JR. The Dietary Inflammatory Index is associated with elevated white blood cell counts in the National Health and Nutrition Examination Survey. *Brain Behav Immun.* 2018;69:296-303. doi:10.1016/j.bbi.2017.12.003
  202. Madhur MS, Lob HE, McCann LA, et al. Interleukin 17 Promotes Angiotensin II–Induced Hypertension and Vascular Dysfunction. *Hypertension.* 2010;55(2):500-507. doi:10.1161/HYPERTENSIONAHA.109.145094
  203. Koep JL, Barker AR, Banks R, et al. The reliability of a breath-hold protocol to determine cerebrovascular reactivity in adolescents. *J Clin Ultrasound.* 2020;48(9):544-552. doi:10.1002/jcu.22891
  204. Grunovas A, Trinkunas E. Cardiovascular Response to Breath-Holding

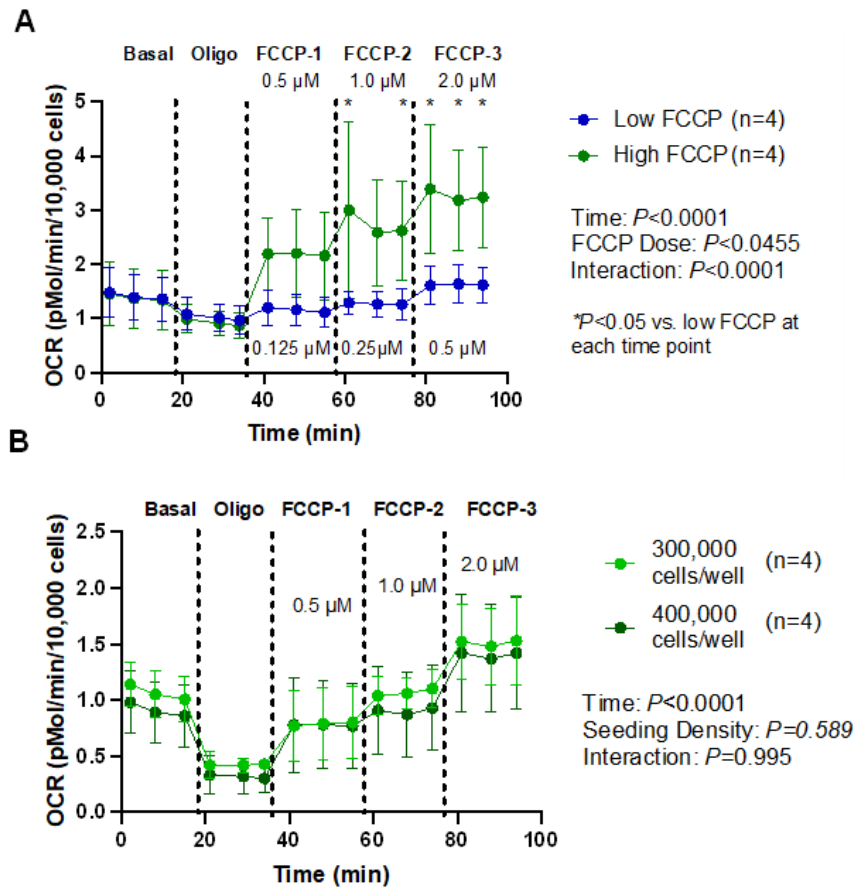
- Explained by Changes of the Indices and their Dynamic Interactions. *Biol Syst Open Access*. 2015;05(01). doi:10.4172/2329-6577.1000152
205. Watanabe H, Washio T, Saito S, Ogoh S. Effect of breath-hold on the responses of arterial blood pressure and cerebral blood velocity to isometric exercise. *Eur J Appl Physiol*. 2022;122(1):157-168. doi:10.1007/s00421-021-04822-1
  206. NAKAHIRA J, OBARA S, JIANG Z-L, YAMAGUCHI H. EFFECTS OF BREATH HOLDING IN AIR ON CARDIAC RESPONSES IN MAN. *Japanese J Phys Fit Sport Med*. 1993;42(5):475-484. doi:10.7600/jspfsm1949.42.475
  207. Trzebski A, Smietanowski M, Zebrowski J. Repetitive apneas reduce nonlinear dynamical complexity of the human cardiovascular control system. *J Physiol Pharmacol*. 2001;52(1):3-19. doi:11321511
  208. Prabhakar NR, Peng Y-JY, Kumar GK, Nanduri J. Peripheral Chemoreception and Arterial Pressure Responses to Intermittent Hypoxia. In: *Comprehensive Physiology*. Vol 5. Wiley; 2015:561-577. doi:10.1002/cphy.c140039
  209. Cooper VL, Pearson SB, Bowker CM, Elliott MW, Hainsworth R. Interaction of chemoreceptor and baroreceptor reflexes by hypoxia and hypercapnia - a mechanism for promoting hypertension in obstructive sleep apnoea. *J Physiol*. 2005;568(2):677-687. doi:10.1113/jphysiol.2005.094151
  210. Hart EC, Charkoudian N, Wallin BG, Curry TB, Eisenach JH, Joyner MJ. Sex Differences in Sympathetic Neural-Hemodynamic Balance. *Hypertension*. 2009;53(3):571-576. doi:10.1161/HYPERTENSIONAHA.108.126391
  211. NOTARIUS CF, MURAI H, MORRIS BL, FLORAS JS. Effect of Fitness on Reflex Sympathetic Neurovascular Transduction in Middle-Age Men. *Med Sci Sport Exerc*. 2012;44(2):232-237. doi:10.1249/MSS.0b013e31822a68a5
  212. Hoiland RL, Smith KJ, Carter HH, et al. SHEAR-MEDIATED DILATION OF THE INTERNAL CAROTID ARTERY OCCURS INDEPENDENT OF HYPERCAPNIA. *Am J Physiol Hear Circ Physiol*. 2018;313(313):24-31. doi:10.1152/ajpheart.00119.2017
  213. Michaud M, Balardy L, Moulis G, et al. Proinflammatory Cytokines, Aging, and Age-Related Diseases. *J Am Med Dir Assoc*. 2013;14(12):877-882. doi:10.1016/j.jamda.2013.05.009
  214. Cullen NC, Mälärstig Anders, Stomrud E, Hansson O, Mattsson-Carlgrén N. Accelerated inflammatory aging in Alzheimer's disease and its relation to amyloid, tau, and cognition. *Sci Rep*. 2021;11(1):1965. doi:10.1038/s41598-021-81705-7
  215. Giunta B, Fernandez F, Nikolic W V, et al. Inflammaging as a prodrome to Alzheimer's disease. *J Neuroinflammation*. 2008;5(1):51. doi:10.1186/1742-2094-5-51
  216. Kosyreva A, Sentyabreva A, Tsvetkov I, Makarova O. Alzheimer's Disease and Inflammaging. *Brain Sci*. 2022;12(9):1237. doi:10.3390/brainsci12091237
  217. Walker AE, Eskurza I, Pierce GL, Gates PE, Seals DR. Modulation of Vascular Endothelial Function by Low-Density Lipoprotein Cholesterol With Aging:

- Influence of Habitual Exercise. *Am J Hypertens*. 2009;22(3):250-256.  
doi:10.1038/ajh.2008.353
218. Bournat JC, Brown CW. Mitochondrial dysfunction in obesity. *Curr Opin Endocrinol Diabetes Obes*. 2010;17(5):446-452.  
doi:10.1097/MED.0b013e32833c3026
  219. Griffiths G, Quinn P, Warren G. Dissection of the Golgi complex. I. Monensin inhibits the transport of viral membrane proteins from medial to trans Golgi cisternae in baby hamster kidney cells infected with Semliki Forest virus. *J Cell Biol*. 1983;96(3):835-850. doi:10.1083/jcb.96.3.835
  220. Moshfegh CM, Elkhatib SK, Collins CW, Kohl AJ, Case AJ. Autonomic and Redox Imbalance Correlates With T-Lymphocyte Inflammation in a Model of Chronic Social Defeat Stress. *Front Behav Neurosci*. 2019;13.  
doi:10.3389/fnbeh.2019.00103
  221. Mukhopadhyay P, Rajesh M, Haskó G, Hawkins BJ, Madesh M, Pacher P. Simultaneous detection of apoptosis and mitochondrial superoxide production in live cells by flow cytometry and confocal microscopy. *Nat Protoc*. 2007;2(9):2295-2301. doi:10.1038/nprot.2007.327
  222. Grotle A-K, Darling AM, Saunders EF, Fadel PJ, Trott DW, Greaney JL. Augmented T-cell mitochondrial reactive oxygen species in adults with major depressive disorder. *Am J Physiol Circ Physiol*. 2022;322(4):H568-H574.  
doi:10.1152/ajpheart.00019.2022
  223. Martínez-Zamudio RI, Dewald HK, Vasilopoulos T, Gittens-Williams L, Fitzgerald-Bocarsly P, Herbig U. Senescence-associated  $\beta$ -galactosidase reveals the abundance of senescent CD8<sup>+</sup> T cells in aging humans. *Aging Cell*. 2021;20(5). doi:10.1111/accel.13344
  224. Roh K, Noh J, Kim Y, et al. Lysosomal control of senescence and inflammation through cholesterol partitioning. *Nat Metab*. 2023;5(3):398-413.  
doi:10.1038/s42255-023-00747-5
  225. Chacko BK, Kramer PA, Ravi S, et al. The Bioenergetic Health Index: a new concept in mitochondrial translational research. *Clin Sci*. 2014;127(6):367-373.  
doi:10.1042/CS20140101
  226. Hill BG, Benavides GA, Lancaster JR, et al. Integration of cellular bioenergetics with mitochondrial quality control and autophagy. *bchm*. 2012;393(12):1485-1512. doi:10.1515/hsz-2012-0198
  227. Lee Y, Siddiqui WJ. *Cholesterol Levels.*; 2023.  
<http://www.ncbi.nlm.nih.gov/pubmed/4337382>.
  228. Barter PJ, Nicholls S, Rye K-A, Anantharamaiah GM, Navab M, Fogelman AM. Antiinflammatory Properties of HDL. *Circ Res*. 2004;95(8):764-772.  
doi:10.1161/01.RES.0000146094.59640.13
  229. Jia C, Anderson JLC, Gruppen EG, et al. High-Density Lipoprotein Anti-Inflammatory Capacity and Incident Cardiovascular Events. *Circulation*. 2021;143(20):1935-1945. doi:10.1161/CIRCULATIONAHA.120.050808
  230. Baixauli F, Acín-Pérez R, Villarroya-Beltrí C, et al. Mitochondrial Respiration

- Controls Lysosomal Function during Inflammatory T Cell Responses. *Cell Metab.* 2015;22(3):485-498. doi:10.1016/j.cmet.2015.07.020
231. Guo C, Sun L, Chen X, Zhang D. Oxidative stress, mitochondrial damage and neurodegenerative diseases. *Neural Regen Res.* 2013;8(21):2003-2014. doi:10.3969/j.issn.1673-5374.2013.21.009
232. Technologies A. Seahorse XF Cell Mito Stress Test User Guide. 2019. [https://www.agilent.com/cs/library/usermanuals/public/XF\\_Cell\\_Mito\\_Stress\\_Test\\_Kit\\_User\\_Guide.pdf](https://www.agilent.com/cs/library/usermanuals/public/XF_Cell_Mito_Stress_Test_Kit_User_Guide.pdf).

## **Appendix A**

### **SUPPLEMENTARY FIGURES**



**Supplementary Figure A.1.** Seeding Density Titration Experiment. A) Pan T-cells were seeded and treated with three low and high doses of FCCP. Oxygen consumption rate (OCR) was then measured using extracellular flux analysis. B) Pan T-cells were seeded at a density of 300,000 cells/well and 400,000 cells/well and treated with varying concentrations of FCCP. OCR was then measured using extracellular flux analysis.

## SUPPLEMENTARY METHODS

### Mito Stress Test Definitions:

- Basal respiration – represents the basal energetic demand of the cells by measuring oxygen consumption at baseline <sup>225,232</sup>.
- ATP-linked O<sub>2</sub> consumption – represents the amount of ATP produced to meet the basal energetic demand of the cell. The injection of oligomycin inhibits ATP synthase, reducing electron flow through the ETC <sup>225,232</sup>.
- Proton leak – represents oxygen consumption that is not linked to the production of ATP. It can also be indicative of mitochondrial damage <sup>225,232</sup>.
- Maximal respiration – represents the maximal response to an energetic demand by measuring oxygen consumption by complex IV after the injection of FCCP. FCCP uncouples the proton gradient in the electron transport chain (ETC), and thus uncouples ATP synthase from the ETC <sup>225,232</sup>.
- Spare respiratory capacity – represents the capacity of a cell to respond to an energetic demand. It is indicative of the cells “fitness” <sup>225,232</sup>.
- Non-mitochondrial O<sub>2</sub> consumption – represents oxygen consumed by processes other than oxidative phosphorylation. It is calculated after the injection complex I and complex III inhibitors <sup>225,232</sup>.
- Coupling Efficiency – represents the proportion of basal respiration that is related to ATP production <sup>192</sup>.

### Mito Stress Test Calculations:

1. *Basal respiration = (Last rate measurement before oligomycin injection) – (Non-mitochondrial oxygen consumption)*
2. *ATP-Production Coupled Respiration = (Last rate measurement before Oligomycin injection) – (Minimum rate measurement after Oligomycin injection)*
3. *Proton Leak = (Minimum rate measurement after Oligomycin injection) – (Non-mitochondrial oxygen consumption)*
4. *Maximal Respiration = (Maximum rate measurement after FCCP injection) – (Non-mitochondrial oxygen consumption)*
5. *Spare Respiratory Capacity = (Maximal Respiration) – (Basal Respiration)*
6. *Coupling Efficiency = (ATP-Production Coupled Respiration) / (Basal Respiration) x 100*

#### Glycolysis Definitions:

- Basal glycolysis – represents the contribution of glycolytic processes to meet basal energetic demands by measuring ECAR at baseline.
- Maximal glycolysis – represents the maximal glycolytic response to an energetic demand by measuring ECAR following FCCP injection.
- Basal OCR/ECAR ratio – represents the metabolic phenotype at baseline.
- Maximal OCR/ECAR ratio – represents the shift in metabolic phenotype in response to an energetic demand.

#### Glycolysis Calculations:

1. *Basal glycolysis = (Last rate measurement before oligomycin injection)*
2. *Maximal glycolysis = (First rate measurement after FCCP injection)*
3. *Basal OCR/ECAR ratio = (basal respiration) / (basal glycolysis)*

4. *Maximal OCR/ECAR ratio = (maximal respiration) / (maximal glycolysis)*

## **Appendix B**

**IRB APPROVED PROTOCOL**



Institutional Review Board  
210H Hullihen Hall  
Newark, DE 19716  
Phone: 302-831-2137  
Fax: 302-831-2828

DATE: June 11, 2021

TO: Theodore DeConne, B.S.  
FROM: University of Delaware IRB

STUDY TITLE: [1753416-1] The effect of low-density lipoprotein cholesterol on human T-cell metabolism and inflammation.

SUBMISSION TYPE: New Project

ACTION: APPROVED  
EFFECTIVE DATE: June 11, 2021  
NEXT REPORT DUE: June 10, 2022

REVIEW TYPE: Expedited Review  
REVIEW CATEGORY: Expedited review category # (2,4)

Thank you for your New Project submission to the University of Delaware Institutional Review Board (UD IRB). The UD IRB has reviewed and APPROVED the proposed research and submitted documents via Expedited Review in compliance with the pertinent federal regulations.

As the Principal Investigator for this study, you are responsible for, and agree that:

- All research must be conducted in accordance with the protocol and all other study forms as approved in this submission. Any revisions to the approved study procedures or documents must be reviewed and approved by the IRB prior to their implementation. Please use the UD amendment form to request the review of any changes to approved study procedures or documents.
- Informed consent is a process that must allow prospective participants sufficient opportunity to discuss and consider whether to participate. IRB-approved and stamped consent documents must be used when enrolling participants and a written copy shall be given to the person signing the informed consent form.
- Unanticipated problems, serious adverse events involving risk to participants, and all non-compliance issues must be reported to this office in a timely fashion according with the UD requirements for reportable events. All sponsor reporting requirements must also be followed.

The UD IRB REQUIRES the submission of a PROGRESS REPORT DUE ON June 10, 2022. A continuing review/progress report form must be submitted to the UD IRB at least 45 days prior to the due date to allow for the review of that report.

If you have any questions, please contact the UD IRB Office at (302) 831-2137 or via email at [hsrb-research@udel.edu](mailto:hsrb-research@udel.edu). Please include the study title and reference number in all correspondence with this office.